THEORETICAL AND EXPERIMENTAL STUDY OF A TIED BACK-TO-BACK RETAINING WALL FOR RAILWAY LOADING

Wilfred W. Wong

A DISSERTATION

in

The Faculty

of

Engineering

Presented in Partial Fulfillment of the Requirements for
the Degree of Master of Engineering at
Sir George Williams University
Montreal, Canada

September 1972

THEORETICAL AND EXPERIMENTAL STUDY OF A TIED BACK-TO-BACK RETAINING WALL FOR RAILWAY LOADING

WILFRED W. WONG

ABSTRACT

The need of environmental control and the high cost of construction have necessitated railway engineers to look for other methods for embankment widening to accommodate new facilities on existing lines. As an alternative to the conventional "haul and fill" method, a tied back-to-back retaining wall was proposed. The scheme calls for parallel walls on each side of the embankment to retain new fill, and the two walls are tied back-to-back to hold the walls against each other in place.

Theoretical study to develop a design procedure was carried out treating the anchor pile as a simple beam, and results for a typical wall are presented.

Model experiment was also carried out on a scaled-down embankment and wall system constructed of sand fill and timber for the walls. Measurements were carried out on the main anchor piles to determine actual deflections to compare them with theory and the overall stability of the wall under maximum loading conditions.

Conclusions were formulated for the wall system as being satisfactory and suggestions were made for modifications from theory in design for practical purposes.

C O N T E N T S

ACKNOWLEDGEMENT

The author wishes to express his sincere gratitude to Dr. M. S. Troitsky, Professor of Civil Engineering, Sir George Williams University, for his valuable advice and stimulating discussions and suggestions in completing this study.

The financial support provided by the Canadian National Railway for the model experiment is gratefully acknowledged.

My thanks are extended to Mr. G. H. Workman, Assistant Chief Engineer of Design and Construction, and Mr. F. L. Peckover, Engineer of Geotechnical Services, of the Office of Chief Engineer, Canadian National Railway, for their support and encouragement.

Thanks also go to my two sons Roland and Colin who helped me to a great extent in constructing the model and conducting the experimental work, and to my wife Eva who typed the manuscript.

LIST OF FIGURES

NOTATIONS

ϕ	angle of internal friction
δ	angle of wall friction
γ	unit weight of fill material
K_a	coefficient of active pressure
K_p	coefficient of passive pressure
p_a	active pressure
p_p	passive pressure
P_b	total active pressure at bottom of anchor pile
P_1	lateral pressure at apex of modified pressure diagram for railway loading
P_o	lateral pressure at bottom of modified pressure diagram for railway loading
s	spacing of anchor piles
μ	Poisson's ratio
H	height of retaining wall
b,B	width of strip load, or length of railway ties
m	horizontal distance factor
n	vertical distance factor
σ_h	intensity of lateral pressure
q	equivalent railway loading
F_1	axial force in upper tie rod
F_2	axial force in lower tie rod
S	shear in anchor pile
E	modulus of elasticity
I	moment of inertia

M	bending moment in anchor pile
y	deflection in anchor pile
λ	model scale factor for lineal dimension
ν	model scale factor for load intensity

1. INTRODUCTION

In the past, railway engineers have almost exclusively employed the conventional construction method of "haul and fill" for the widening of existing railway embankment to accommodate additional tracks. Nowadays, such a method may not be practical or economical especially if the work is to be undertaken on existing embankments located within city, suburban and other crowded or restricted areas where environmental consideration must be taken into account. Land properties for additional right-of-way are costly to secure and the fill material needed to construct the additional embankment widths must be hauled in from distant sources. Even in less populated areas, the conventional method is undesirable if the site or foundation soil condition in the general area of the existing embankment is poor, making it necessary to add stabilizing berms or other measures to obtain a safe finished embankment. This would increase construction cost as more fill and additional properties are required.

As an alternative to the "haul and fill" method, a tied back-to-back retaining wall system is proposed. It assumes the form of a wall system built on top of the embankment feasible from a soil mechanics and foundation point of view. A generalized case is illustrated in Fig.1-1 in which a 90 ft. high embankment on the Canadian National Railway mainline located near Hamilton, Ontario, was proposed for widening for the construction of additional tracks. It shows features

of comparative advantage for using this type of retaining walls. It should be mentioned that the idea of tied back-to-back retaining walls was originated by Mr. F. L. Peckover of the Chief Engineer's Office, Canadian National Railway, in September 1970. As there has been no known precedent case of such a wall system, and also due to certain factors unknown, no real attempt has since been made by the Railway to develop the idea for application to design and construction.

This study is undertaken to develop an analytical procedure which could be used for design of a tied back-to-back retaining wall system applicable to railway loading. The general scheme calls for parallel walls, one on each side of the embankment to retain the new fill and the two walls are tied back-to-back by tie rods to hold the walls in place against each other.

The wall system chosen for this study consists of horizontal tie rods fastened to vertical anchor piles between which horizontal laggings are placed. It can be seen that the anchor piles of the wall system will be the most important structural component to be investigated. As the walls are tied against each other and held in place by fill, their resistance to movement or deflection by applied surface loads is inter-dependent of the passive resistance provided by the fill or by the surface loads if such loads are imposed simultaneously on both walls. These combinations of lateral pressure and passive resistance are difficult to assess by theory since the walls would be flexible in varying degree to adjust or yield under such actions.

Theoretical analysis will be carried out for the anchor pile together with the other components of the wall. It will treat the effects of earth pressure and railway loading seperately. The anchor pile will be assumed as an "equivalent beam" and its two points of anchor rod connection as hinged and non-yielding supports.

A model experiment of the retaining wall system is carried out using results from theoretical study. The main object of the experiment is to compare the validity of theoretical results relating to railway loading and the assumptions made therewith. Measurements are to be taken for deflection of the anchor piles and to compare them with those obtained by theory. Finally, conclusions are drawn from the test results and observations on the overall stability of such a retaining wall system.

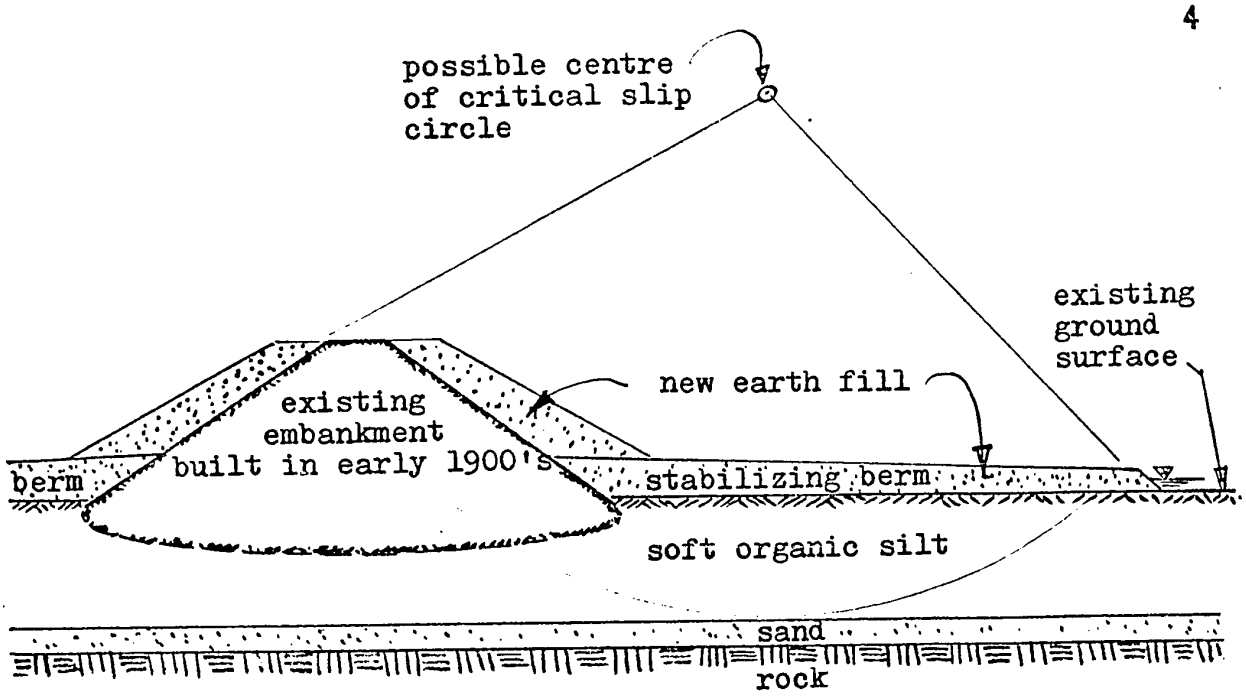

(a) Embankment widening using conventional "haul and fill" method.
Note: Berms are necessary for stability of final embankment, requiring large quantities of fill and wide additional land for new right-of-way.

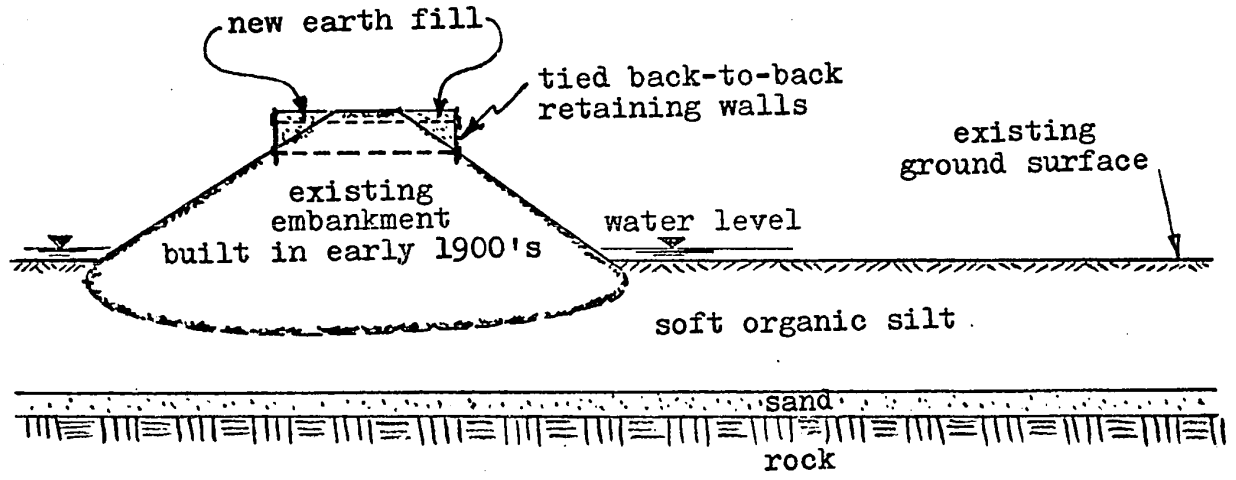

(b) Embankment widening using tied back-to-back retaining walls.
Note: Comparatively small amount of new fill on top of existing embankment generally has negligible effect on the overall stability of the final embankment.

Fig.1-1 - Generalized case illustrating features of comparative advantage of using tied back-to-back retaining walls. (Approximate scale 1" = 100')

2. LATERAL EARTH PRESSURE

2.1 - GENERAL BACKGROUND

The methods commonly used nowadays for design practice are derived from classical earth theories developed by Coulomb (1776) and Rankine (1857). Since that time, various other engineers and scientists have made significant contributions to earth pressure theories. Experiments have shown that classical theories for cohesionless soil lead to quite accurate results for backfills of clean dry sand.

Developments[7] since 1920, largely due to the influence of Dr. Karl Terzaghi, have led to a better understanding of the limitation and appropriate application of the theories. Results have shown that the lateral pressures in a soil mass are greatly affected by any deformation which the mass may have experienced. This phenomena was well demonstrated by Terzaghi (1934) in a series of large scale-model tests with retaining walls backfilled with sand which showed the importance of wall movement on the development of earth pressure.

Earth pressures are generally classified into three important types (a) active pressure, (b) passive pressure, (c) pressure at rest, depending on the state of stress which may exist in a soil mass in accordance with the manner in which it has been deformed. These are discussed in subsequent section.

2.2 - EARTH PRESSURE PHENOMENA

Consider the retaining wall backfilled with a granular cohesionless material as shown in Fig.2-1.(9)

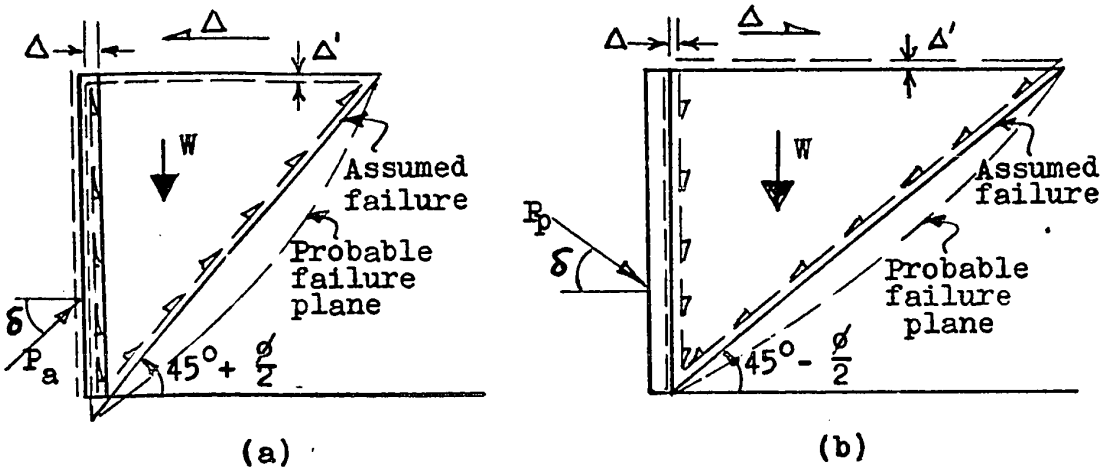

Fig.2-1 - Wall movements to develop (a) active pressure, (b) passive pressure.

When the wall moves forward slightly, the soil would tend to move forward also. As it does so, friction forces would become mobilized, and an analysis would indicate that the critical surface of failure is approximately a plane surface at an angle of $45^o + \frac{\phi}{2}$ with a horizontal plane as shown in Fig.2-1 (a). In this case the failure wedge and the driving weight are a minimum. This is termed "active pressure". The magnitude of the lateral extension of the soil required to develop active state of stress depends upon the kind of soil, the manner in which it is deposited, and the pattern of deformation. It is larger for loose sand than for sense sand.

However, after a deformation has been reached which is sufficient to develop or mobilize the full shearing resistance of the soil, further deformation does not appreciably affect the magnitude of the active pressure.

On the other hand, if the wall is moved into the backfill, the failure wedge can be approximated by a plane surface at an angle of $45^{o} - \frac{\phi}{2}$ with the horizontal, the retaining wall must provide a sufficient push against the soil to overcome the friction resistance along the rupture plane and to lift the weight of the wedge of soil upward along the failure plane as shown in Fig.2-1 (b). The pressure developed in this case is termed "passive pressure". The magnitude of the lateral compression of the soil required to develop the passive state of stress in a given soil is somewhat greater than that of the lateral extension required to produce the active state of stress in that soil. Also, after a deformation has been reached which is sufficient to develop or mobilize the full shearing resistance of the soil, further deformation does not greatly affect the magnitude of the passive pressure. In the case of this study, passive pressure may be called passive resistance.

Earth pressure termed "at rest" is associated with the forces acting on the retaining structure before any movement takes place either into or away from the backfill mass. In fact, earth pressure at rest is a special case of elastic equilibrium. Again the magnitude of these pressures depends upon the manner in which the soil is deposited and upon the physical properties of the soil. Earth pressure at rest will

exist in natural soil deposits which have remained undisturbed. They may occur in backfill or soil deposits retained laterally by rigid structures which do not yield appreciably under the action of earth pressure. It is not possible to compute the magnitudes of earth pressure at rest. Such values can only be determined by experiments.

The relative magnitude of active, passive and at rest pressures are illustrated in Fig.2-2.

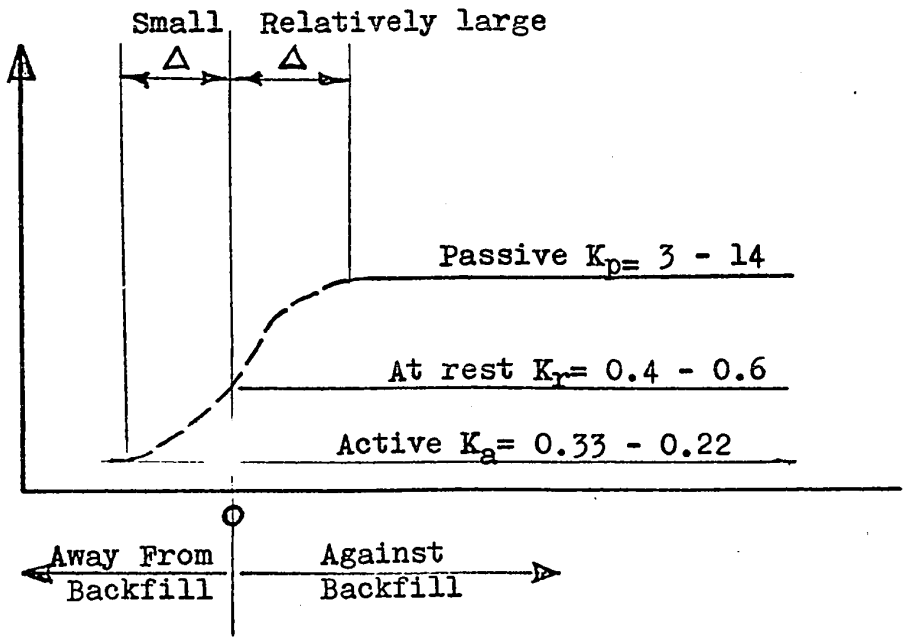

Fig.2-2 - Illustration of active and passive pressures with usual range of values for cohesionless soil.

2.3 - RANKINE THEORY OF EARTH PRESSURE

Rankine's[9] method of determining lateral earth pressure will be used in this study since it is appropriate to omit effect of wall friction in view of vibrations from railway traffic.

The theory considers that the major and minor principal axes are in the x and y directions. This state of stress is not changed if a perfectly smooth vertical wall is introduced as a boundary. Since there is no shear stress between the backfill soil and the frictionless wall, the vertical wall remains as a principal plane.

Rankine's case of lateral earth pressure is illustrated in Fig.2-3.

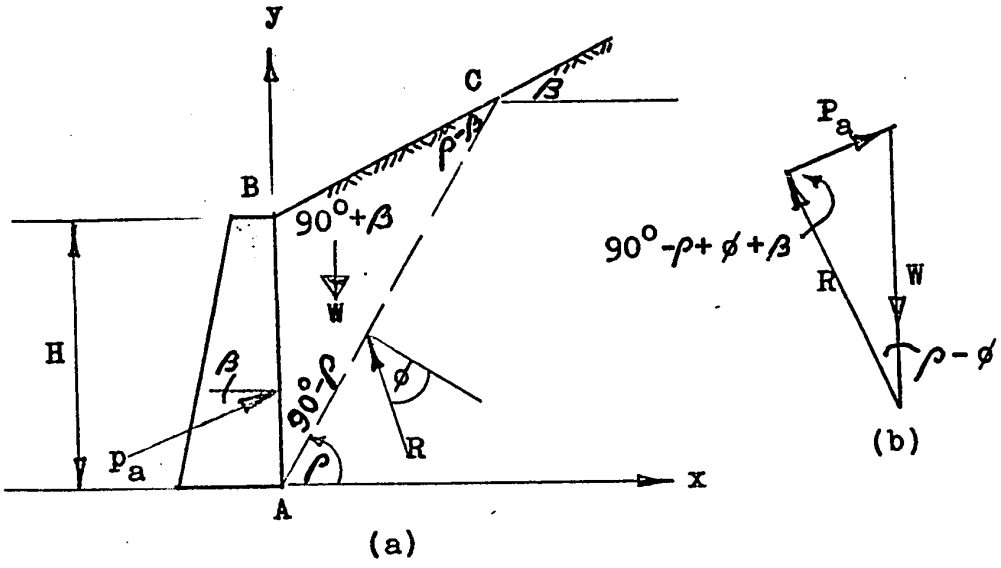

Fig.2-3 - (a) Soil-Structure System for Rankine Solution, (b) Force Triangle in the Rankine Solution.

$$\text{Area ABC} = \tfrac{1}{2}\gamma H^2 \frac{\sin(90^\circ-\rho)\,\sin(90^\circ+\beta)}{\sin(\rho-\beta)}$$

$$W = \tfrac{1}{2}\gamma H^2 \frac{\cos\rho\,\cos\beta}{\sin(\rho-\beta)} \qquad \text{.....Eq.(2-1)}$$

$$P_a = \frac{W\sin(\rho-\phi)}{\sin(90^\circ-\rho+\phi+\beta)} \qquad \text{.....Eq.(2-2)}$$

Substituting Eq.(2-1) into Eq.(2-2), differentiating and setting

$$\frac{dP_a}{d\rho} = 0, \quad \text{then}$$

$$P_a = \frac{\gamma H^2}{2}\cos\beta\,\frac{\cos\beta-\sqrt{\cos^2\beta-\cos^2\phi}}{\cos\beta+\sqrt{\cos^2\beta-\cos^2\phi}}$$

or $$P_a = \frac{\gamma H^2}{2} K_a$$

where $$K_a = \cos\beta\,\frac{\cos\beta-\sqrt{\cos^2\beta-\cos^2\phi}}{\cos\beta+\sqrt{\cos^2\beta-\cos^2\phi}}$$

In the case of this study, ground surface at top of retaining wall level, $\beta = 0$, and K_a simplifies to

$$K_a = \frac{1-\sqrt{1-\cos^2\phi}}{1+\sqrt{1-\cos^2\phi}}$$

or $$K_a = \frac{1-\sin\phi}{1+\sin\phi} \qquad \text{.....Eq.(2-3)}$$

By analogy, the passive pressure for the Rankine solution can be derived as

$$P_p = \frac{\gamma H^2}{2}\cos\beta\,\frac{\cos\beta+\sqrt{\cos^2\beta-\cos^2\phi}}{\cos\beta-\sqrt{\cos^2\beta-\cos^2\phi}}$$

or $$P_p = \frac{\gamma H^2}{2} K_p$$

where $K_p = \cos\beta \frac{\cos\beta + \sqrt{\cos^2\beta - \cos^2\phi}}{\cos\beta - \sqrt{\cos^2\beta - \cos^2\phi}}$

Again, as ground surface is level, $\beta = 0$, and K_p simplifies to

$$K_p = \frac{1 + \sqrt{1 - \cos^2\phi}}{1 - \sqrt{1 - \cos^2\phi}}$$

or $$K_p = \frac{1 + \sin\phi}{1 - \sin\phi} \qquad \text{.....Eq.(2-4)}$$

Hence, at any depth z of the retaining wall,

active pressure, $p_a = \gamma z K_a$ .....Eq.(2-5)

passive pressure, $p_p = \gamma z K_p$ .....Eq.(2-6)

Therefore, Rankine's theory in this case has considered only the weight of the failure wedge behind the wall as contributing to the wall pressure. Thus three important limitations on the Rankine solution are:

(a) backfill must be a plane surface,

(b) wall must not interfere with the failure wedge,

(c) there is no wall friction.

It will be seen that these limitaions are satisfied in this study only when friction resistance between wall and backfill can reach zero value, as the retaining wall will be subjected to vibration from rail traffic.

The effects of equivalent surcharge resulting from railway loading in the form of line load and uniform strip load are dealt with in a subsequent section.

2.4 - SOIL PARAMETERS OF BACKFILL MATERIAL

The backfill to be placed behind retaining walls in this study will be a granular cohesionless material such as gravel, sand, crushed stone, crushed rock, slag or other suitable light-weight material. The lateral earth pressure is dependent on the following factors:(9)

Unit Weight of Backfill Material, γ

Lateral earth pressure is directly proportional to the unit weight of the backfill soil material. Table 2-1 gives some typical values for the common granular backfill material.

Table 2-1

Material	Loose γ_{dry} pcf	Loose Void Ratio e	Dense γ_{dry} pcf	Dense Void Ratio e	Range of ϕ degree
Gravel	100-110	0.7 - 0.5	115-125	0.5 - 0.3	35 - 45
Coarse Sand	95-100	0.8 - 0.5	115-125	0.45-0.35	28 - 40
Fine/Med. Sand	90-100	0.9 - 0.7	100-110	0.7 - 0.5	28 - 35

Whenever possible, the values of dry unit weight γ_{dry} should be determined by test. Density depends on both the kind of material and the amount of water present in the voids. Density may vary with time through vibrations. Consolidation effects may also increase the density if surcharges are imposed on the backfill.

Angle of Internal Friction ϕ

This parameter is dependent on the density of the material, type of material, shape of the granular particles, and presence of water. Water tends to reduce the angle of internal friction in moist material. The less the ϕ, the larger the lateral pressure for the active case, i.e. the term $K_a = \frac{1 - \sin \phi}{1 + \sin \phi}$ will approach unity as in the case of a frictionless material. For this reason, it is desirable to use granular materials because of their free draining characteristics.

Angle of Wall Friction, δ

This parameter is dependent on the degree of smoothness of the wall, and the type and density of the backfill material that comes in contact with the wall. Presence of water, temperature and vibration may also affect the wall friction. If the wall is smooth, $\delta \rightarrow 0$, or if it is excessively rough, the wall cavities will fill with soil and any shear failure will take place by shear along soil surface, or $\delta \rightarrow \phi$. The angle of wall friction may be positive or negative, dependent on the relative movement of the wall with respect to the backfill soil mass. A downward drag of the wall will occur if only the backfill settles or consolidates.

Since the retaining walls in this study will be subjected to vibrations by railway traffic, the effect of wall friction will be omitted when calculating for lateral earth pressure.

3. THEORETICAL ANALYSIS CONSIDERING LATERAL EARTH PRESSURE

3.1 - DEFINITIONS AND ASSUMPTIONS

The typical retaining wall system chosen for the study will be one which is to be built on both side slopes of an existing embankment. It will consist of horizontal laggings supported by vertical anchor piles which are tied back-to-back with tie rods as shown in Fig.3-1(a). The anchor piles with their tie rods are spaced at suitable regular interval.

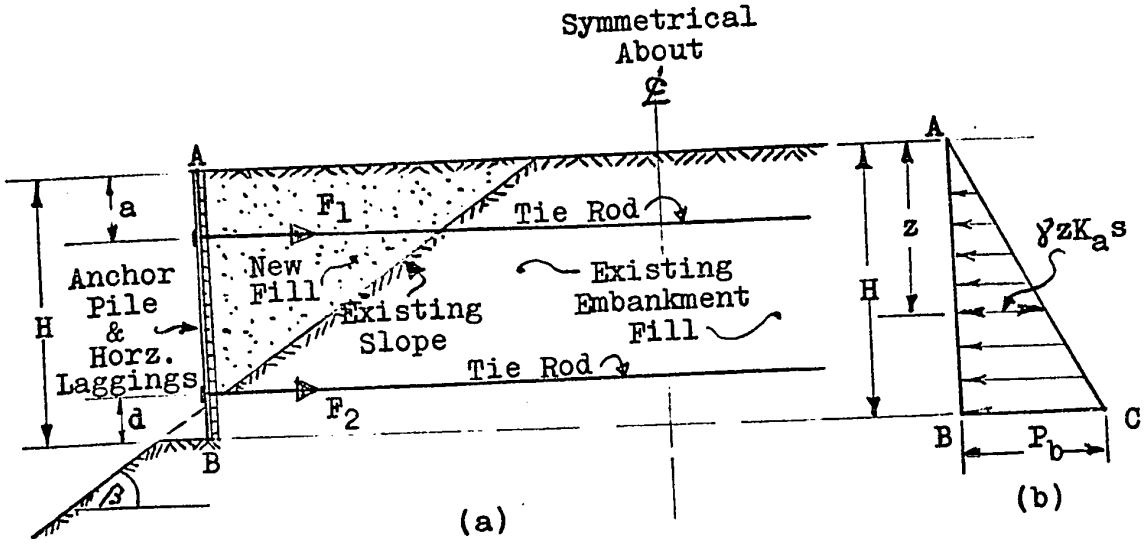

Fig.3-1 - (a) Cross-section of typical retaining wall system, (b) Lateral earth pressure diagram.

The horizontal laggings supporting the backfill are considered simply-supported, and therefore their end reactions are transfered directly to the anchor piles which are supported and held in place by the tie rods. Point of connection of the tie rod to the anchor pile is assumed hinged, and thereis no

distortion or rotation of the tie rod about this point so that the anchor pile may be analysed as an " equivalent beam ".

For practical reason, bottom end of the anchor pile will bear on a cut bench made in the embankment slope, and earth pressure from backfill will be considered effective on the entire depth of the pile. The pile is assumed free to deflect from its vertical axis, except at the points held by the tie rods. These points are assumed as non-yielding supports.

3.2 - LATERAL EARTH PRESSURE DIAGRAM

Since the walls will be subjected to vibrations from railway traffic, the effect of wall friction will not be considered in evaluating earth pressure.

Therefore, with $\delta = 0$, and using a granular backfill material of given γ and ϕ values, at any depth z of the wall, the unit pressure per unit width of wall is

$$p_a = \gamma z K_a, \text{ where } K_a = \frac{1 - \sin \phi}{1 + \sin \phi} .$$

If 's' is the spacing between anchor piles, then the total reaction from the horizontal laggings on the anchor pile at depth z will be

$$P_z = \gamma z K_a s.$$

At the bottom of the pile, this pressure or reaction becomes

$$P_b = \gamma H K_a s \quad \ldots\ldots\ldots\ldots\ldots\ldots\ldots\ldots \text{Eq.(3-1)}$$

Eq.(3-1) gives the maximum pressure per unit height of pile at depth H and gives a triangular pressure diagram in Fig.3-1(b).

3.3 - EQUIVALENT BEAM METHOD

The anchor pile will be analysed as an equivalent beam loaded with the triangular pressure diagram, and supported at non-yielding points R_1 and R_2 held by the tie rods as shown in Fig.3-2.

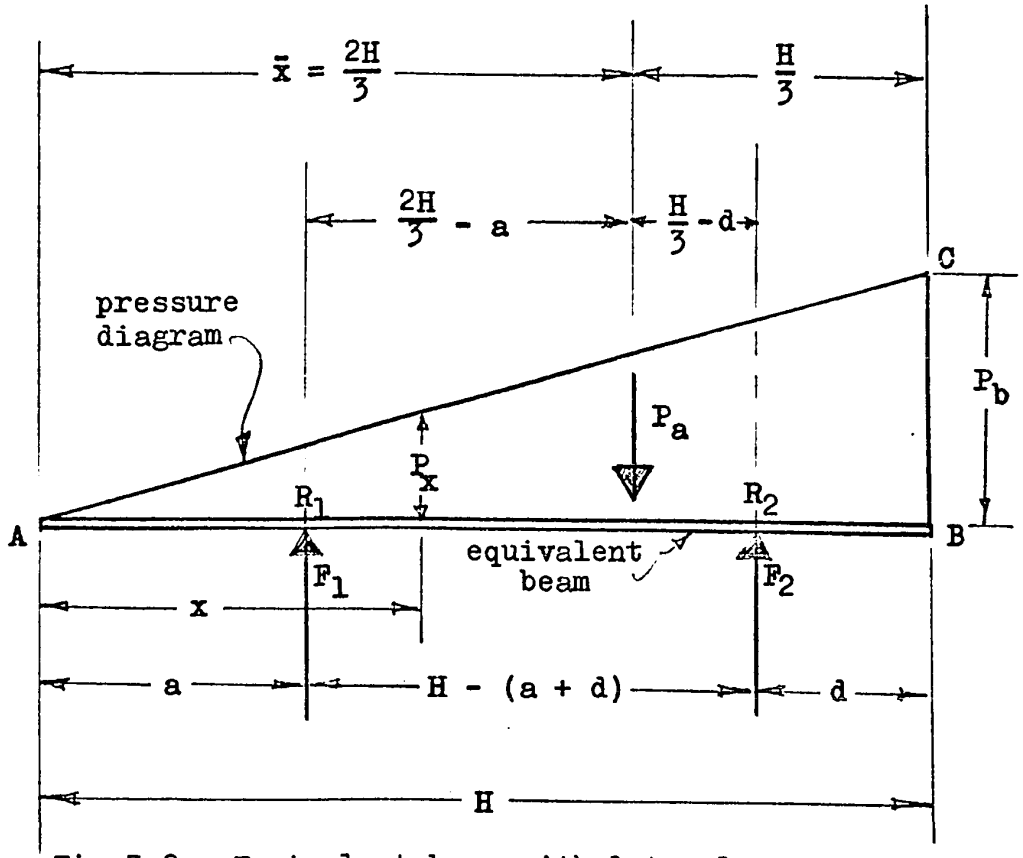

Fig.3-2 - Equivalent beam with lateral pressure diagram.

Equations for axial forces F_1 and F_2 in the two tie rods; the shear S, the bending moment M and the deflection y at any point along the length of the anchor are all derived using static and simple beam theory.

3.4 - FORCES IN TIE RODS

The total load from the triangular pressure diagram ABC is $P_a = \frac{P_b H}{2}$.

Distance of the centre of gravity of pressure diagram from point A is $\bar{x} = \frac{2H}{3}$.

Taking moments about point R_2, therefore

$$F_1(H - a - d) = \frac{P_b H}{2}\left(\frac{H}{3} - d\right)$$

Hence, $$F_1 = \frac{P_b H}{6} \frac{(H - 3d)}{(H - a - d)} \quad \text{..... Eq.(3-2)}$$

Similarly taking moments about R_1, therefore

$$F_2 = \frac{P_b H}{6} \frac{(2H - 3a)}{(H - a - d)} \quad \text{..... Eq.(3-3)}$$

3.5 - SHEAR IN ANCHOR PILE

Let S be the shear at any point x along the beam AB.

Case (a) - for x = 0 to x = a :-

Since $P_x = \frac{P_b x}{H}$,

$$S = \frac{P_x x}{2}.$$

Hence $$S = \frac{P_b x^2}{2H} \quad \text{..... Eq.(3-4a)}$$

Case (b) - for x = a to x = H - d :-

$$S = \frac{P_b x^2}{2H} - F_1 \quad \text{..... Eq.(3-4b)}$$

Case (c) - for x = H - d to x = H :-

$$S = \frac{P_b x^2}{2H} - F_1 - F_2 \quad \text{..... Eq.(3-4c)}$$

3.6 - BENDING MOMENT IN ANCHOR PILE

Let M be the bending moment at any point x along the beam AB.

Case (a) - for x = 0 to x = a :-

$$\text{Since } P_x = \frac{P_b x}{H} ,$$

$$M = P_x \cdot \frac{x}{2} \cdot \frac{x}{3} .$$

$$\text{Hence, } M = \frac{P_b x^3}{6H} \quad \ldots\ldots\ldots\ldots\ldots\ldots\ldots \text{Eq.(3-5a)}$$

Case (b) - for x = a to x = H - d :-

$$M = \frac{P_b x^3}{6H} - F_1(x - a) \quad \ldots\ldots\ldots\ldots\ldots \text{Eq.(3-5b)}$$

Case (c) - for x = H - d to x = H :-

$$M = \frac{P_b x^3}{6H} - F_1(x - a) - F_2(x - H - d) \ldots\ldots \text{Eq.(3-5c)}$$

3.7 - MAXIMUM BENDING MOMENT IN ANCHOR PILE

Maximum positive bending moment will occur at zero shear between points R_1 and R_2. To find location of zero shear, differentiate the bending moment equation for Case (b) and equate to zero.

$$M = \frac{P_b x^3}{6H} - F_1(x - a)$$

$$\frac{dM}{dx} = \frac{P_b x^2}{2H} - F_1$$

$$= 0$$

Substituting for the value of F_1, therefore

$$x = \frac{H}{\sqrt{3}}\sqrt{\frac{H - 3d}{H - a - d}} .$$

Substituting x = h for location of maximum moment, therefore

$$h = \frac{H}{\sqrt{3}}\sqrt{\frac{H - 3d}{H - a - d}} \quad \text{..... Eq.(3-6)}$$

Hence, $M_{max} = \frac{P_b h^3}{6H} - F_1(h - a)$ ..... Eq.(3-7)

3.8 - DEFLECTION OF ANCHOR PILE

Let y be the deflection at any point along the beam AB. Then the deflection is obtained by integrating the equation of deflection: $\frac{d^2y}{dx^2} = -\frac{M}{EI}$ using the bending moment equations derived in Section 3.6.

Case (a) - for x = 0 to x = a :-

Since $M = \frac{P_b x^3}{6H}$, therefore

$$\frac{d^2y}{dx^2} = -\frac{1}{EI} \cdot \frac{P_b x^3}{6H}$$

$$\frac{dy}{dx} = -\frac{1}{EI} \cdot \frac{P_b}{6H}\left[\frac{x^4}{4} + C_1\right]$$

$$y = -\frac{1}{EI} \cdot \frac{P_b}{6H}\left[\frac{x^5}{20} + C_1 x + C_2\right] \quad \text{.....Eq.(3-8a)}$$

The constants of integration C_1 and C_2 are obtained as follows:-

At x = a, $\frac{dy}{dx} = 0$, and therefore,

$$C_1 = -\frac{a^4}{4}.$$

At x = a, y = 0 , and therefore,

$$C_2 = \frac{a^5}{5}$$

Case (b) - for x = a to x = H - d :-

$$\frac{d^2y}{dx^2} = -\frac{M}{EI}$$

$$= -\frac{1}{EI}\left[\frac{P_b x^3}{6H} - F_1(x - a)\right]$$

Integrating, therefore,

$$\frac{dy}{dx} = -\frac{1}{EI}\left[\frac{P_b x^4}{24H} - F_1\left(\frac{x^2}{2} - ax\right) + C_1\right]$$

$$y = -\frac{1}{EI}\left[\frac{P_b x^5}{120H} - F_1\left(\frac{x^3}{6} - \frac{ax^2}{2}\right) + C_1 x + C_2\right] \quad \ldots \text{ Eq.(3-8b)}$$

The constants of integration C_1 and C_2 are obtained as follows:-

Since maximum positive bending moment occurs at point 'h', therefore at x = h, $\frac{dy}{dx} = 0$.

Hence, $C_1 = -\frac{P_b h^4}{24H} + F_1\left(\frac{h^2}{2} - ah\right)$

At x = a, y = 0, and therefore,

$$C_2 = -\frac{P_b a^5}{120H} - F_1\frac{a^3}{3} - C_1 a$$

Case (c) - for x = H - d to x = H :-

$$\frac{d^2y}{dx^2} = -\frac{M}{EI}$$

$$= -\frac{1}{EI}\left[\frac{P_b x^3}{6H} - F_1(x - a) - F_2\left[x - (H - d)\right]\right]$$

Letting (H - d) = k and integrating, therefore,

$$\frac{dy}{dx} = -\frac{1}{EI}\left[\frac{P_b x^4}{24H} - F_1\left(\frac{x^2}{2} - ax\right) - F_2\left(\frac{x^2}{2} - kx\right) + C_1\right]$$

$$y = -\frac{1}{EI}\left[\frac{P_b x^5}{120H} - F_1\frac{x^2}{2}\left(\frac{x}{3} - a\right) + F_2\frac{x^2}{6}(3k - x) + C_1 x + C_2\right]$$

.....Eq.(3-8c)

The constants of integration C_1 and C_2 are obtained as follows:-

At $x = k$, $\frac{dy}{dx} = 0$, and therefore,

$$C_1 = -\frac{P_b k^4}{24H} - F_1 ak + (F_1 - F_2)\frac{k^2}{2}$$

At $x = k$, $y = 0$, and therefore,

$$C_2 = -\frac{P_b k^5}{120H} + F_1 \frac{k^2}{6}(k - 3a) - F_2 \frac{k^3}{3} - C_1 k$$

4. LATERAL PRESSURE FROM SURFACE LOADS BY THEORY OF ELASTICITY

4.1 - APPLICATION OF THE THEORY

Most of the methods currently used in the study of lateral pressures resulting from surcharge loads placed at ground surface are based on the theory of elasticity, with certain emphirical modification to precise mathematical solutions of elasticity. The solutions to pressure or stress distribution within a medium are available in text books on the theory of elasticity and the purely analytical approaches are found in them.

The early theories concerning lateral pressures resulting from surface loads were used practically unchallenged until experiments were carried out to verify their validity. Tests which were carried out by Gerber (1929)[1], Terzaghi (1954)[5] and Spangler & Mickle (1956)[6] indicate that lateral pressures can be computed for various types of surcharges by using modified forms of equations from the theory of elasticity.

The most well-known equation for lateral pressure was one originally presented by Bossinesq in 1883.

The following will outline the development of Boussinesq's equation with subsequent modifications from experimental results to suit its application in practical problem.[9]

4.2 - BOUSSINESQ'S EQUATION

Boussinesq's equation for lateral stress is given in the form

$$\sigma_h = \frac{V}{2\pi z^2}\left[3\sin^2\theta\cos^3\theta - \frac{(1-2\mu)\cos^2\theta}{1+\cos\theta}\right] \quad \text{....Eq.(4-1)}$$

where the terms are illustrated as in Fig.4-1,

and μ = Poisson's ratio.

It is assumed that the unit weight of the supporting elastic material is zero.

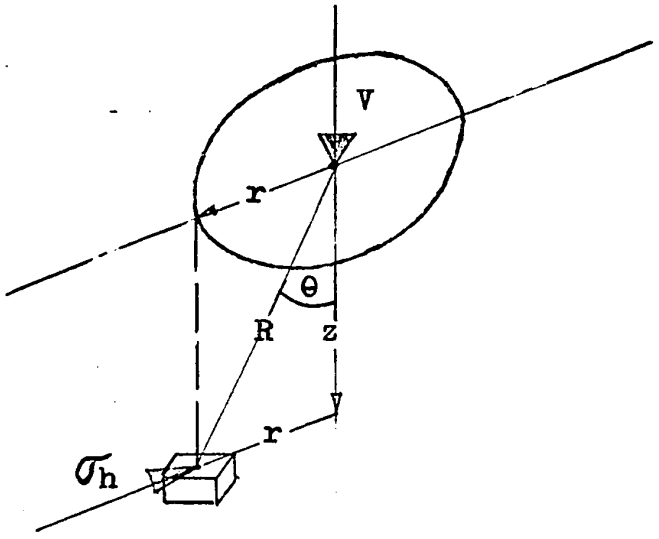

Fig.4-1 - Intensity of stress, σ_h, based on Boussinesq's approach.

The assumptions for applying Boussinesq's equation are that the soil material is:

(a) semi-infinite in extent,

(b) isotropic,

(c) homogeneous,

(d) elastic and obeys Hooke's Law.

Referring to Fig.4-1

Let r = x, and redefining the terms slightly,

$x = mH$

$z = nH$

Now taking Poisson's ratio $\mu = 0.5$ for soil, then Eq.(4-1) may be re-written as

$$\sigma_h = \frac{3V}{2\pi} \frac{m^2n^2}{(m^2+n^2)} \qquad \text{.....Eq.(4-2)}$$

The theoretical form of Eq.(4-2) requires adjustment when computing the lateral pressure against a rigid wall to make the equation values compare with the measured test values obtained by Terzaghi in his experiments in 1954.

4.3 - POINT LOAD PRESSURE

The problem for point load application was investigated by both Gerber and Spangler for which Eq.(4-2) was given coefficients which have been adjusted to make the theoretical agree with the measured pressures.

The equations are based on mH being the perpendicular distance to the wall, and nH, a point in the wall below the surface, as shown in Fig.4-2 and Fig4-3.

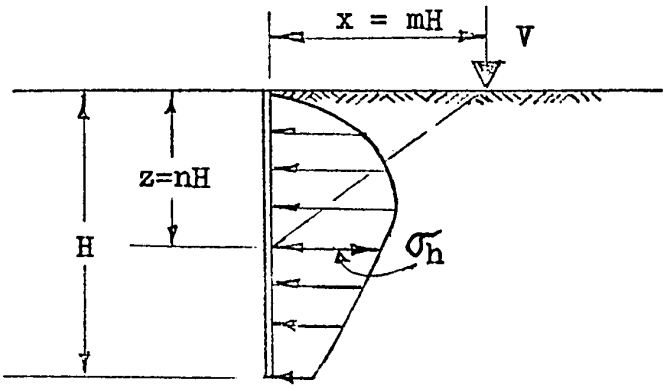

Fig.4-2 - Lateral pressure due to point load.

Case (a) - For $m \leq 0.4$:-

$$\sigma_h = \frac{0.28\ V}{H^2} \frac{n^2}{(0.16 + n^2)^3} \qquad \text{.....Eq.(4-3a)}$$

Case (b) - For $m > 0.4$:-

$$\sigma_h = \frac{1.77\ V}{H^2} \frac{m^2 n^2}{(m^2 + n^2)^3} \qquad \text{.....Eq.(4-3b)}$$

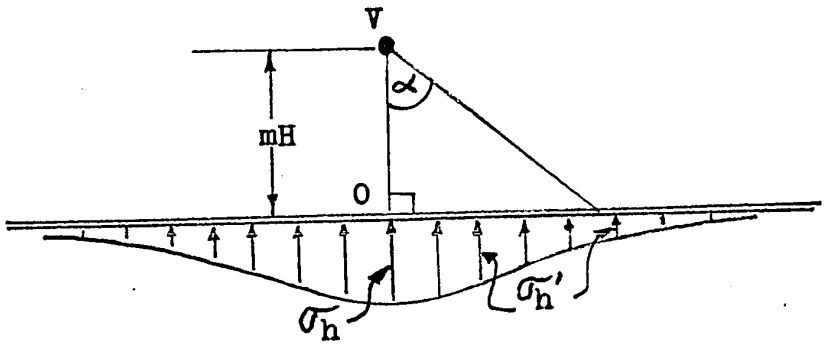

Fig.4-3 - Lateral Pressure at points along the wall on each side of perpendicular line V-0.

If the pressure intensity is desired at points on either side of the perpendicular line V-0 as shown in Fig.4-3, the intensity may be computed as

$$\sigma_h' = \sigma_h (\cos^2 1.1\alpha) \qquad \text{.....Eq.(4-4)}$$

where α = angle between V-0 and point for which σ_h' is desired,

σ_h' = intensity of pressure at point defined by angle α.

4.4 - LINE LOAD PRESSURE

A continuous narrow foundation wall, block wall and conduit laid on the ground are some examples which may be considered as line load.

Early attempt to calculate line load pressure was based on Coulomb's earth pressure theory that the intensity and the position of the centre of the pressure depend on the angle of internal friction ϕ and the angle of wall friction δ. This approach remained practically unchallenged until both the intensity and distribution of the lateral pressure were determined experimentally, also by Gerber and Spangler to show that Coulomb's theory is somewhat incompatible with the experimental result. There was however satisfactory agreement between the measured pressure and the theory of Boussinesq according to which

$$\sigma_h = \frac{2q}{\pi H} \frac{m^2 n}{(m^2 + n^2)^2} \qquad \text{.....Eq.(4-5)}$$

However, further experiments by Terzaghi (1954) showed that the measured values by tests were found to be approximately double the value given by Eq.(4-5). Therefore modifying, Eq.(4-5) becomes:

Case (a) - For $m > 0.4$:-

$$\sigma_h = \frac{4q}{\pi H} \frac{m^2 n}{(m^2 + n^2)^2} \qquad \text{.....Eq.(4-6a)}$$

Case (b) - For $m < 0.4$ (taking m as $m=0.4$ only):-

$$\sigma_h = \frac{q}{H} \frac{0.203\, n}{(0.16 + n^2)^2} \qquad \text{.....Eq.(4-6b)}$$

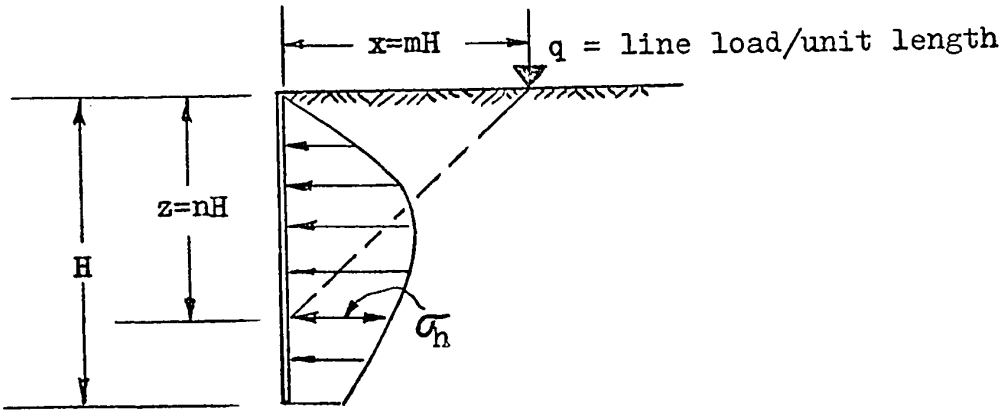

Fig.4-4 - Lateral pressure due to line load.

Wide strip loads may be considered as a series of parallel-loads. Therefore Eq.(4-6) may be used to calculate the lateral pressure from railway loading considering distribution of load on track as a series of parallel-line loads of equal intensity.

4.5 - STRIP LOAD PRESSURE

Loadings with finite width such as earth embankment, highway, railway, etc. which run parallel to the retaining wall may be considered as strip loads.

For this purpose, Terzaghi (1934)[2] presented an equation which he formulated using Boussinesq's equation for horizontal stress

$$\sigma_x = \frac{2\,q'}{\pi z}\cos^2\theta \sin^2\theta \qquad \text{.....Eq.(4-7)}$$

q' in the equation is considered as a line load per unit of the length of infinite extension on the surface as represented in Fig.4-5(a).

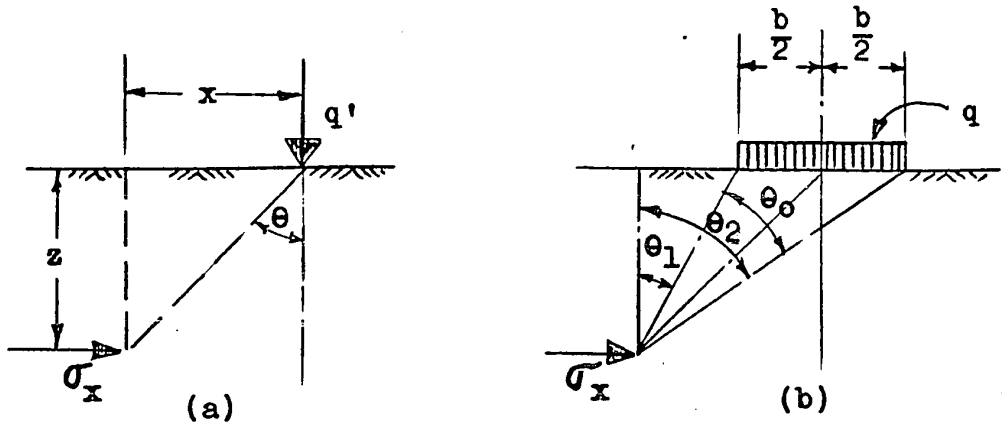

Fig.4-5 - (a) Line load,
(b) Strip load, acting on surface of semi-infinite solid material.

By intergration of Eq.(4-7) one obtains the horizontal stress due to a load q per unit of area on a strip of infinite length and a constant width b as represented in Fig.4-5(b). This results in an equation of the form:

$$\sigma_x = \frac{q}{\pi}\left[-\sin\theta\cos\theta + \theta\right]_{\theta_1}^{\theta_2} \quad \text{.....Eq.(4-8)}$$

Now, redefining the terms in Fig.4-5(b), and letting

$$\theta_o = \beta$$
$$\theta_1 = \alpha - \frac{\beta}{2}$$
$$\theta_2 = \alpha + \frac{\beta}{2}$$

Eq.(4-8) can be reduced to Terzaghi's form of equation which is:

$$\sigma_h = \frac{2q}{\pi}\left(\beta + \sin\beta\sin^2\alpha - \sin\beta\cos^2\alpha\right) \quad \text{...Eq.(4-9)}$$

where β is in radians and the other terms are defined in Fig.4-6, and $\sigma_h = \sigma_x$

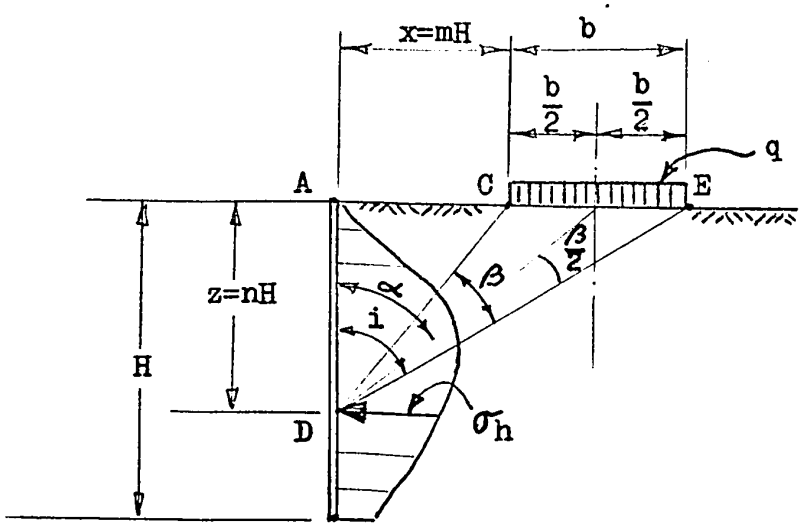

Fig.4-6 - Lateral Pressure due to strip load.

In Eq.(4-9), the values of β and α in terms of the parameters H, b, m and n may be obtained as follows:

Let distance $\overline{DE} = \sqrt{(mH + b)^2 + (nH)^2}$

$$= H\sqrt{(m + \frac{b}{H})^2 + n^2}$$

$$\overline{DC} = \sqrt{(mH)^2 + (nH)^2}$$

$$= H\sqrt{m^2 + n^2}$$

$$\sin i = \frac{\overline{AE}}{\overline{DE}}$$

$$= \frac{mH + b}{H\sqrt{(m + \frac{b}{H})^2 + n^2}}$$

$$= \frac{m + \frac{b}{H}}{\sqrt{(m + \frac{b}{H})^2 + n^2}}$$

Therefore, $$i = \sin^{-1}\left[\frac{m + \frac{b}{H}}{\sqrt{(m + \frac{b}{H})^2 + n^2}}\right] \quad \text{.....Eq.(4-10)}$$

$$\sin (i - \beta) = \frac{\overline{AC}}{\overline{DC}}$$

$$= \frac{mH}{H\sqrt{m^2 + n^2}}$$

$$= \frac{m}{\sqrt{m^2 + n^2}}$$

Hence, $$\beta = \sin^{-1}\left[\frac{m + \frac{b}{H}}{\sqrt{(m + \frac{b}{H})^2 + n^2}}\right] - \sin^{-1}\left[\frac{m}{\sqrt{m^2 + n^2}}\right] \quad \text{....Eq.(4-11)}$$

$$\alpha = i - \frac{\beta}{2}$$

Hence, $$\alpha = \frac{1}{2}\left\{\sin^{-1}\left[\frac{m + \frac{b}{H}}{\sqrt{(m + \frac{b}{H})^2 + n^2}}\right] + \sin^{-1}\left[\frac{m}{\sqrt{m^2 + n^2}}\right]\right\} \text{..Eq.(4-12)}$$

The strip load equations are particularly useful for calculating lateral pressure due to railway loading if the width "b" and an equivalent uniform load "q" are given.

5. LATERAL PRESSURE FROM RAILWAY LOADING

5.1 - GENERAL CONSIDERATION

Influence of railway cars and locomotives in static or moving positions on track structure and roadbed requires complex analyses. It depends on axle loads, wheel arrangement, stiffness of rails and ties, and the contact of the ties with soil beneath. The horizontal and vertical pressures created on the supporting soil are at best determined by generalization of the load distribution at the level of the ties.

Vibrations from railway traffic may increase the lateral pressure but such effects are not usually considered significant. Allowance for vibration however, is provided by making " δ " angle of wall friction equal to zero. Also, moving or braking cars and locomotives do subject the embankment and backfill to impact forces. However, the cushioning due to the large mass of earth in the embankment reduces this effect to such an extent that impact is not usually considered in calculating lateral pressure on the wall.

For most routine design purposes, railway loadings are usually taken from Manual of Recommended Practice, by Construction and Maintenance Division of the Association of American Railroads Chicago 1958. The Manual recommends that railway loading to have an equivalent surcharge of 10 ft. of fill over the track bed of 14 ft. width at top of the embankment slope.

However, for purpose of this study, a series of 100-ton ore cars,[12] each having gross weight of 263,000 lbs, is chosen and considered as giving the most severe loading condition on track. Each car consists of a set of axles at the front and at the back. The spacings between individual axles, and the overall length of the car between couplings are shown in Fig.5-1.

5.2 - EQUIVALENT RAILWAY LOADING

For the 100-ton ore cars, the most severe loading condition will come from combination of the back and front set of axles on each coupled pair of cars. These back-to-front combination of axles will therefore altogether exert load equal to the gross weight of one single car.

Under this loading condition, it seems reasonable to assume that the gross weight imposed on the track bed should spread uniformly over a restricted rectangular area of width equal to length of ties, and length equal to the distances covered by the four axles plus two tie spacings, as represented in Fig.5-1. One tie spacing beyond centre of each outer axle is considered because the influence of wheel reaction is not significant enough to be accounted for those ties beyond the outer adjacent tie.

Therefore, the loading from a series of 100-ton ore cars on track bed may be taken as equivalent to a series of rectangular loads of uniform intensity "q" per unit area, as shown in Fig.5-2.

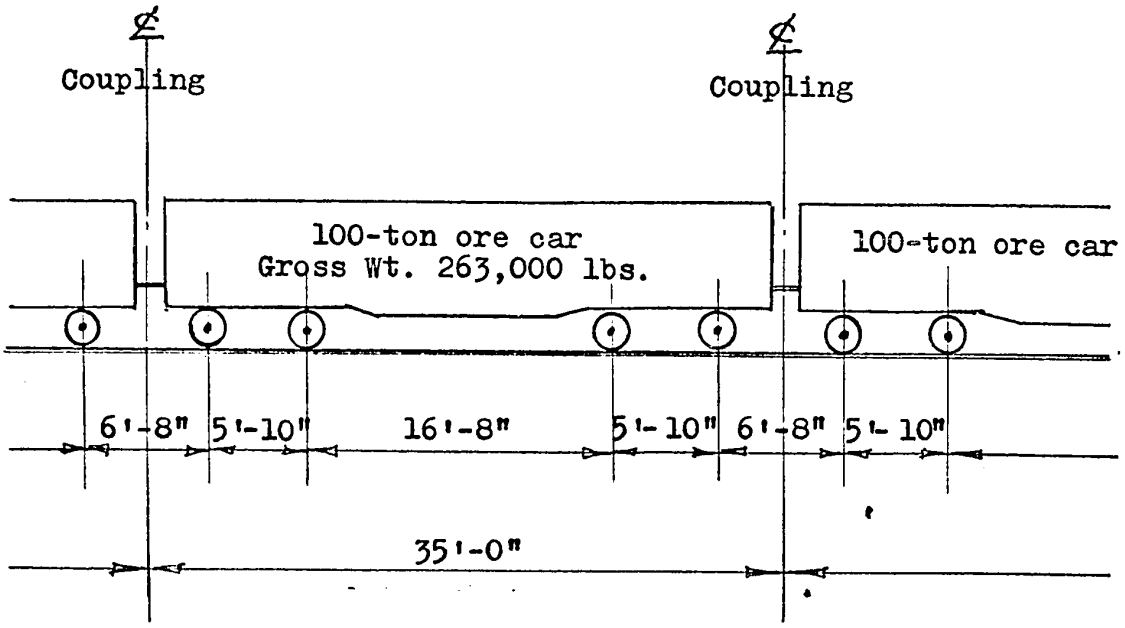

Fig.5-1 (a) Axle spacings of 100-ton ore car series.

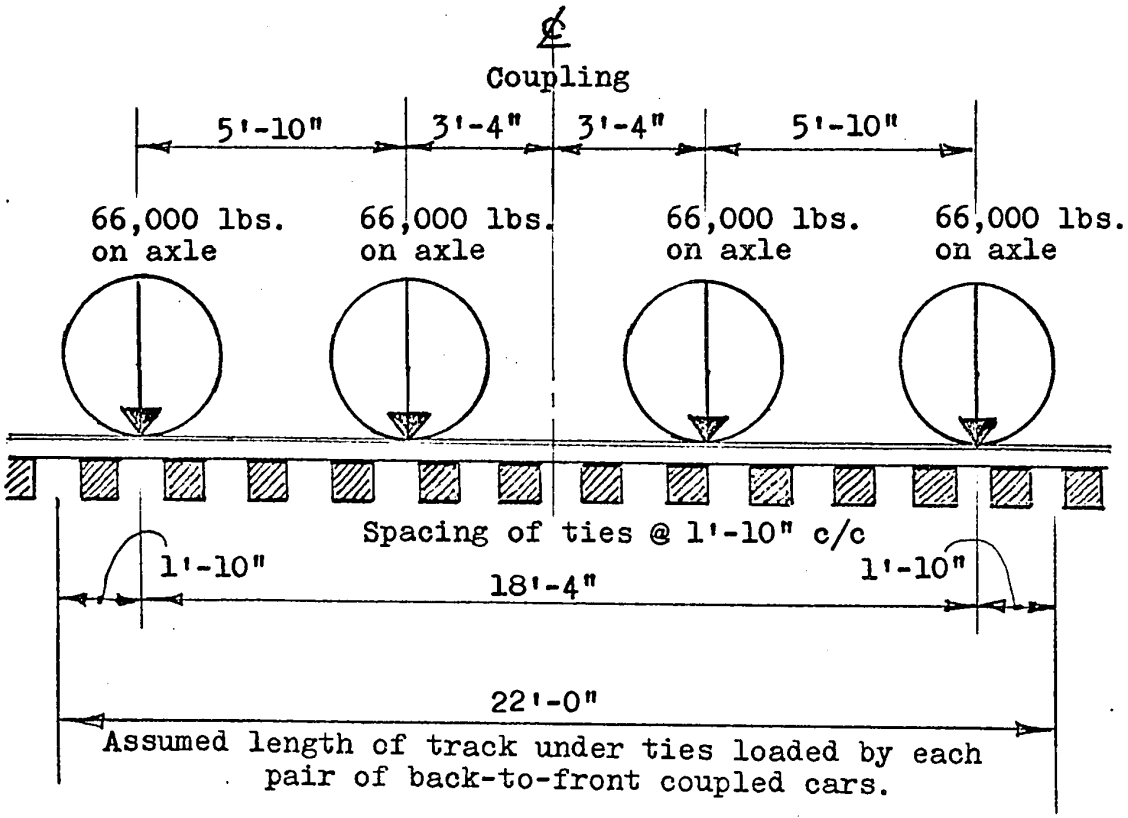

Fig.5-1 (b) Axle loadings and spacing of back-to-front coupled cars.

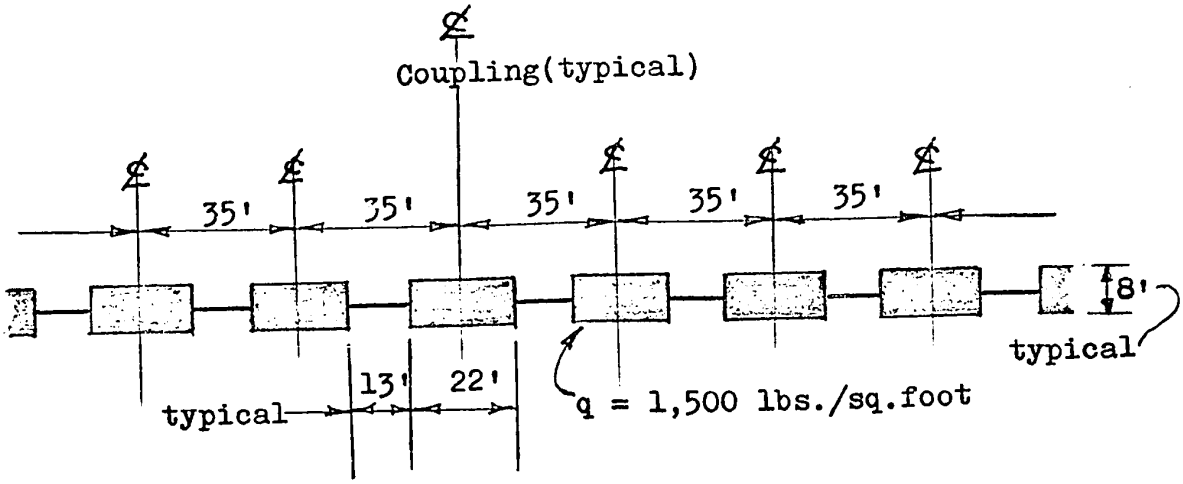

Fig.5-2 - Equivalent railway loading resulting from 100-ton ore car series.

To obtain "q", divide gross weight per car by area of one rectangular load. Thus,

$$q = \frac{263{,}000 \text{ lbs.}}{22' \times 8'}$$

$$= 1{,}489 \text{ lbs./sq.foot.}$$

$$\text{Use } q = 1{,}500 \text{ lbs./sq.foot.}$$

5.3 - COMPUTER SOLUTION OF LATERAL PRESSURE DISTRIBUTION

Lateral pressure on wall subjected to railway loading will be computed by the strip load method. A Fortran program is presented in Table 5-1 for the computation of the strip load Eq.(4-9)

$$\sigma_h = \frac{2q}{\pi}\left(\beta + \sin\beta \sin^2\alpha - \sin\beta \cos^2\alpha\right)$$

where

$$\beta = \sin^{-1}\left[\frac{m + \frac{b}{H}}{\sqrt{\left(m + \frac{b}{H}\right)^2 + n^2}}\right] - \sin^{-1}\left[\frac{m}{\sqrt{m^2 + n^2}}\right]$$

$$\alpha = \frac{1}{2}\left\{\sin^{-1}\left[\frac{m + \frac{b}{H}}{\sqrt{\left(m + \frac{b}{H}\right)^2 + n^2}}\right] + \sin^{-1}\left[\frac{m}{\sqrt{m^2 + n^2}}\right]\right\}$$

Computations are made for a 20 ft. high wall. Location of the tracks relative to the wall and other pertinent dimensions required for the computation are given in Fig.5-3 The results obtained for loading from each of the two tracks are displayed on Tables 5-2 and 5-3. The results are also plotted in Fig.5-4 to give the lateral pressure intensity curves which will be used for the numerical example given in Appendix B and for the design of the experimental model presented in Section 8.

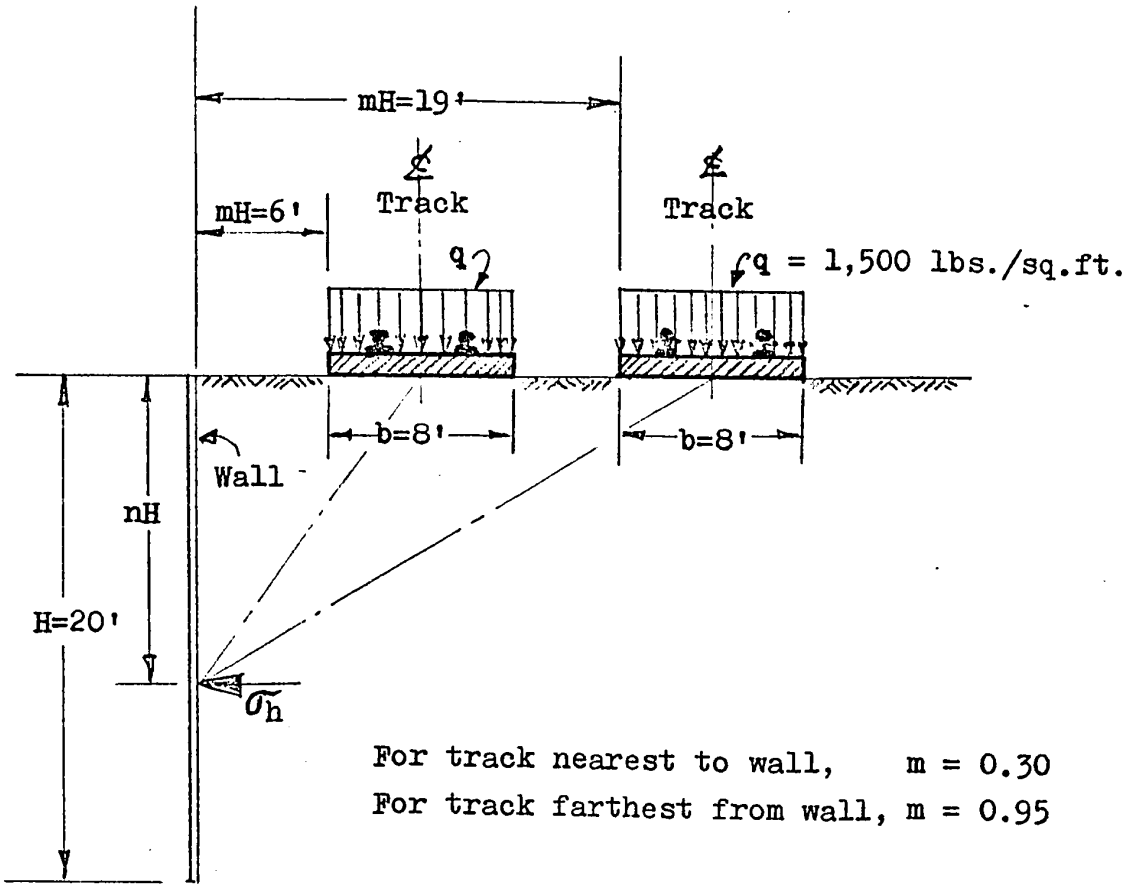

Fig.5-3 - Dimensions for loadings of two tracks.

```
      DIMENSION XXM(10)
      NT=0
      IT=1
      READ(5,5)NO,H,(XXM(I),I=1,NO)
5     FORMAT(I5,11F5.0)
      N=H
3     XM=XXM(IT)/H
      WRITE(6,4)H,XM
4     FORMAT(/////1X,'LATERAL PRESSURE FROM RAILWAY LOADING'//
     11X,'EQUIVALENT VERTICAL LOAD ON TRACK BED (Q)  1500 LB./SQ.FT.'/
     11X,'HEIGHT OF RETAINING WALL (H)',15X,F4.1,' FT.'/
     21X,'LENGTH OF TIES (B)',26X,'8.0 FT.'/
     31X,'DISTANCE FACTOR FROM EDGE OF TIE'/
     42X,'TO FACE OF WALL (M)',23X,F4.2//
     533X,'BETA',27X,'ALPHA',5X,'PRESSURE'/
     63X,'N',13X,'BETA',11X,'(RAD.)',10X,'ALPHA',10X,'(RAD.)',
     73X,'(LB./SQ.FT.)'/)
      XN=0.
      DO 1 I=1,N
      XN=XN+.05
      TERM1=ARSIN((XM+8./H)/SQRT((XM+8./H)**2+XN**2))
      TERM2=ARSIN(XM/SQRT(XM**2+XN**2))
      BETA=TERM1-TERM2
      ALPHA=(TERM1+TERM2)/2.
      DEGB=BETA*57.29578
      DEGA=ALPHA*57.29578
      THETA=3000./3.14159*(BETA+SIN(BETA)*(SIN(ALPHA)**2)-SIN(BETA)*
     1(COS(ALPHA)**2))
      NDEGB=DEGB
      XMINB=(DEGB-FLOAT(NDEGB))*60.
      MINB=XMINB
      NSECB=(XMINB-FLOAT(MINB))*60.
      NDEGA=DEGA
      XMINA=(DEGA-FLOAT(NDEGA))*60.
      MINA=XMINA
      NSECA=(XMINA-FLOAT(MINA))*60.
      WRITE(6,2)XN,NDEGB,MINB,NSECB,BETA,NDEGA,MINA,NSECA,ALPHA,
     1THETA
2     FORMAT(1X,F5.2,I7,' DEG.',I3,1H',I3,1H",F12.4,I7,' DEG.',I3,1H',
     1I3,1H",F11.4,F12.2)
1     CONTINUE
      IF(IT.EQ.NO)STOP
      IT=IT+1
      GO TO 3
      END
/DATA
    2  20.   6.  19.
*END

*GO
```

Table 5-1 - Fortran Program for Computation of Lateral Pressure From Strip Loads. (see Section 5.3 for equations)

LATERAL PRESSURE FROM RAILWAY LOADING

EQUIVALENT VERTICAL LOAD ON TRACK BED (Q)	1500 LB./SQ.FT.
HEIGHT OF RETAINING WALL (H)	20.0 FT.
LENGTH OF TIES (B)	8.0 FT.
DISTANCE FACTOR FROM EDGE OF TIE TO FACE OF WALL (M)	0.30

N	BETA	BETA (RAD.)	ALPHA	ALPHA (RAD.)	PRESSURE (LB./SQ.FT.)
0.05	5 DEG. 22' 35"	0.0938	83 DEG. 13' 33"	1.4526	176.60
0.10	10 DEG. 18' 17"	0.1799	76 DEG. 43' 2"	1.3390	324.53
0.15	14 DEG. 28' 12"	0.2526	70 DEG. 40' 12"	1.2334	427.50
0.20	17 DEG. 44' 40"	0.3097	65 DEG. 10' 56"	1.1376	484.23
0.25	20 DEG. 9' 6"	0.3517	60 DEG. 16' 13"	1.0519	503.03
0.30	21 DEG. 48' 4"	0.3805	55 DEG. 54' 2"	0.9757	495.07
0.35	22 DEG. 50' 0"	0.3985	52 DEG. 1' 5"	0.9079	470.44
0.40	23 DEG. 23' 6"	0.4081	48 DEG. 33' 45"	0.8476	436.77
0.45	23 DEG. 34' 28"	0.4115	45 DEG. 28' 38"	0.7937	399.28
0.50	23 DEG. 29' 54"	0.4101	42 DEG. 42' 46"	0.7455	361.28
0.55	23 DEG. 13' 56"	0.4055	40 DEG. 13' 35"	0.7021	324.73
0.60	22 DEG. 50' 1"	0.3985	37 DEG. 58' 54"	0.6629	290.69
0.65	22 DEG. 20' 45"	0.3900	35 DEG. 56' 53"	0.6274	259.62
0.70	21 DEG. 48' 5"	0.3805	34 DEG. 5' 57"	0.5951	231.64
0.75	21 DEG. 13' 25"	0.3704	32 DEG. 24' 47"	0.5657	206.68
0.80	20 DEG. 37' 47"	0.3601	30 DEG. 52' 15"	0.5388	184.54
0.85	20 DEG. 1' 56"	0.3496	29 DEG. 27' 22"	0.5141	164.97
0.90	19 DEG. 26' 24"	0.3393	28 DEG. 9' 17"	0.4914	147.71
0.95	18 DEG. 51' 31"	0.3291	26 DEG. 57' 17"	0.4705	132.49
1.00	18 DEG. 17' 34"	0.3193	25 DEG. 50' 44"	0.4511	119.08

Table 5-2 - Computer results of lateral pressure from railway loading - for track nearest to wall.

LATERAL PRESSURE FROM RAILWAY LOADING

EQUIVALENT VERTICAL LOAD ON TRACK BED (Q)	1500 LB./SQ.FT.
HEIGHT OF RETAINING WALL (H)	20.0 FT.
LENGTH OF TIES (B)	8.0 FT.
DISTANCE FACTOR FROM EDGE OF TIE TO FACE OF WALL (M)	0.95

N	BETA	BETA (RAD.)	ALPHA	ALPHA (RAD.)	PRESSURE (LB./SQ.FT.)
0.05	0 DEG. 53' 31"	0.0156	87 DEG. 26' 0"	1.5260	29.68
0.10	1 DEG. 46' 23"	0.0309	84 DEG. 52' 39"	1.4814	58.63
0.15	2 DEG. 37' 58"	0.0460	82 DEG. 20' 37"	1.4372	86.19
0.20	3 DEG. 27' 42"	0.0604	79 DEG. 50' 32"	1.3935	111.78
0.25	4 DEG. 15' 8"	0.0742	77 DEG. 22' 57"	1.3506	134.92
0.30	4 DEG. 59' 48"	0.0872	74 DEG. 58' 22"	1.3085	155.27
0.35	5 DEG. 41' 25"	0.0993	72 DEG. 37' 13"	1.2675	172.63
0.40	6 DEG. 19' 45"	0.1105	70 DEG. 19' 51"	1.2275	186.91
0.45	6 DEG. 54' 40"	0.1206	68 DEG. 6' 34"	1.1887	198.15
0.50	7 DEG. 26' 7"	0.1298	65 DEG. 57' 33"	1.1512	206.48
0.55	7 DEG. 54' 7"	0.1379	63 DEG. 52' 57"	1.1150	212.11
0.60	8 DEG. 18' 47"	0.1451	61 DEG. 52' 51"	1.0800	215.28
0.65	8 DEG. 40' 13"	0.1513	59 DEG. 57' 17"	1.0464	216.29
0.70	8 DEG. 58' 36"	0.1567	58 DEG. 6' 14"	1.0141	215.42
0.75	9 DEG. 14' 7"	0.1612	56 DEG. 19' 39"	0.9831	212.96
0.80	9 DEG. 27' 0"	0.1649	54 DEG. 37' 27"	0.9534	209.19
0.85	9 DEG. 37' 27"	0.1680	52 DEG. 59' 31"	0.9249	204.37
0.90	9 DEG. 45' 42"	0.1704	51 DEG. 25' 44"	0.8976	198.73
0.95	9 DEG. 51' 56"	0.1722	49 DEG. 55' 58"	0.8715	192.46
1.00	9 DEG. 56' 23"	0.1735	48 DEG. 30' 4"	0.8465	185.76

Table 5-3 - Computer results of lateral pressure from railway loading - for track furthest from wall.

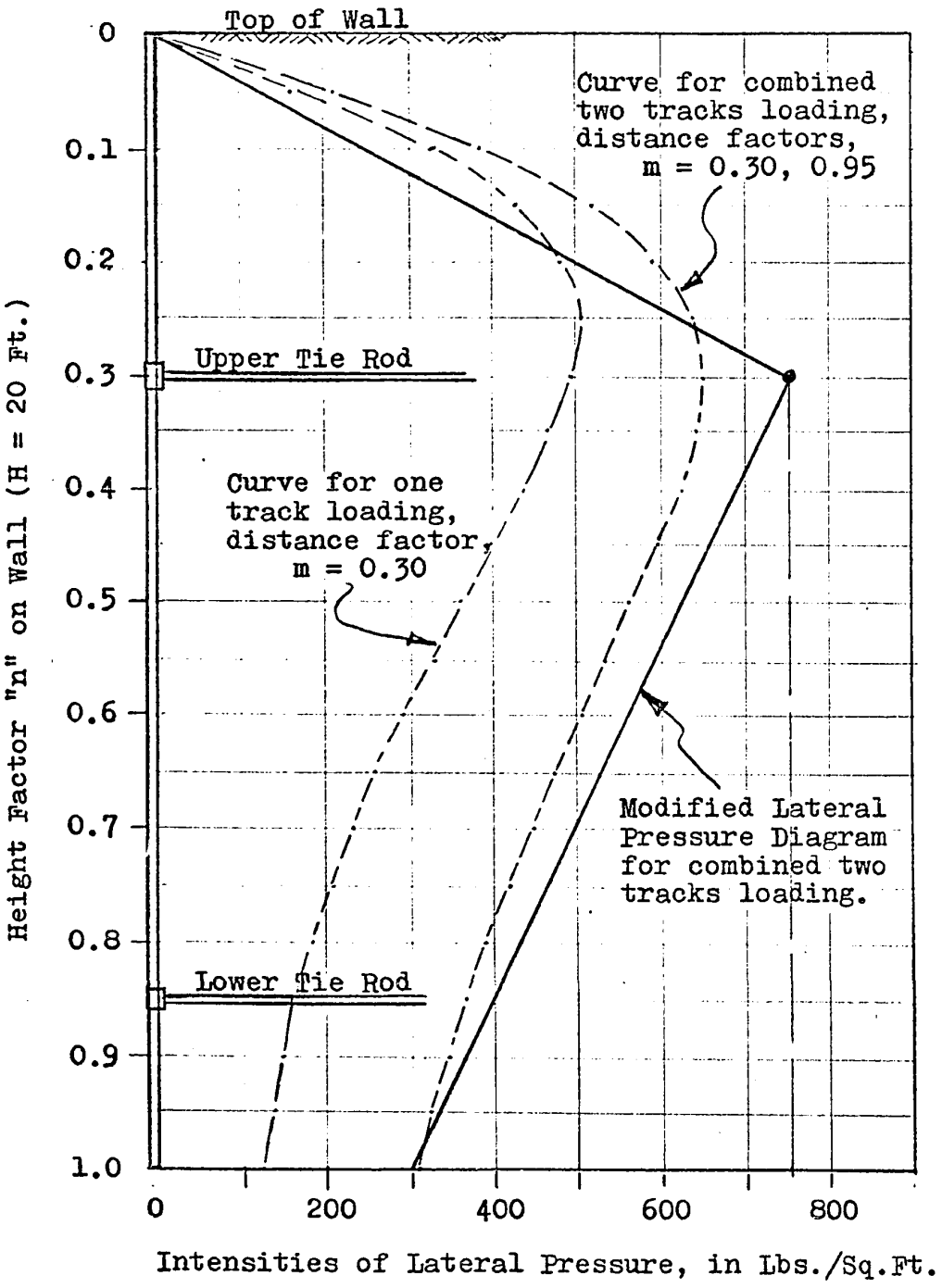

Fig.5-4 Curves for Lateral Pressure Intensities by Railway Loading on Wall, H = 20 Ft.

6. THEORETICAL ANALYSIS CONSIDERING LATERAL PRESSURE FROM RAILWAY LOADING

6.1 - DEFINITIONS AND ASSUMPTIONS

The analysis will base on the same embankment and retaining wall system shown in Fig.3-1(a), taking similar analytical assumptions as for earth pressure analysis. Railway tracks will be located parallel to the wall, with the outside track at a minimum allowable distance from the back of the wall. The bottom of ties is assumed at the level of top of the wall. General arrangement of the tracks to the wall is shown in Fig.6-1(a).

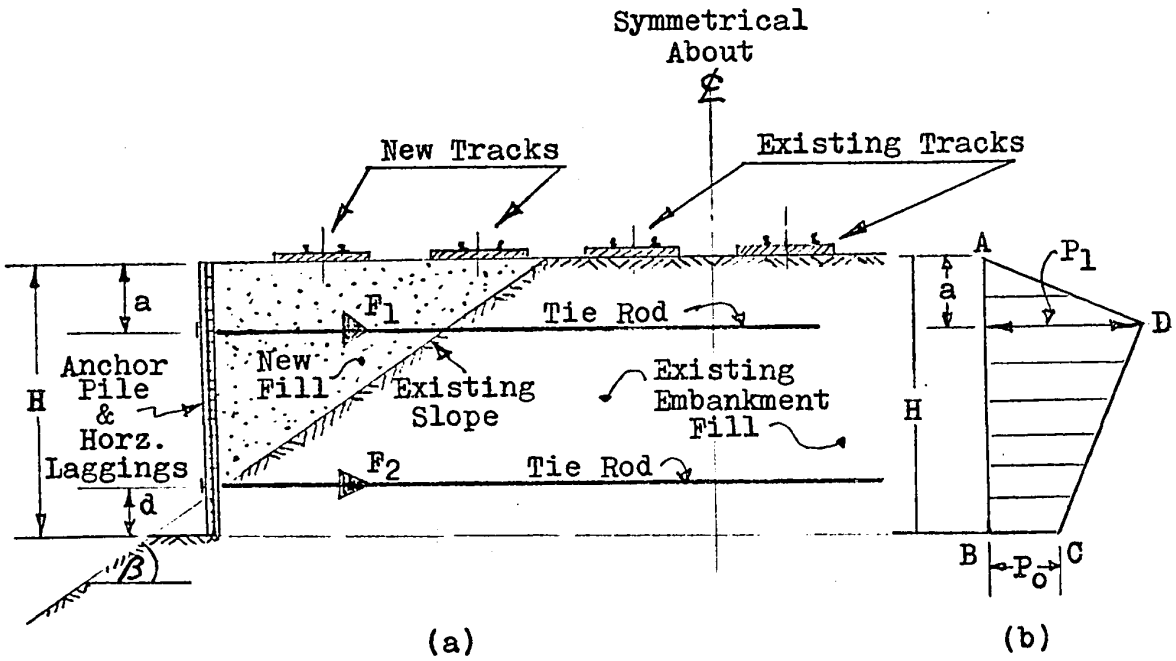

Fig.6-1 - (a) Typical retaining wall system with tracks,
(b) Modified diagram for lateral pressure from railway loading.

From the numerical results computed in Section 5.3, because of the characteristic of the equation for lateral pressure from strip loading (similarly for equations for line load), it can be observed that the general curve derived, whether for one track or two tracks, will more or less take on similar shape. In order to develop general design equations, it seems reasonable as well as desirable to lineally modify the shape of the pressure diagram to be used for the wall, so that a simplified and more practical analysis can be carried out.

The degree of approximation involved in the simplified representation may be judged by comparing the curves shown in Fig.5-4. It can be observed that the depth of maximum intensity of lateral pressure on the wall occurs in direct function with the distance of the nearest tie from the back of the wall. This is illustrated by the curves that when the edge of the nearest tie is at a minimum distance of 6 ft. from the back of the wall, maximum intensity of lateral pressure on the wall would occur in the depth region of 6 ft. For this reason, a modified pressure diagram ADCB as shown in Fig.6-1(b) is assumed for the analysis. The maximum intensity line through apex D of the diagram will coincide with the level of the upper anchor rod. In adjusting or modifying, the pressure distribution above the apex line may generally assume a lower value, but that below the apex line could take on a slightly higher value.

6.2 - EQUIVALENT DIAGRAM FOR LATERAL PRESSURE

The magnitude of the pressure diagram will be a function of the maximum intensity of lateral pressure σ_1 through apex

line at D and the lateral pressure σ_o at the base of the wall along line BC. The modified pressure diagram thus obtained and represented in Fig.6-1(b) should be applicable to loadings from either one track only or two tracks.

Let 's' be the spacing between anchor piles. Then the resulting reaction from horizontal laggings on anchor pile at depth 'a' will be: $\sigma_1 s = P_1$ .....Eq.(6-1a)

and that at depth 'H' will be:

$$\sigma_o s = P_o \quad \text{.....Eq.(6-1b)}$$

The pressure lines for P_1 and P_o are represented in Fig.6-1(b).

6.3 - EQUIVALENT BEAM METHOD

Similar method of analysis as discussed in Section 3-3, treating the anchor pile as an equivalent beam will be used. In this case, the beam will be loaded with the pressure diagram ADCB and supported at anchor rod points R_1 and R_2 as shown in Fig.6-2

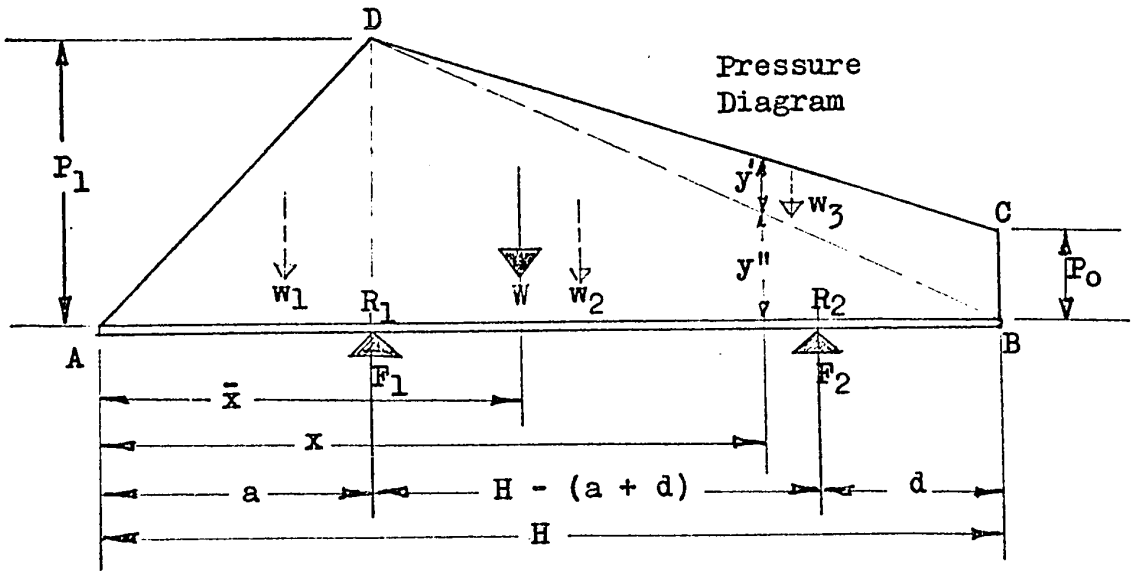

Fig.6-2 - Equivalent beam loaded with diagram of lateral pressure from Railway Loading.

Similarly, equations for tie rod forces, shear, bending moment and deflection are derived using static and simple beam theory.

Let load represented by ΔADR_1 be $w_1 = \frac{P_1 a}{2}$

ΔDBR_1 be $w_2 = \frac{P_1(H - a)}{2}$

ΔDCB be $w_3 = \frac{P_o(H - a)}{2}$

Then, total load of pressure diagram ADCB is:

$$W = w_1 + w_2 + w_3$$

By substituting for values of w_1, w_2 and w_3, and simplifying,

$$W = \tfrac{1}{2}\left[H(P_1 + P_o) - aP_o\right] \quad \text{.....Eq.(6-2)}$$

Distance of centre of gravity of pressure diagram ADCB from point A on the beam is:

$$\bar{x} = \frac{w_1 \frac{2}{3}a + (a + \frac{H - a}{3})w_2 + a + \frac{2(H - a)}{3} w_3}{W}$$

Again, by substituting for values of w_1, w_2 and w_3, and simplifying,

$$\bar{x} = \frac{\left[aH(P_1 - P_o) + H^2(P_1 + 2P_o) - a^2P_o\right]}{W} \quad \text{... Eq.(6-3)}$$

6.4 - FORCES IN TIE RODS

Take moments about point R_2,

$$F_1(H - a - d) = \left[(H - d) - \bar{x}\right] W$$

Hence, $$F_1 = \frac{\left[(H - d) - \bar{x}\right] W}{(H - a - d)} \quad \text{..... Eq.(6-4)}$$

Similarly, take moments about point R_1,

$$F_2(H - a - d) = (\bar{x} - a)W$$

Hence, $$F_2 = \frac{(\bar{x} - a)W}{(H - a - d)} \quad \text{.....Eq.(6-5)}$$

6.5 - SHEAR IN ANCHOR PILE

Let S be the shear at any point x along the beam AB.

Case (a) - for x = 0 to x = a :-

$$\text{Since } P_x = \frac{P_1 x}{a},$$

$$S = \frac{P_x x}{2}.$$

$$\text{Hence } S = \frac{P_1 x^2}{2a} \quad \ldots\ldots\ldots\ldots\ldots\ldots \text{ Eq.(6-6a)}$$

Case (b) - for x = a to x = H - d :-

$$\text{Let } y' = \frac{(x - a)}{(H - a)} P_o$$

$$y'' = \frac{(H - x)}{(H - a)} P_1$$

$$\text{Then } S = \frac{(x - a)}{2} (y' + y'' + P_1) + \frac{P_1 a}{2} - F_1$$

By substituting for the values of y' and y'', and simplifying,

$$S = \frac{(x - a)}{2(H - a)} 2HP_1 - a(P_1 + P_o) - x(P_1 - P_o) + \frac{P_1 a}{2} - F_1 \quad \ldots\ldots\ldots\ldots\ldots \text{ Eq.(6-6b)}$$

Case (c) - for x = H - d to x = H :-

$$S = \frac{(x - a)}{2(H - a)} 2HP_1 - a(P_1 + P_o) - x(P_1 - P_o) + \frac{P_1 a}{2} - F_1 - F_2 \quad \ldots\ldots\ldots\ldots \text{ Eq.(6-6c)}$$

6.6 - BENDING MOMENT IN ANCHOR PILE

Let M be the bending moment at any point x along the beam AB.

Case (a) - for x = 0 to x = a :-

$$\text{Since } P_x = \frac{P_1 x}{a},$$

$$M = P_x \cdot \frac{x}{2} \cdot \frac{x}{3} .$$

Hence, $$M = \frac{P_1 x^3}{6a} \quad \ldots\ldots\ldots\ldots\ldots\ldots\ldots \text{Eq.(6-7a)}$$

Case (b) - for x = a to x = H - d :-

Since $$y' = \frac{(x - a)}{(H - a)} P_o$$

$$y'' = \frac{(H - x)}{(H - a)} P_1$$

then $$M = \frac{P_1 a}{2}(x - \frac{2}{3}a) - F_1(x - a) + \frac{P_1}{2}(x - a) \cdot \frac{2}{3}(x - a)$$

$$+ (y' + y'') \cdot \frac{(x - a) \cdot (x - a)}{2} \frac{}{3} .$$

By subsituting for the values of y' and y", and simplifying,

$$M = \frac{P_1 a}{2}(x - \frac{2}{3}a) - F_1(x - a) + \frac{P_1}{3}(x - a)^2$$

$$+ \frac{P_1 (H - x)(x - a)^2}{6(H - a)} + \frac{P_o (x - a)^3}{6(H - a)} \quad \ldots\ldots \text{Eq.(6-7b)}$$

Case (c) - for x = H - d to x = H :-

Extending Eq.(6-7b) for this case, and letting (H - d) = k,

$$M = \frac{P_1 a}{2}(x - \frac{2}{3}a) - F_1(x - a) + \frac{P_1}{3}(x - a)^2$$

$$+ \frac{P_1 (H - x)(x - a)^2}{6(H - a)} + \frac{P_o (x - a)^3}{6(H - a)} - F_2(x - k) \ldots$$

$$\ldots\ldots\ldots \text{Eq.(6-7c)}$$

6.7 - MAXIMUM BENDING MOMENT IN ANCHOR PILE

Maximum positive bending moment will occur at zero shear between points R_1 and R_2. To find location of zero shear, differentiate the bending moment equation for Case (b) and equate to zero. For this purpose, Eq.(6-7b) may be re-written in the form of:

$$M = \frac{P_1 a}{2}(x - \frac{2}{3}a) - F_1(x - a) + \frac{P_1}{3}(x^2 - 2ax + a^2)$$
$$+ \frac{P_1}{6(H - a)}\left[Hx^2 - 2axH + a^2H - x^3 + 2ax^2 - a^2x\right]$$
$$+ \frac{P_o}{6(H - a)}\left[x^3 - 3ax^2 + 3a^2x - a^3\right]$$

$$\frac{dM}{dx} = \frac{P_1 a}{2} - F_1 + \frac{2P_1}{3}x - \frac{2aP_1}{3}$$
$$+ \frac{P_1}{6(H - a)}\left[2Hx - 2Ha - 3x^2 + 4ax - a^2\right]$$
$$+ \frac{P_o}{6(H - a)}\left[3x^2 - 6ax + 3a^2\right]$$

$$= 0$$

By simplifying and sorting out the x^2 and x, therefore

$$3(P_1 - P_o)x^2 - 6(P_1H - P_oa)x + 3P_1aH + 6F_1(H - a) - 3P_oa^2 = 0$$

Substituting x = h for location of maximum moment, therefore

$$h^2 - \left[\frac{2(P_1H - P_oa)}{(P_1 - P_o)}\right]h + \left[\frac{P_1aH + 2F_1(H - a) - P_oa^2}{(P_1 - P_o)}\right] = 0$$

..... Eq.(6-8)

Eq.(6-8) is a quadratic equation from which the location of maximum bending moment 'h' can be determined.

$$\text{Hence, } M_{max} = \frac{P_1 a}{2}(h - \frac{2}{3}a) - F_1(h - a) + \frac{P_1}{3}(h - a)^2$$
$$+ \frac{P_1(H - h)(h - a)^2}{6(H - a)} + \frac{P_o(h - a)^2}{6(H - a)} \quad \text{..... Eq.(6-9)}$$

6.8 - DEFLECTION OF ANCHOR PILE

Let y be the deflection at any point x along the beam AB. Then the deflection is obtained by integrating the equation of deflection: $\frac{d^2y}{dx^2} = -\frac{M}{EI}$ using the bending moment equations derived in Section 6.6.

Case (a) - for x = 0 to x = a :-

Since $M = \frac{P_1 x^3}{6a}$, therefore

$$\frac{d^2y}{dx^2} = -\frac{1}{EI}\cdot\frac{P_1 x^3}{6a}$$

$$\frac{dy}{dx} = -\frac{1}{EI}\cdot\frac{P_1}{6a}\left[\frac{x^4}{4} + C_1\right]$$

$$y = -\frac{1}{EI}\cdot\frac{P_1}{6a}\left[\frac{x^5}{20} + C_1 x + C_2\right] \quad \ldots\ldots\ldots\ldots\ldots \text{Eq.(6-10a)}$$

The constants of integration C_1 and C_2 are obtained as follows:-

At x = a, $\frac{dy}{dx} = 0$, and therefore,

$$C_1 = -\frac{a^4}{4}.$$

At x = a, y = 0, and therefore,

$$C_2 = \frac{1}{5}a^5$$

Case (b) - for x = a to x = H - d :-

$$\frac{d^2y}{dx^2} = -\frac{M}{EI}$$

$$= -\frac{1}{EI}\left\{\left[\frac{P_1 a}{2}\left(x - \frac{2}{3}a\right) - F_1(x - a) + \frac{P_1}{3}(x^2 - 2ax + a^2)\right.\right.$$

$$+ \frac{P_1}{6(H - a)}\left[Hx^2 - 2axH + a^2H - x^3 + 2ax^2 - a^2x\right]$$

$$\left.\left. + \frac{P_o}{6(H - a)}\left[x^3 - 3ax^2 + 3a^2x - a^3\right]\right\}$$

Integrating, therefore,

$$\frac{dy}{dx} = -\frac{1}{EI}\left\{\left[\frac{P_1 a}{2}\left(\frac{x^2}{2} - \frac{2}{3}ax\right) - F_1\left(\frac{x^2}{2} - ax\right) + \frac{P_1}{3}\left(\frac{x^3}{3} - ax^2 + a^2x\right)\right.\right.$$

$$+\frac{P_1}{6(H-a)}\left[\frac{Hx^3}{3}-Hax^2+Ha^2x-\frac{x^4}{4}+\frac{2}{3}ax^3-\frac{a^2x^2}{2}\right]$$
$$+\frac{P_o}{6(H-a)}\left[\frac{x^4}{4}-ax^3+\frac{3}{2}a^2x^2-a^3x\right]+C_1\Bigg\}$$

$$y=-\frac{1}{EI}\Bigg\{\frac{P_1a}{2}\left(\frac{x^3}{6}-\frac{ax^2}{3}\right)-F_1\left(\frac{x^3}{6}-\frac{ax^2}{2}\right)+\frac{P_1}{3}\left(\frac{x^4}{12}-\frac{ax^3}{3}+\frac{a^2x^2}{2}\right)$$
$$+\frac{P_1}{6(H-a)}\left[\frac{Hx^4}{12}-\frac{Hax^3}{3}+\frac{Ha^2x^2}{2}-\frac{x^5}{20}+\frac{ax^4}{6}-\frac{a^2x^3}{6}\right]$$
$$+\frac{P_o}{6(H-a)}\left[\frac{x^5}{20}-\frac{ax^4}{4}+\frac{a^2x^3}{2}-\frac{a^3x^2}{2}\right]+C_1x+C_2\Bigg\}$$

..... Eq.(6-10b)

The constants of integration C_1 and C_2 are obtained as follows:-
Since maximum positive bending moment occurs at point 'h', therefore

at $x = h$, $\frac{dy}{dx} = 0$.

Hence, $$C_1=\frac{P_1h^2}{3}\left(\frac{a}{4}-\frac{h}{3}\right)+F_1h\left(\frac{h}{2}-a\right)$$
$$-\frac{P_1h}{6(H-a)}\left[Hh\left(\frac{h}{3}-a\right)+a^2\left(H-\frac{h}{2}\right)-h^2\left(\frac{h}{4}-\frac{2a}{3}\right)\right]$$
$$-\frac{P_oh}{6(H-a)}\left[\frac{h^3}{4}-ah^2+\frac{3}{2}a^2h-a^3\right]$$

At $x = a$, $y = 0$, and therefore,

$$C_2=-F_1\frac{a^3}{3}-\frac{P_1a^4}{24(H-a)}\left[H-\frac{a}{5}\right]+\frac{P_oa^5}{30(H-a)}-C_1a$$

Case (c) - for $x = H - d$ to $x = H$:-

The deflection for this case can be conveniently derived by appropriate extension of Case (b) above, using Eq.(6-7c) and setting limiting conditions $\frac{dy}{dx} = 0$ and $y = 0$ for $x = k$.

7. DERIVATION OF EQUATIONS FOR DESIGN OF MODEL

7.1 - DEFINITIONS AND ASSUMPTIONS

The experimental study will use a model designed geometrically similar to the retaining wall system given in the numerical examples in Appendices A and B. To develop model design equations,[3][4] a scale factor λ will be used to scale down all principal dimensions of the prototype using equations derived in Sections 3 and 6.

The principal dimensions of the model scaled down by the factor λ are designated as: H_m, a_m, d_m, x_m, s_m, B_m, and L_m. Therefore,

$$H_m = \lambda H, \qquad s_m = \lambda s$$
$$a_m = \lambda a \qquad B_m = \lambda B$$
$$d_m = \lambda d \qquad L_m = \lambda L$$
$$x_m = \lambda x$$

The same backfill material for the prototype will be used for the model, and therefore,

$$\gamma_m = \gamma$$
$$K_{am} = K_a = \frac{1 - \sin \phi}{1 + \sin \phi} \quad \text{since } \phi \text{ is dimensionless.}$$

7.2 - MODEL EQUATIONS FOR EARTH PRESSURE ONLY

Lateral earth pressure on horizontal laggings:

Let $p_b = \gamma H K_a$ ..... for the prototype

$p_{bm} = \gamma_m H_m K_{am}$ ..... for the model

Substituting the required values given in Section 7.1 into the equation for the model,

$$p_{bm} = \lambda p_b \qquad \text{..... Eq.(7-1)}$$

Maximum bending moment in horizontal laggings:

Let $M = \frac{p_b s^2}{8}$ ..... for the prototype

$M_m = \frac{p_{bm} s_m^2}{8}$ ..... for the model.

Substituting the required values given in Section 7.1 into the equation for the model,

$$M_m = \lambda^3 M \qquad \text{.....Eq.(7-2)}$$

Lateral pressure on anchor pile:

Let $P_b = \gamma H K_a s$ .... for the prototype, by Eq.(3-1)

$P_{bm} = \gamma_m H_m K_{am} s_m$ .. for the model.

Substituting the required values given in Section 7.1 into the equation for the model,

$$P_{bm} = \lambda^2 P_b \qquad \text{.....Eq.(7-3)}$$

Forces in tie rods:

Let $F_1 = \frac{P_b H}{6} \frac{(H - 3d)}{(H - a - d)}$ .... for the prototype, Eq.(3-2)

$F_{1m} = \frac{P_{bm} H_m}{6} \frac{(H_m - 3d_m)}{(H_m - a_m - d_m)}$ for the model.

Substituting the required values given in Section 7.1 into the equation for the model,

$$F_{1m} = \lambda^3 F_1 \qquad \text{.....Eq.(7-4)}$$

Similarly,

$$F_{2m} = \lambda^3 F_2 \qquad \text{.....Eq.(7-5)}$$

Shear in anchor pile:

Let $S = \frac{P_b x^2}{2H}$ .... for the prototype, by Eq.(3-4a)

$S_m = \frac{P_{bm} x_m^2}{2 H_m}$ .... for the model.

Substituting the required values given in Section 7.1 into the equation for the model,

$$S_m = \lambda^3 S \qquad \text{..... Eq.(7-6)}$$

Bending moment in anchor pile:

Let $M = \frac{P_b x^3}{6H}$ .... for the prototype, by Eq.(3-5a)

$M_m = \frac{P_{bm} x_m^3}{6H_m}$ .... for the model.

Substituting the required values given in Section 7.1 into the equation for the model,

$$M_m = \lambda^4 M \qquad \text{..... Eq.(7-7)}$$

Deflection in anchor pile:

Let $y = -\frac{1}{EI} \cdot \frac{P_b}{6H} \left[\frac{x^5}{20} - \frac{a^4 x}{4} + \frac{a^5}{5} \right]$ ... for the prototype, by Eq.(3-8a)

$y_m = -\frac{1}{E_m I_m} \cdot \frac{P_{bm}}{6H_m} \left[\frac{x_m^5}{20} - \frac{a_m^4 x_m}{4} + \frac{a_m^5}{5} \right]$ for the model.

Substituting the required values given in Section 7.1 into the equation for the model,

$$y_m = -\lambda^6 \frac{E\ I}{E_m\ I_m} y \qquad \text{..... Eq.(7-8)}$$

7.3 - MODEL EQUATIONS FOR EQUIVALENT RAILWAY LOADING

Equivalent load on track:

Consider the section of track with uniform strip load as shown in Fig.7-1.

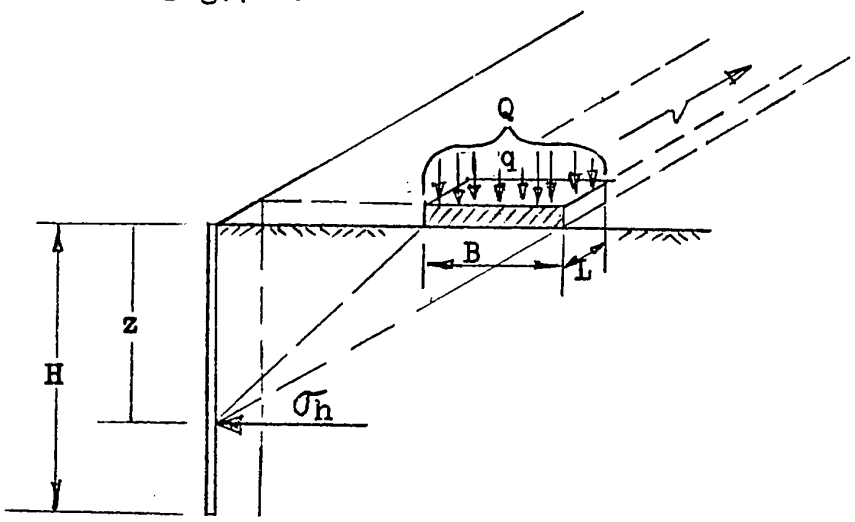

Fig.7-1 - Section of continuous strip load on track.

Let q = load intensity per unit area on prototype,

B = length of railway tie, or width of strip load,

L = unit length of strip load

ν = scale factor for load intensity, or

$q_m = \nu q$ for the model. ..... Eq.(7-9)

Then $Q = BLq$ ..... for the prototype,

$Q_m = B_m L_m q_m$ ..... for the model.

Substituting the required values given in Section 7.1 into the equation for the model,

$$Q_m = \nu \lambda^2 Q \quad \text{..... Eq.(7-10)}$$

Lateral pressure:

Let $\sigma_h = \frac{2q}{\pi}(\beta + \sin\beta\sin^2\alpha - \sin\beta\cos^2\alpha)$ ...

... for the prototype, Eq(4-9)

All terms in Eq.(4-9) except q are dimensionless.

Since $q_m = \nu q$, therefore

$\sigma_{hm} = \nu\sigma_h$ for the model ..... Eq.(7-11)

Maximum bending moment in horizontal laggings:

Let $M = \frac{\sigma_h s^2}{8}$ ..... for the prototype,

$M_m = \frac{\sigma_{hm} s_m^2}{8}$ ..... for the model

Substituting the required values obtained in this Section into the equation for the model,

$M_m = \nu\lambda^2 M$ ..... Eq.(7-12)

Lateral pressure on anchor pile:

Let $P_1 = \sigma_1 s$ ..... for the prototype, by Eq.(6-1a)

$P_{1m} = \sigma_{1m} s_m$ ..... for the model.

Substituting the required values obtained in this Section into the equation for the model,

$P_{1m} = \nu\lambda P_1$ .....Eq.(7-13)

Similarly,

$P_{om} = \nu\lambda P_o$ .....Eq.(7-14)

Forces in tie rods:

Since $W = \frac{1}{2}\left[H(P_1 + P_o) - aP_o\right]$ for prototype, by Eq.(6-2), it will be seen that by substitution of Eqs.(7-13) and (7-14) that

$W_m = \nu\lambda^2 W$ .....Eq.(7-15)

Also, $\bar{x}_m = \lambda \bar{x}$

$F_2 = \dfrac{(x - a)W}{(H - a - d)}$ for prototype, by Eq.(6-5),

$F_{2m} = \dfrac{(x_m - a_m)W_m}{(H_m - a_m - d_m)}$ for model.

Substituting the required values obtained in this section into the equation for the model,

$$F_{2m} = \nu\lambda^2 F_2 \quad \text{..... Eq(7-16)}$$

Similarly,

$$F_{1m} = \nu\lambda^2 F_1 \quad \text{..... Eq.(7-17)}$$

Shear in anchor pile:

This is derived by using Eq.(6-6a) and substituting required values obtained in this section, and therfore

$$S_m = \nu\lambda^2 S \quad \text{..... Eq.(7-18)}$$

Bending moment in anchor pile:

This is derived by using Eq.(6-7a) and substituting required values obtained in this section , and therefore

$$M_m = \nu\lambda^3 M \quad \text{.....Eq.(7-19)}$$

Deflection in anchor pile:

This is derived by using Eq.(6-10a) and substituting required values obtained in this section, and therefore

$$y_m = -\nu\lambda^5 \frac{E\ I}{E_m\ I_m} y \quad \text{..... Eq.(7-20)}$$

8. EXPERIMENTAL PROGRAM

8.1 - GENERAL CONSIDERATION

The most important structural component of the model to be investigated in this experiment is the anchor pile. It is required to measure the deflections of the pile compared to those derived by theory, and to assess the stability of the entire wall system. Various materials[3] have been investigated for the anchor pile.

An examination of the curves for anchor pile presented in Fig.8-1 shows that wood is the preferred material considering its flexural strength necessary to withstand combined laterial pressures but flexible enough for measurable deflection on anchor pile due to railway loading only.

The material chosen is prefabricated yellow pine wood strips of small rectangular sections. Only dry and straight grained pieces were selected. As the model was to be set up out-door, they were painted over with two thin coatings of shellac to make them water-proof prior to testing for flexural properties and installing them as walls.

8.2 - DETERMINATION OF FLEXURAL PROPERTIES OF WOOD STRIPS

Before any meaningful test could be conducted on the wood material, appropriate material properties[8] had to be determined. Representative pieces of the pine wood strips were tested to determine their flexural properties.

The wood strips are of rectangular sections of 1-1/16

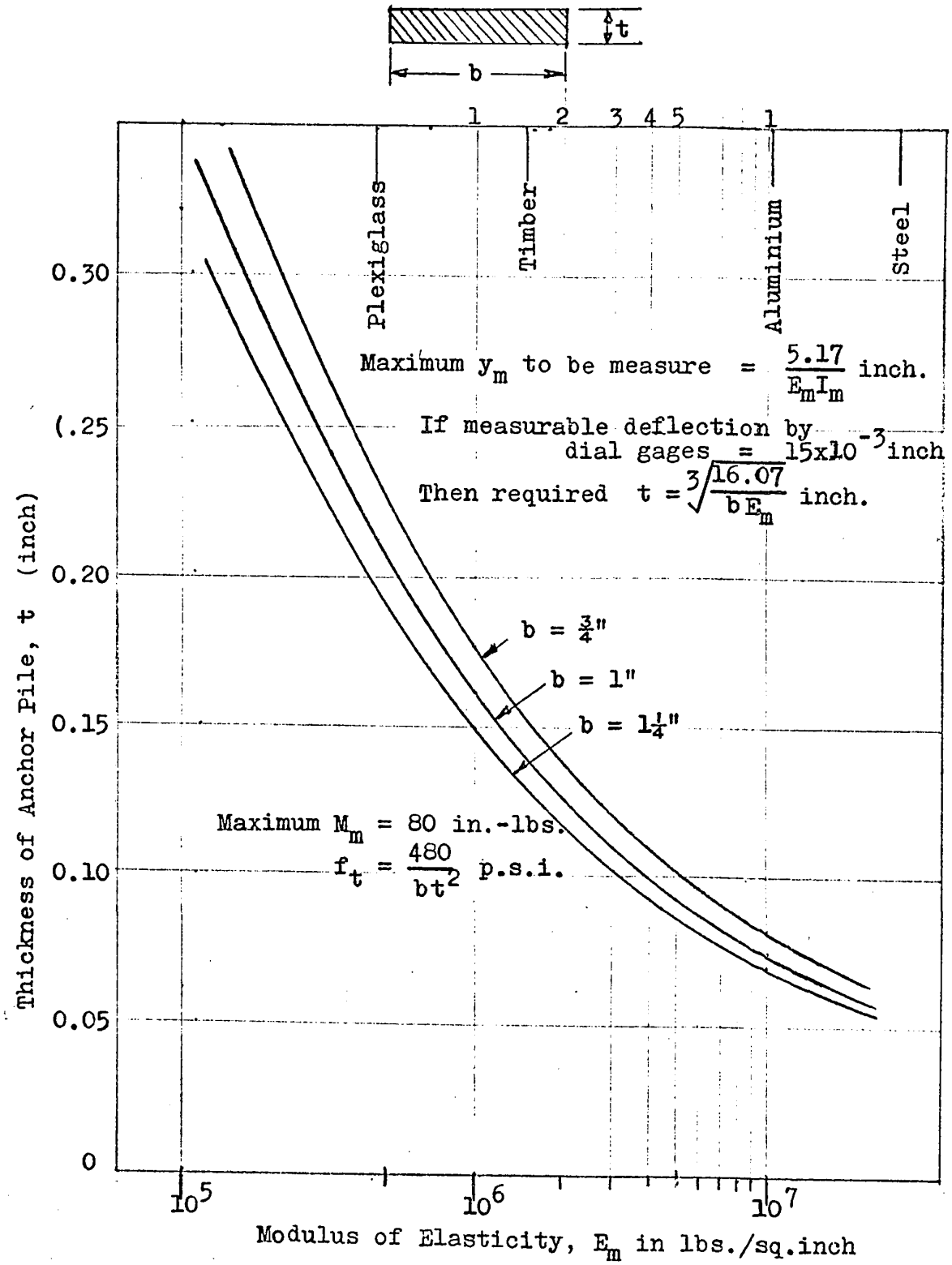

Fig.8-1 - Curves for choice of model material for anchor pile design, based on rectangular section of width b and thickness t.

inches wide by 1/4 inch thick. They were tested as beams of 18 inches span between knife-edge supports. To find the load-deflection relationship, a series of test loads was applied at mid-span and the deflection of the beams at the loading position was recorded by a dial gage. Loading, starting from a low value, was increased in regular steps. For each loading, the dial gage reading was recorded fifteen minutes after loading to ensure deflection was complete for that load. The load was then removed and a higher load was placed on the beam after an interval of fifteen minutes which was considered sufficient for full recovery of the beam. Typical deflections so obtained were plotted against loads and are shown in Fig.8-2.

From the load-deflection curve, it was observed that the wood material behaved linearly up to a load level giving a probable maximum stress of 7,000 p.s.i. which may be taken as the upper limit of stress that could be allowed for the material to obey Hooke's law. An average value of modulus of elasticity, E, was taken from the load-deflection relationship as equal to 1.40×10^6 p.s.i.

8.3 - DESIGN AND SET-UP OF MODEL

The model required was made geometrically similar to the railway embankment and retaining wall system given by the numerical example in Appendices A and B. Scale factor $\lambda = \nu = \frac{1}{12}$ was used in the design of the model, using model equations derived in Section 7. The layout and details of the model are shown in Figs.8-3 and 8-4.

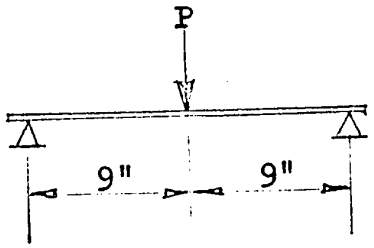

Test-Beam is of rectangular section of
1-1/16 inches by 1/4 inch.

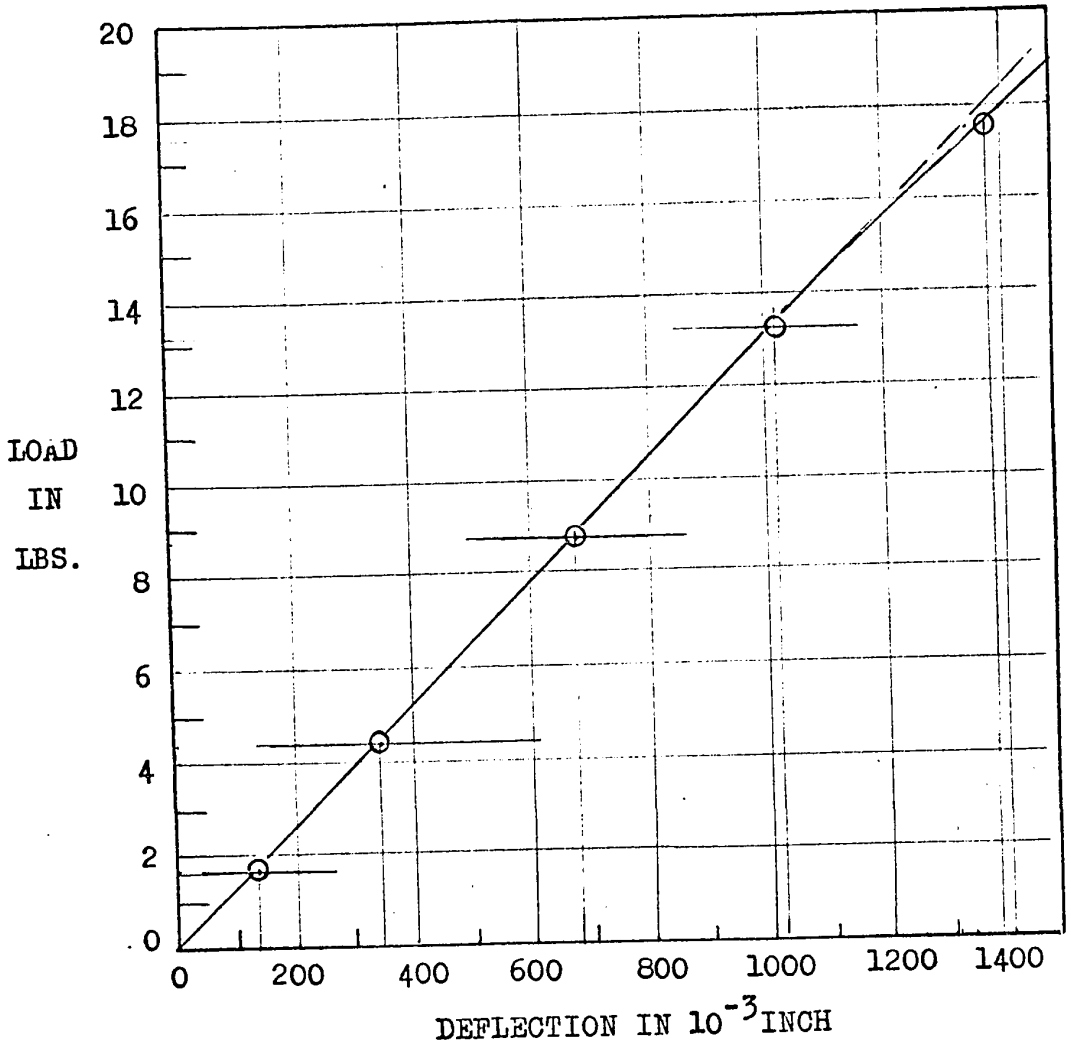

Fig.8-2 - Typical Load Deflection Curve For Test-Beam

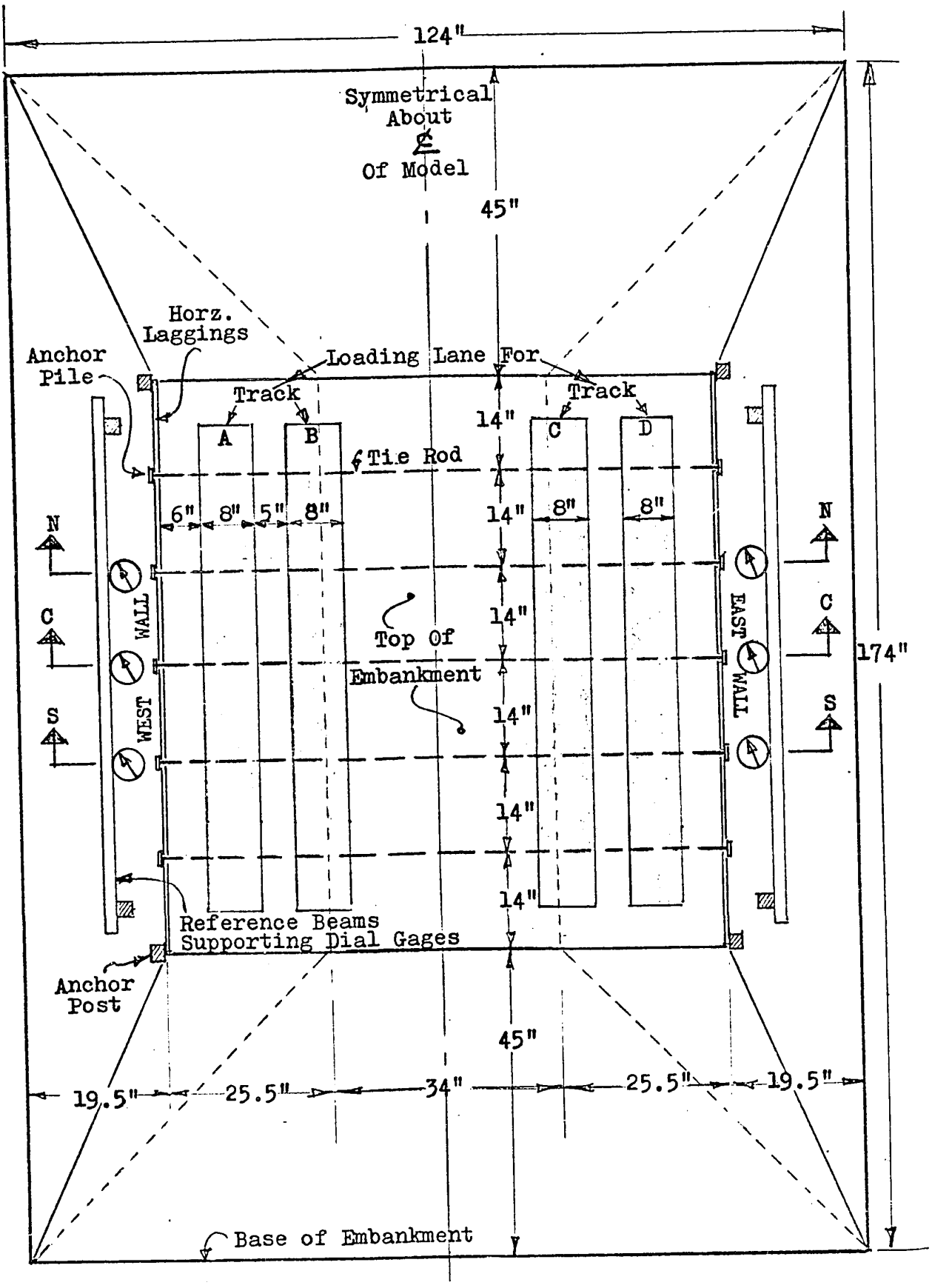

Fig.8-3 - General Layout of Model

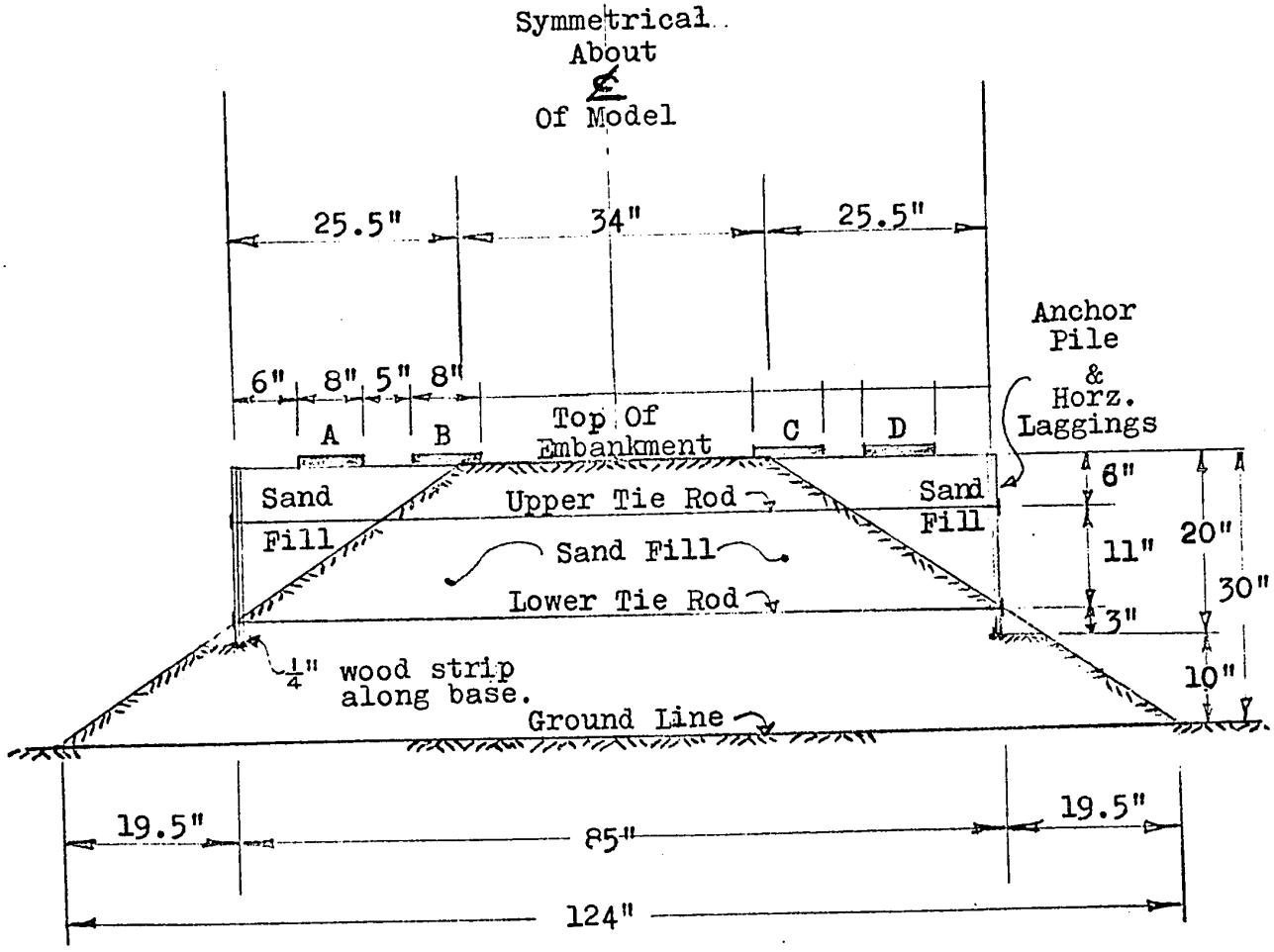

Fig.8-4 - Typical Cross Section of Model

(For location of dial gages, see Figs. 8-5 and 8-6)

The embankment for the model was constructed of a fine-medium sand having about 8% passing the U.S.Sieve 200. The sand was compacted in thin layers by watering and rolling. Density of the sand was estimated at about 115 lbs./cu. foot prior to application of test loads on the model.

Tie rods, $\frac{1}{4}$" diameter threaded steel rods, were initially placed and embedded in the fill during construction of the embankment. The embankment and the tie rods placed are shown on Plates 1 to 4.

The horizontal laggings and anchor piles for the walls are both fabricated with pine wood strips. The laggings are of rectangular section of 1-1/16 inches wide by 3/8 inch thick. They were taped together in panels for ease of installation. The anchor piles are of section 1-1/16 inches wide by 1/4 inch thick. Proper fittings and connection from the anchor rod to the anchor piles were provided by turn-buckles and anchor snaps. The turn-buckles were essential for the proper tension on the tie rods during installation. Details of the laggings, anchor piles, the fittings and their installation are shown on Plates 5, 6 and 7.

Similar sand material was used for filling between the embankment and the walls. Filling was carried out simultaneously on both walls to ensure that they are in proper alignment and in proper contact with the inner face of the wall. The sand was carefully placed and packed-in behind the walls in small quantities to avoid possible formation of cavities. Water was used to aid in achieving proper packing behind the

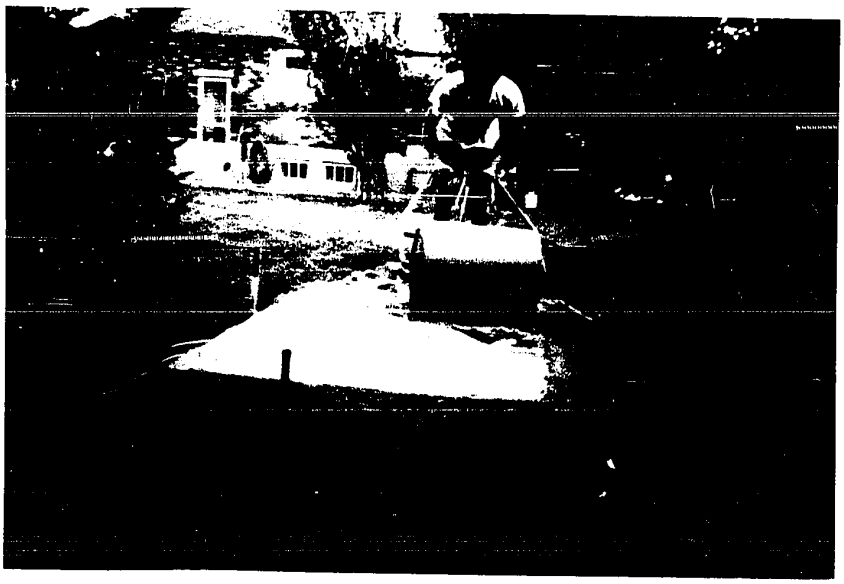

Plate 1 - Construction of model embankment using sand fill. Compaction achieved by watering and rolling on thin layers.

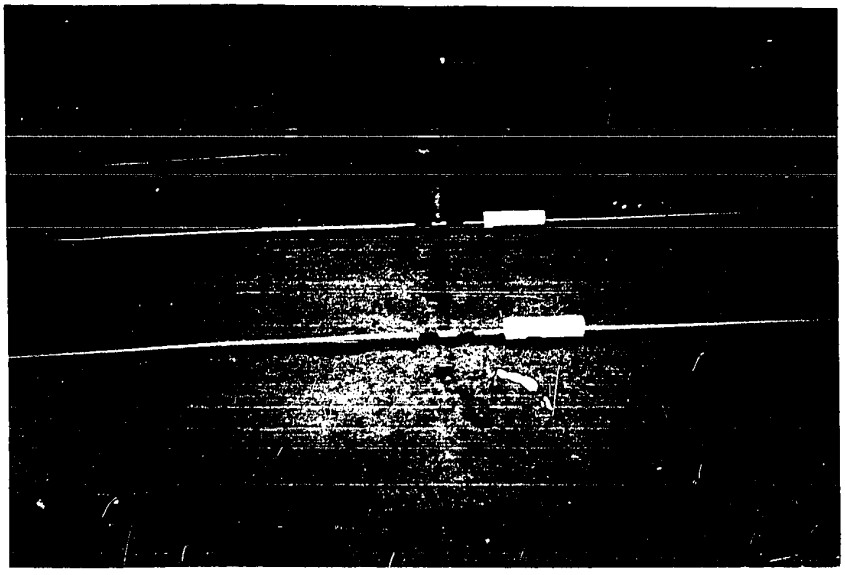

Plate 2 - Placing and aligning tie rods on embankment. Rods encased in plastic tubing allow free movement inside embankment.

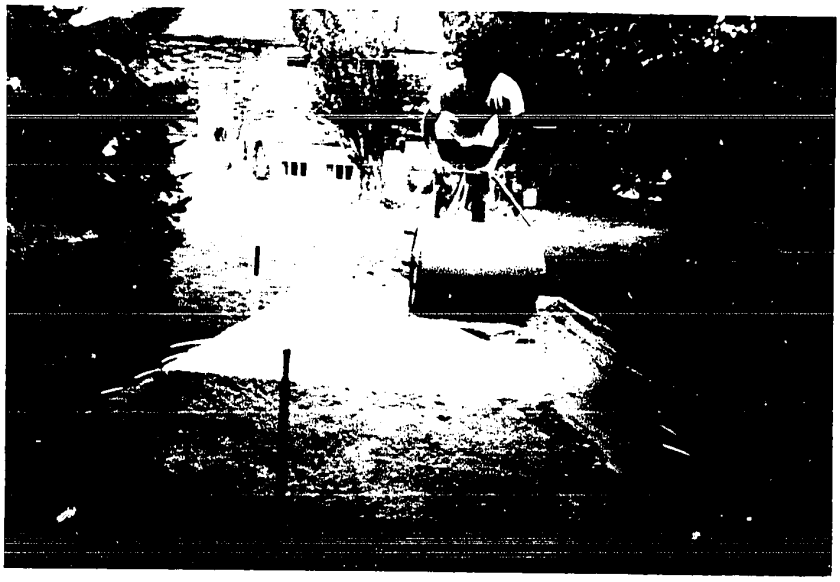

Plate 1 - Construction of model embankment using sand fill. Compaction achieved by watering and rolling on thin layers.

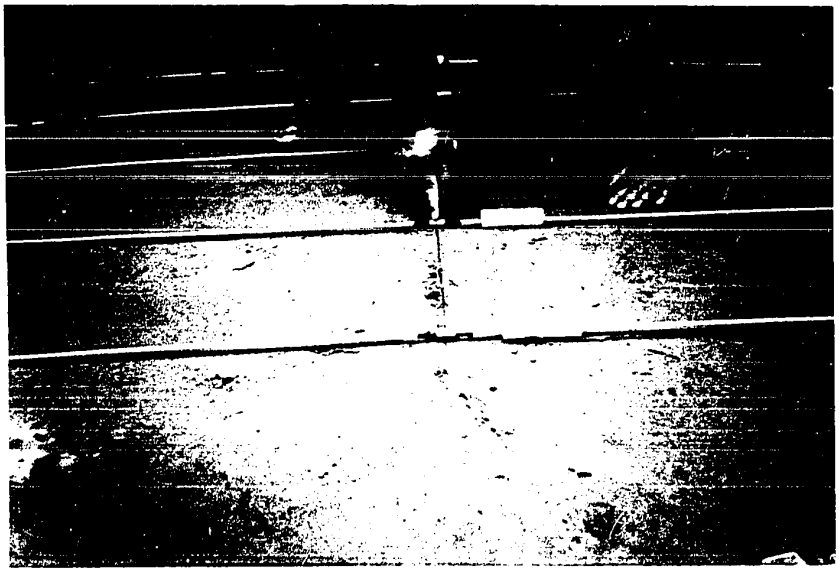

Plate 2 - Placing and aligning tie rods on embankment. Rods encased in plastic tubing allow free movement inside embankment.

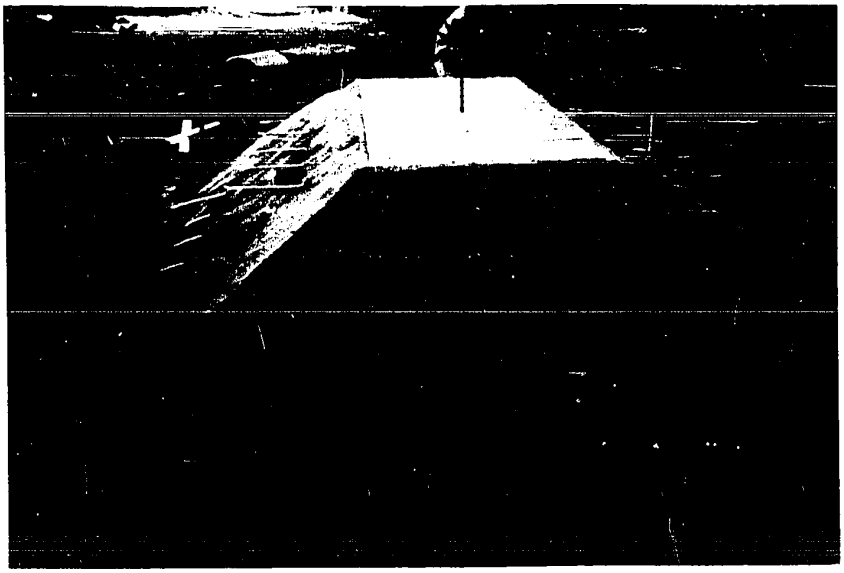

Plate 3 - Final model embankment with tie rods in place.

Plate 4 - Model embankment ready for erection of walls.

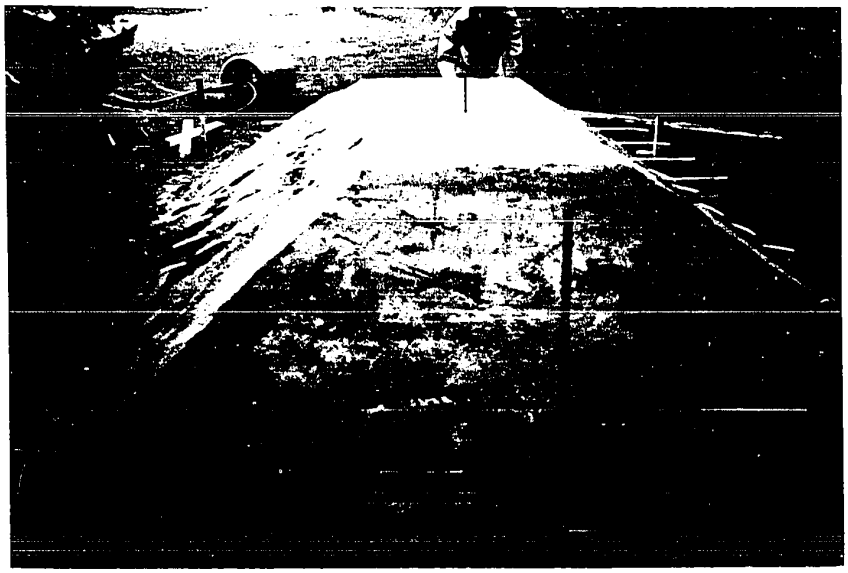

Plate 3 - Final model embankment with tie rods in place.

Plate 4 - Model embankment ready for erection of walls.

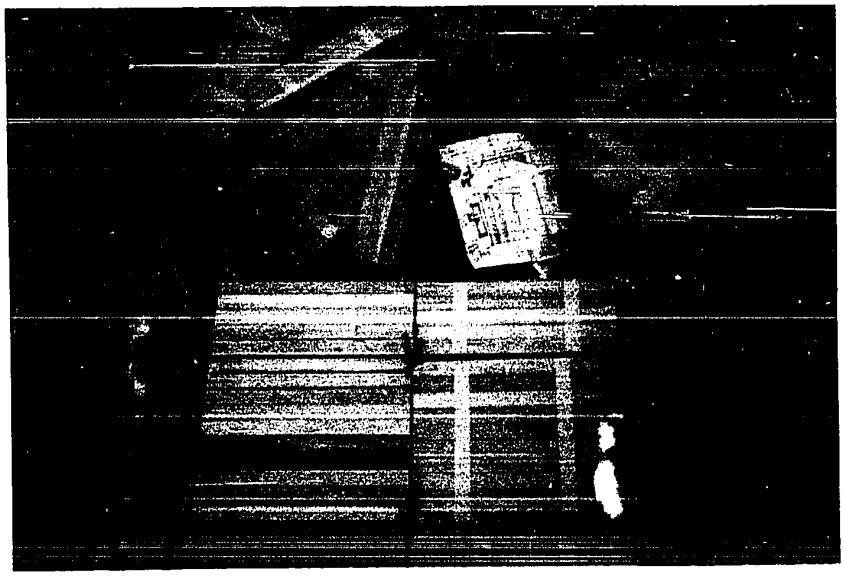

Plate 5 - Some details of wood strips fabricated for walls and hardware pieces used for tie rod system.

Plate 6 - Adjusting and aligning tie rod system to the anchor piles.

Plate 5 - Some details of wood strips fabricated for walls and hardware pieces used for tie rod system.

Plate 6 - Adjusting and aligning tie rod system to the anchor piles.

Plate 7 - Adjusting vertical alignment of anchor piles and wall panels to anchor rod system.

Plate 7 - Adjusting vertical alignment of anchor piles and wall panels to anchor rod system.

walls. The walls before filling and after filling are shown on Plates 8 and 9.

The dial gages were mounted on vertical steel rods which were rigidly attached to two cross beams. The beams were rigidly connected to solid posts driven into ground outside the influence of the test sections. The installation and general layout of the dial gages at each wall are shown on Plates 10 and 11. Gages were located to measure the deflection or movement of the main anchor piles in such a pattern that their locations on one wall corresponded to those on the other wall. As resulting deflections were anticipated to be small, special care was exercised to protect the set-up of the gages to ensure that proper readings could be taken.

Loading surface on top of the walled embankment was properly consolidated and levelled off to receive the test loads. Railway loadings were provided by layers of bricks laid on 8" wide lanes simulating tracks on the prototype. Each brick $3\frac{3}{4}$" wide by 8" long weighed 4.4 lbs. A lane with 6 layers of bricks provided a load of 84.6 lbs./lin. foot which will be equivalent to 1,500 lbs./sq. foot on a loaded track of the prototype. The loading lanes, and some of the loadings imposed on the walls during the experiment are shown on Plates 12, 13 and 14.

8.4 - TEST SEQUENCE AND MEASUREMENTS

Three series of tests were carried out. Loadings were applied in the sequences and the time duration designated on

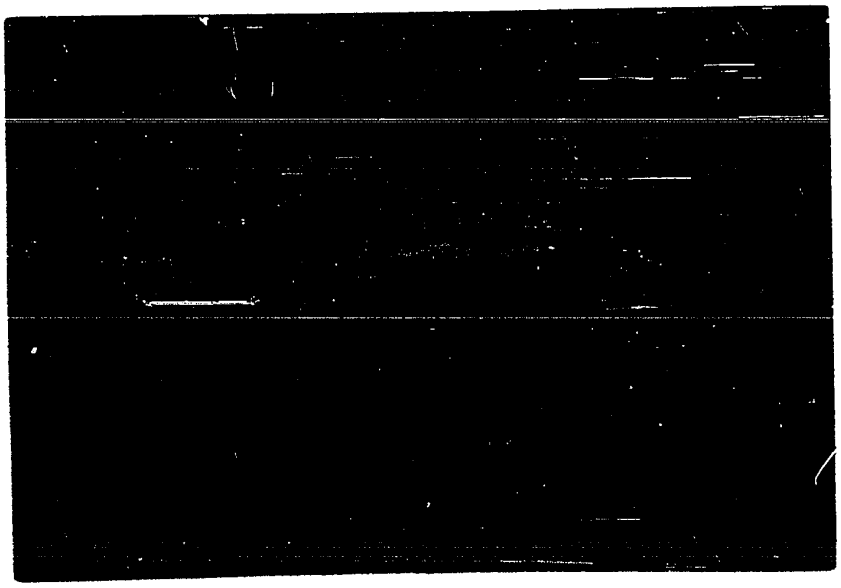

Plate 8 - Layout of wall system on embankment before filling.

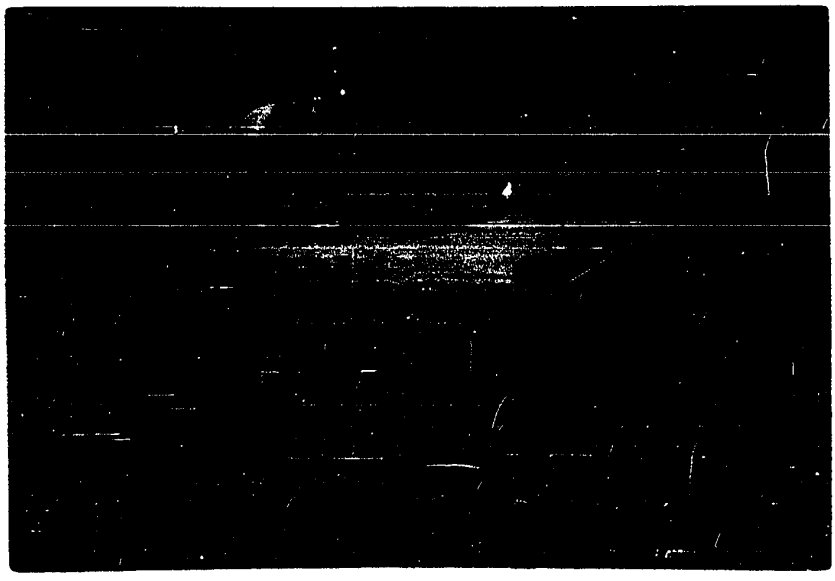

Plate 9 - View of walls after filling.

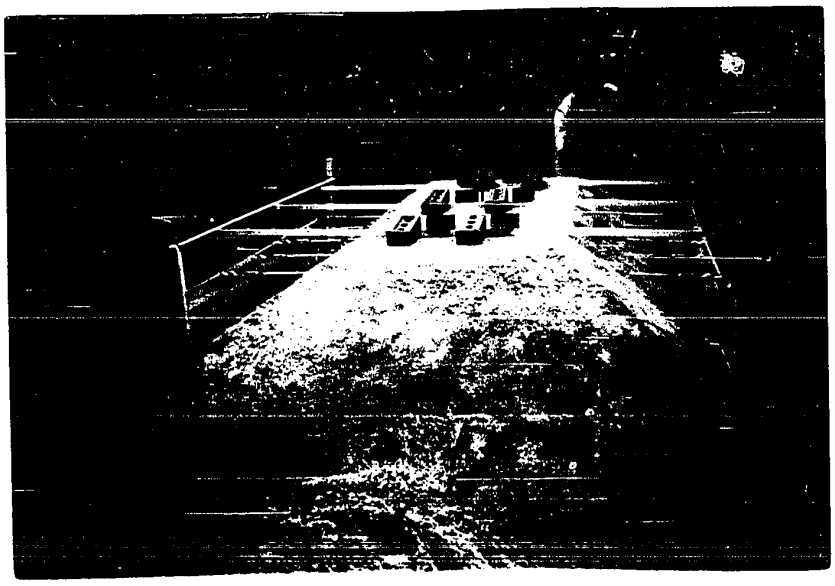

Plate 8 - Layout of wall system on embankment before filling.

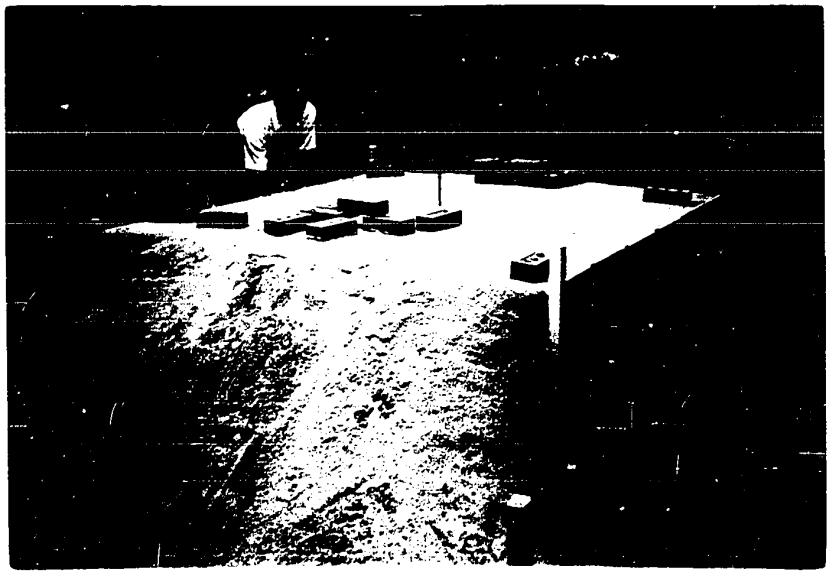

Plate 9 - View of walls after filling.

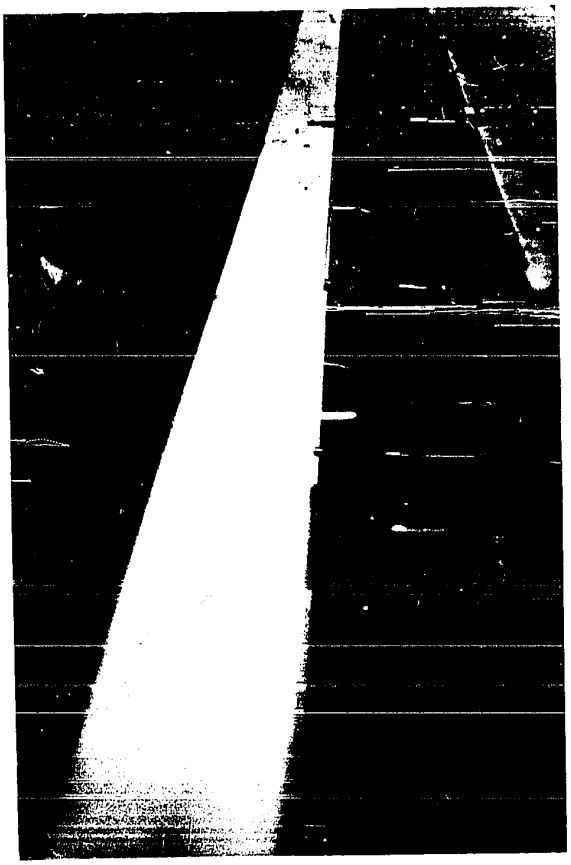

Plate 10 -

Details of dial gage installation to measure deflection of anchor piles.

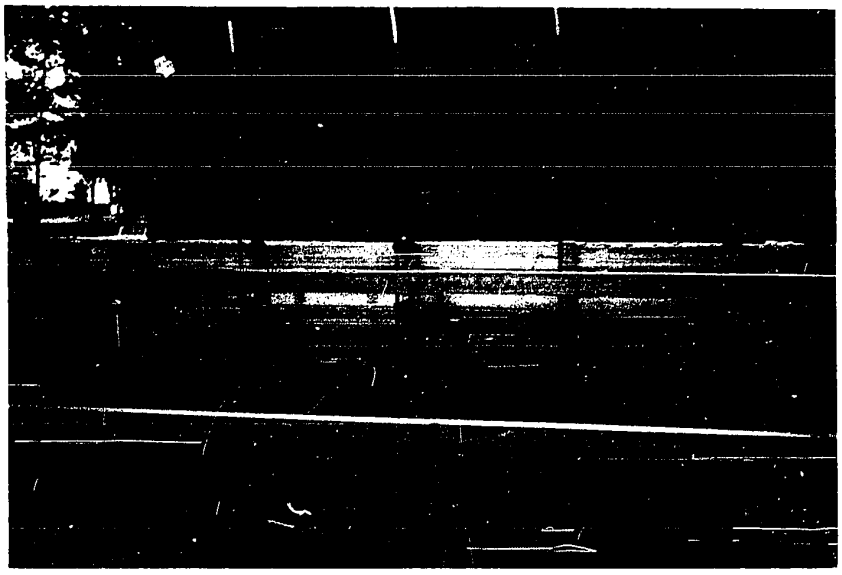

Plate 11 - View of west wall showing location of dial gages. Corresponding dial gage installation also located on the east wall.

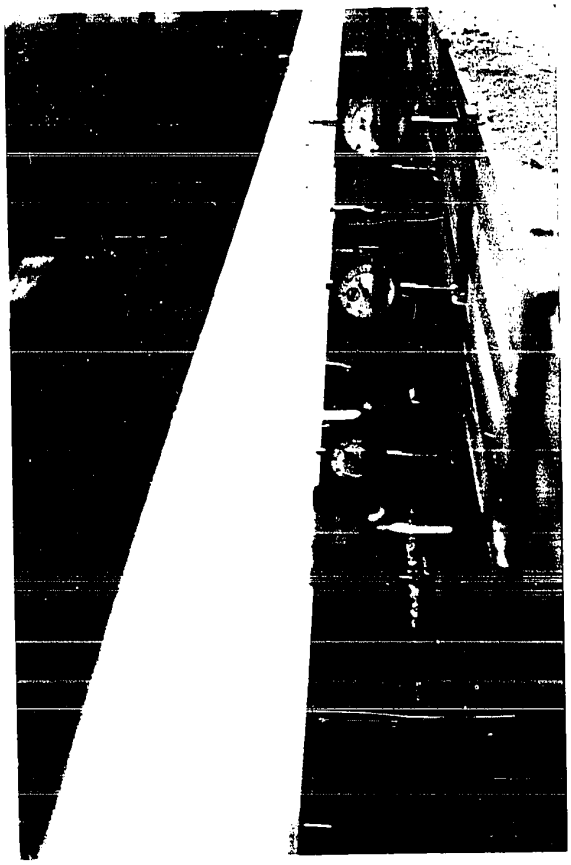

Plate 10 -

Details of dial gage installation to measure deflection of anchor piles.

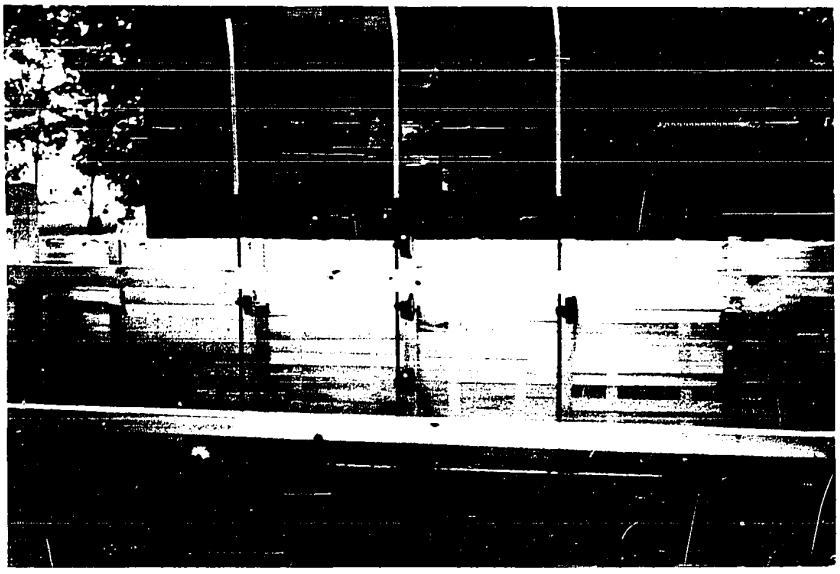

Plate 11 - View of west wall showing location of dial gages. Corresponding dial gage installation also located on the east wall.

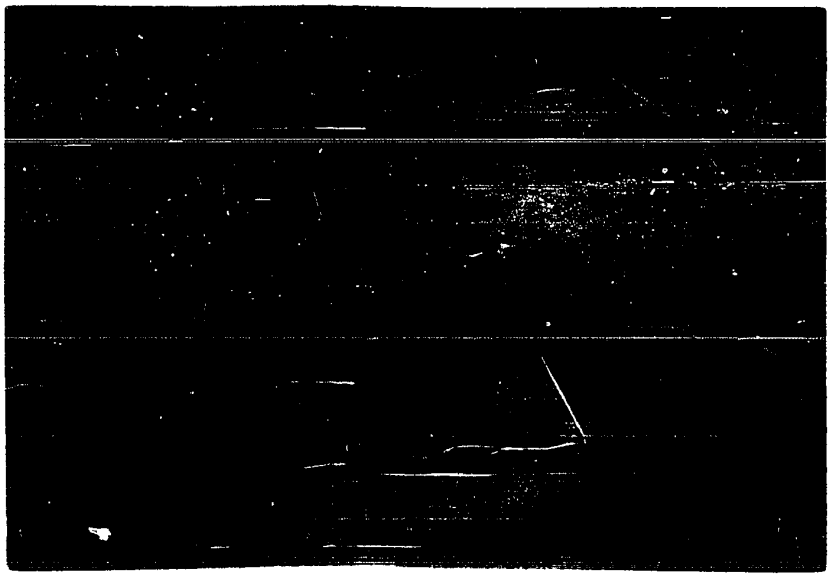

Plate 12 - Layout of loading lanes for strip loads simulated by layers of bricks.

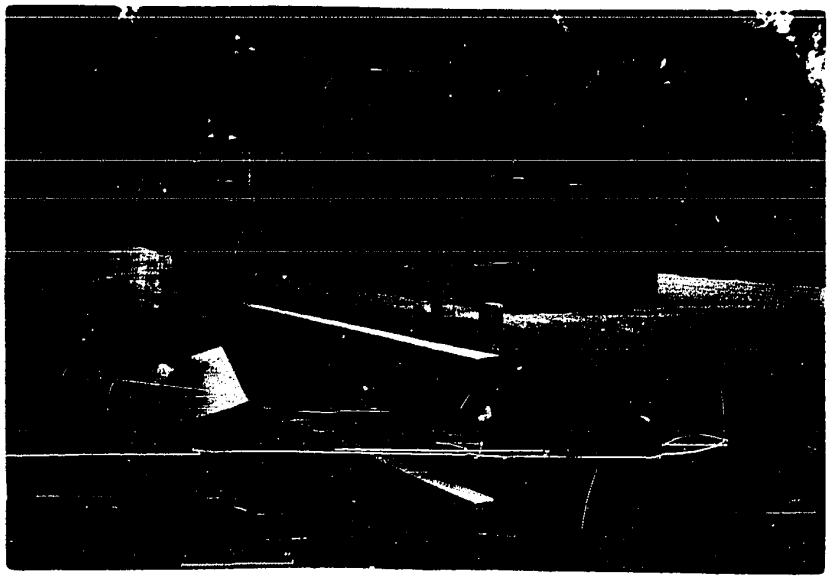

Plate 13 - View of model loaded with two parallel strip loads. Each strip load represents twice the equivalent load by 100-ton ore cars on track.

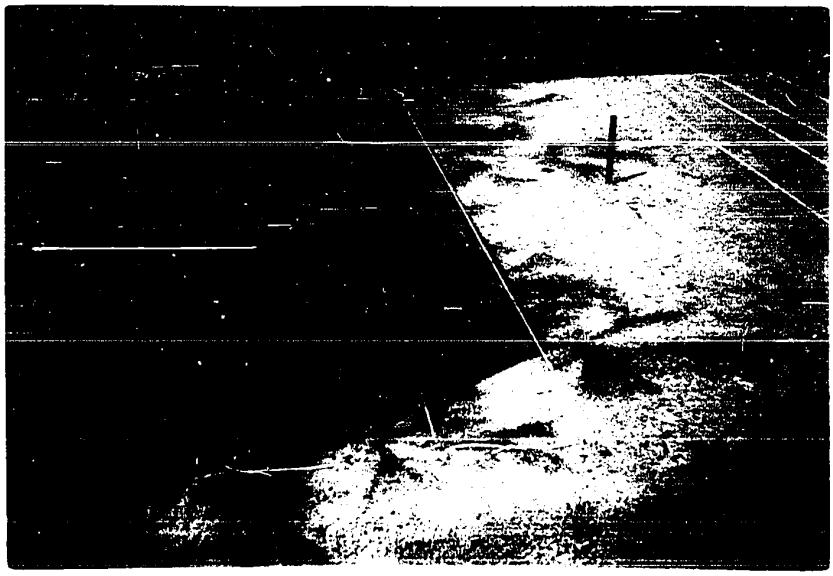

Plate 12 - Layout of loading lanes for strip loads simulated by layers of bricks.

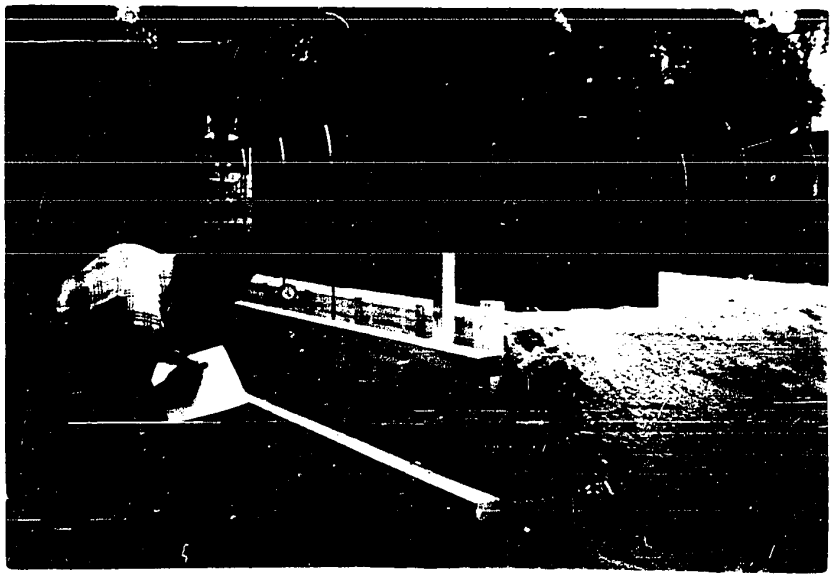

Plate 13 - View of model loaded with two parallel strip loads. Each strip load represents twice the equivalent load by 100-ton ore cars on track.

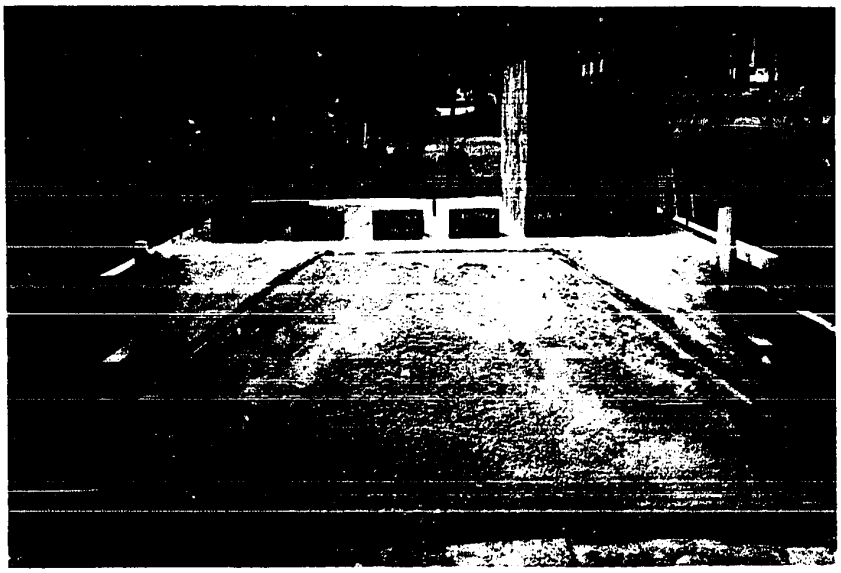

Plate 14 - General view with model loaded at both walls.

the test data sheets.

Test Series I, which comprises of Tests 1 to 7 inclusive, was carried out to design load of 84.6 lbs./lin. foot which is equivalent to q = 1,500 lbs./sq. foot derived in Section 5.2 for loading from the 100-ton ore cars. The locations of the dial gages to measure deflections of anchor piles on each wall are given in cross sections in Fig.8-5,and Fig.8-6.

As the wall system was observed to be rather stable from Test Series I, and that the observed relative deflection of the anchor piles or movement of the walls appeared to be so small, it was decided that loadings for Test Series II and III were increased to twice the design loads.

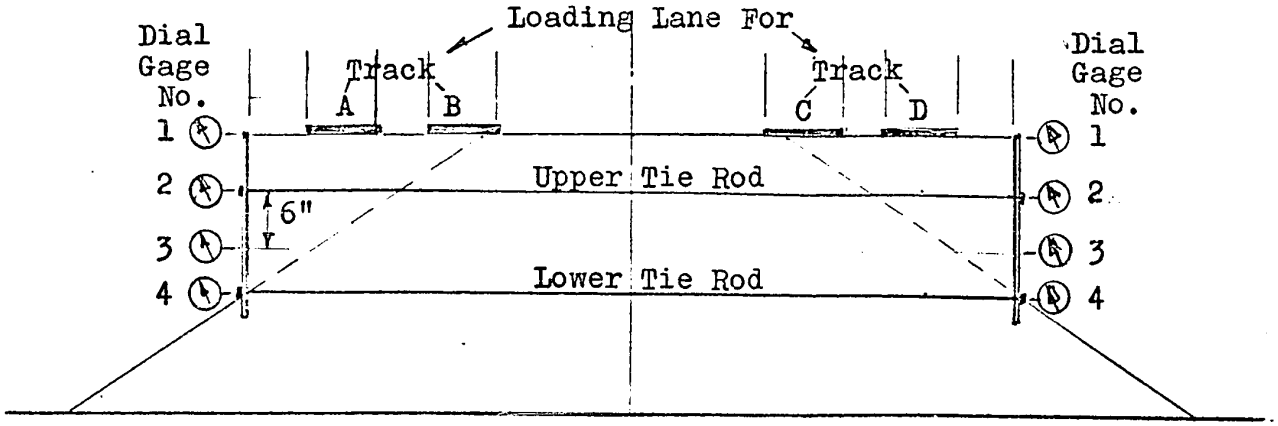

Section C - C

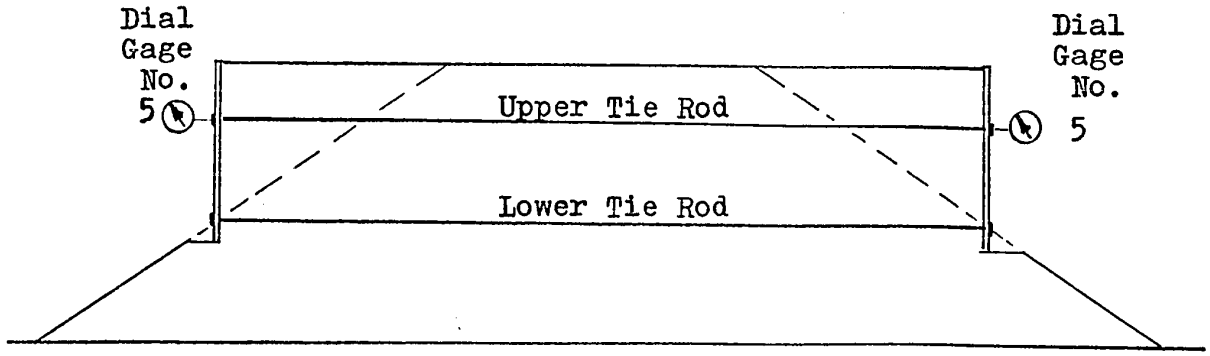

Section S - S

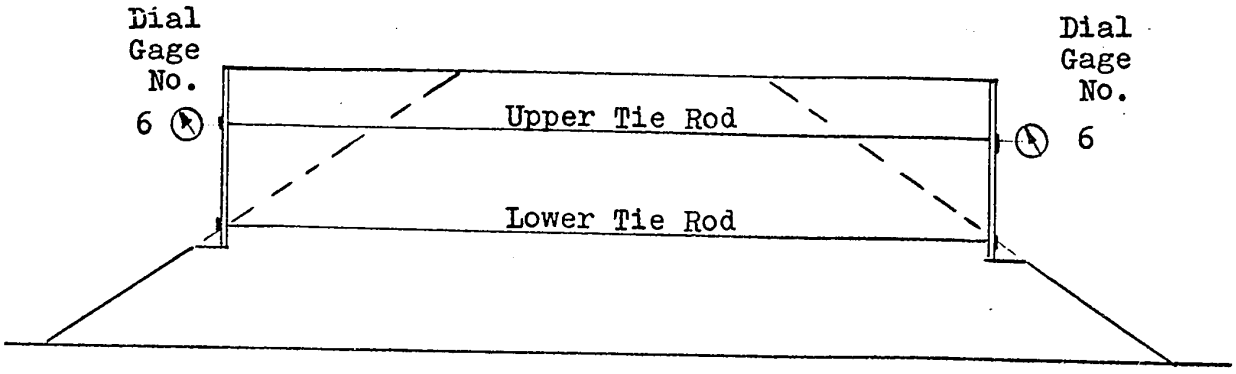

Section N - N

Fig.8-5 - Location of Dial Gages for Test Series I & II.

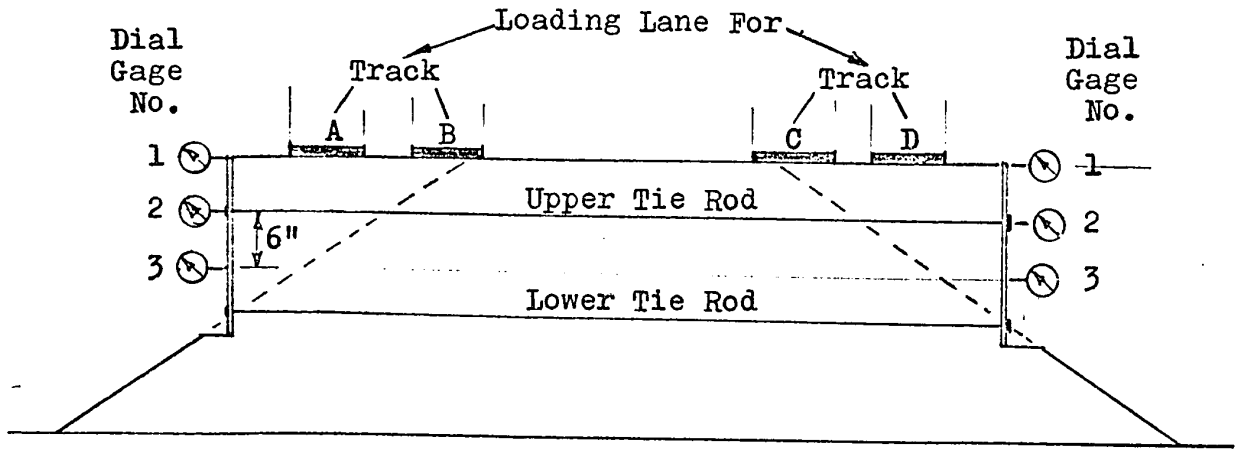

Section C - C

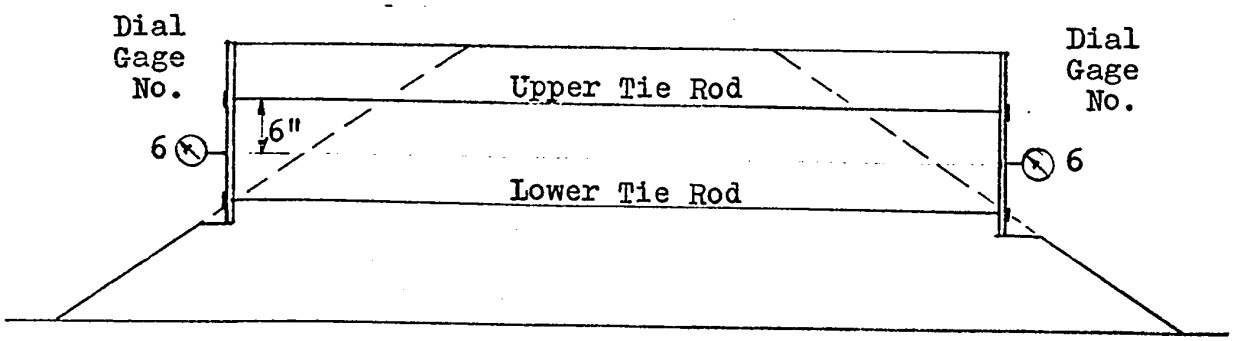

Section N - N

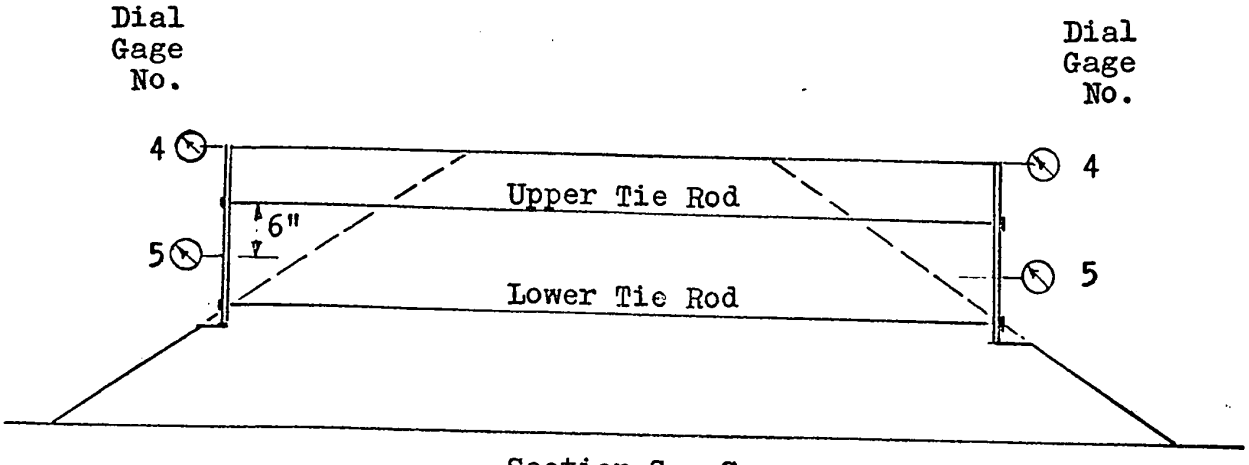

Section S - S

Fig.8-6 - Location of Dial Gages for Test Series III.

9. TEST RESULTS

All tests were carried out in 72° to 80°F weather under sunny condition. Temperature effect on the model materials and dial gages was considered to be negligible.

Results of measured deflections on the anchor piles under the various application of load combinations are presented in tabulated forms grouped under Table 9-1 consisting of Tests 1 to 16 inclusive. The main results are represented by load-deflection curves in Figures 9-1, 9-2 and 9-3.

Movement of the wall observed in Test Series I was relatively larger compared with the other Test Series II and III with higher applied loads. This was probably due to an improper initial contact of fill with wall components, or an initial slack in the tie rod system. It could also be due to an initial state of the sand fill which allowed itself to adjust and consolidate under the application of surface loads.

Actual deflections measured on all tests are small as predicted. The movements of the walls are generally considered non-linear. It would require a trial analysis to interpolate any intermediate condition by load-deflection relationship.

TEST 1 - TEST SERIES I (Tests 1 to 7 inclusive)

LOADING SEQUENCE: - Loading on Track A to design load of 84.6 lbs./lin. ft.

WEST WALL							
TIME, Elapsed in Minutes	LOADING, Uniform Load in lbs./lin.ft.	MEASURED DEFLECTION IN 10^{-4} INCH Of Anchor Pile at Section & Dial Gage No.					
		C - C				S - S	N - N
		1	2	3	4	5	6
0	0	0	0	0	0	0	0
15	28.2	+ 10	+ 17	+ 15	0	+ 10	+ 10
30	56.4	+ 35	+ 24	+ 25	0	+ 20	+ 35
60	84.6	+ 45	+ 39	+ 55	0	+ 40	+ 45
Calculated deflection at design load		+ 8	0	+ 20	0	0	0

EAST WALL							
TIME, Elapsed in Minutes	LOADING, Uniform Load in lbs./lin.ft.	MEASURED DEFLECTION IN 10^{-4} INCH Of Anchor Pile at Section & Dial Gage No.					
		C - C				S - S	N - N
		1	2	3	4	5	6
0	0	0	0	0	0	0	0
15	28.2	- 5	- 5	0	+ 2	- 5	- 4
30	56.4	- 15	- 11	+ 5	+ 4	- 15	- 12
60	84.6	- 35	- 16	0	+ 2	- 20	- 18
No calculations made for inward deflection		x	x	x	x	x	x

+ = outward deflection
- = inward deflection

Table 9-1 - Anchor pile deflection results, Tests 1 to 16 inclusive.

TEST 2 - TEST SERIES I (Tests 1 to 7 inclusive)

LOADING SEQUENCE: - Track A loaded with existing load of 84.6 lbs./lin. ft. resulting at end of Test 1.
- Loading on Track B to design load of 84.6 lbs./lin. ft.

WEST WALL

TIME, Elapsed in Minutes	LOADING, Uniform Load in lbs./lin.ft.	MEASURED DEFLECTION IN 10^{-4} INCH Of Anchor Pile at Section & Dial Gage No.					
		C - C				S - S	N - N
		1	2	3	4	5	6
0	0	0	0	0	0	0	0
60	84.6	+ 15	+ 11	+ 10	+ 5	+ 10	+ 5
Deflection at end of Test 1.		+ 45	+ 38	+ 55	0	+ 40	+ 45
Resulting deflection at end of Test 2.		+ 60	+ 49	+ 65	+ 5	+ 50	+ 50
Calculated deflection with Tracks A & B at design load.		+ 10	0	+ 27	0	0	0

EAST WALL

TIME, Elapsed in Minutes	LOADING, Uniform Load in lbs./lin.ft.	MEASURED DEFLECTION IN 10^{-4} INCH Of Anchor Pile at Section & Dial Gage No.					
		C - C				S - S	N - N
		1	2	3	4	5	6
0	0	0	0	0	0	0	0
60	84.6	- 20	- 16	- 5	- 2	- 15	- 15
Deflection end of Test 1.		- 35	- 16	0	+ 2	- 20	- 18
Resulting deflection at end of Test 2.		- 55	- 32	- 5	0	- 35	- 33
No calculation made for inward deflection.		x	x	x	x	x	x

+ = outward deflection
- = inward deflection

TEST 3 - TEST SERIES I (Tests 1 to 7 inclusive)

LOADING SEQUENCE: - Tracks A & B each loaded with existing load of 84.6 lbs./lin. ft. resulting at end of Test 2.
- Loading on Track D to design load of 84.6 lbs./lin. ft.

WEST WALL

TIME, Elapsed in Minutes	LOADING, Uniform Load in lbs./lin.ft.	MEASURED DEFLECTION IN 10^{-4} INCH Of Anchor Pile at Section & Dial Gage No.					
		C - C				S - S	N - N
		1	2	3	4	5	6
0	0	0	0	0	0	0	0
60	84.6	0	- 4	0	0	- 5	- 5
Resulting deflection at end of Test 2.		+ 60	+ 49	+ 65	+ 5	+ 50	+ 50
Resulting deflection at end of Test 3.		+ 60	+ 45	+ 65	+ 5	+ 45	+ 45

EAST WALL

TIME, Elapsed in Minutes	LOADING, Uniform Load in lbs./lin.ft.	MEASURED DEFLECTION IN 10^{-4} INCH Of Anchor Pile at Section & Dial Gage No.					
		C - C				S - S	N - N
		1	2	3	4	5	6
0	0	0	0	0	0	0	0
60	84.6	+ 55	+ 14	+ 15	- 10	+ 10	+ 14
Resulting deflection at end of Test 2.		- 55	- 32	- 5	0	- 35	- 33
Resulting deflection at end of Test 3.		0	- 18	+ 10	- 10	- 25	- 19

+ = outward deflection
- = inward deflection

TEST 4 - TEST SERIES I (Tests 1 to 7 inclusive)

LOADING SEQUENCE: - Tracks A, B & D each loaded with existing load of 84.6 lbs./lin. ft. resulting at end of Test 3.
- Loading on Track C to design load of 84.6 lbs./lin. ft. with load transferred directly from Track B.

WEST WALL

TIME, Elapsed in Minutes	LOADING, Uniform Load in lbs./lin.ft.	MEASURED DEFLECTION IN 10^{-4} INCH Of Anchor Pile at Section & Dial Gage No.					
		C - C				S - S	N - N
		1	2	3	4	5	6
0	0	0	0	0	0	0	0
60	84.6	- 5	- 8	- 10	0	- 10	- 5
Resulting deflection at end of Test 3		+ 60	+ 45	+ 65	+ 5	+ 45	+ 45
Resulting deflection at end of Test 4		+ 55	+ 37	+ 55	+ 5	+ 35	+ 40

EAST WALL

TIME, Elapsed in Minutes	LOADING, Uniform Load in lbs./lin.ft.	MEASURED DEFLECTION IN 10^{-4} INCH Of Anchor Pile at Section & Dial Gage No.					
		C - C				S - S	N - N
		1	2	3	4	5	6
0	0	0	0	0	0	0	0
60	84.6	+ 15	+ 7	+ 5	- 2	+ 25	+ 8
Resulting deflection at end of Test 3		0	- 18	+ 10	- 10	- 25	- 19
Resulting deflection at end of Test 4		+ 15	- 11	+ 15	- 12	0	- 11

+ = outward deflection
- = inward deflection

TEST 5 - TEST SERIES I (Tests 1 to 7 inclusive)

LOADING SEQUENCE: - Tracks A, C & D each loaded with existing load of 84.6 lbs./lin. ft. resulting at end of Test 4.
- Unloading Track A only.

WEST WALL

TIME, Elapsed in Minutes	LOADING, Uniform Load in lbs./lin.ft.	MEASURED DEFLECTION IN 10^{-4} INCH Of Anchor Pile at Section & Dial Gage No.					
		C - C				S - S	N - N
		1	2	3	4	5	6
0	84.6	0	0	0	0	0	0
60	0	- 20	- 19	- 15	- 5	- 15	- 15
Resulting deflection at end of Test 4.		+ 55	+ 37	+ 55	+ 5	+ 35	+ 40
Resulting deflection at end of Test 5.		+ 35	+ 18	+ 40	0	+ 20	+ 25

EAST WALL

TIME, Elapsed in Minutes	LOADING, Uniform Load in lbs./lin.ft.	MEASURED DEFLECTION IN 10^{-4} INCH Of Anchor Pile at Section & Dial Gage No.					
		C - C				S - S	N - N
		1	2	3	4	5	6
0	84.0	0	0	0	0	0	0
60	0	+ 10	+ 5	0	- 2	- 10	+ 4
Resulting deflection at end of Test 4.		+ 15	- 11	+ 15	- 12	0	- 11
Resulting deflection at end of Test 5.		+ 25	- 6	+ 15	- 14	- 10	- 7
Calculated deflection with Tracks C & D at design load.		+ 10	0	+ 27	0	0	0

+ = outward deflection
- = inward deflection

TEST 6 - TEST SERIES I (Tests 1 to 7 inclusive)

LOADING SEQUENCE: - Tracks C & D each loaded with existing load of 84.6 lbs./lin. ft. resulting at end of Test 5.
- Unloading Track C only.

WEST WALL							
TIME, Elapsed in Minutes	LOADING, Uniform Load in lbs./lin.ft.	MEASURED DEFLECTION IN 10^{-4} INCH Of Anchor Pile at Section & Dial Gage No.					
		C - C				S - S	N - N
		1	2	3	4	5	6
0	84.6	0	0	0	0	0	0
60	0	0	- 12	- 5	0	- 5	- 5
Resulting deflection at end of Test 5.		+ 35	+ 18	+ 40	0	+ 20	+ 25
Resulting deflection at end of Test 6.		+ 35	+ 6	+ 35	0	+ 15	+ 20

EAST WALL							
TIME, Elapsed in Minutes	LOADING, Uniform Load in lbs./lin.ft.	MEASURED DEFLECTION IN 10^{-4} INCH Of Anchor Pile at Section & Dial Gage No.					
		C - C				S - S	N - N
		1	2	3	4	5	6
0	84.6	0	0	0	0	0	0
60	0	+ 5	- 3	- 5	0	0	0
Resulting deflection at end of Test 5.		+ 25	- 6	+ 15	- 14	- 10	- 7
Resulting deflection at end of Test 6		+ 30	- 9	+ 10	- 14	- 10	- 7
Calculated deflection with Track D at design load.		+ 8	0	+ 20	0	0	0

+ = outward deflection
- = inward deflection

TEST 7 - TEST SERIES I (Tests 1 to 7 inclusive)

LOADING SEQUENCE: - Track D loaded with existing load of 84.6 lbs./lin. ft. resulting at end of Test 6.
- Unloading Track D, only.

WEST WALL							
TIME, Elapsed in Minutes	LOADING, Uniform Load in lbs./lin.ft.	MEASURED DEFLECTION IN 10^{-4} INCH Of Anchor Pile at Section & Dial Gage No.					
		C - C				S - S	N - N
		1	2	3	4	5	6
0	84.6	0	0	0	0	0	0
60	0	0	+ 3	0	- 5	- 5	0
Resulting deflection at end of Test 6.		+ 35	+ 6	+ 35	0	+ 15	+ 20
Resulting deflection with all loads removed.		+ 35	+ 9	+ 35	- 5	+ 10	+ 20

EAST WALL							
TIME, Elapsed in Minutes	LOADING, Uniform Load in lbs./lin.ft.	MEASURED DEFLECTION IN 10^{-4} INCH Of Anchor Pile at Section & Dial Gage No.					
		C - C				S - S	N - N
		1	2	3	4	5	6
0	84.6	0	0	0	0	0	0
60	0	- 15	- 14	- 20	- 3	- 10	- 13
Resulting deflection at end of Test 6.		+ 30	- 9	+ 10	- 14	- 10	- 7
Resulting deflection with all loads removed.		+ 15	- 23	- 10	- 17	- 20	- 20

+ = outward deflection
- = inward deflection

TEST 8 - TEST SERIES II (Tests 8 to 12 inclusive)

LOADING SEQUENCE: - Loading Tracks A & B simultaneously to maximum load of 169.2 lbs./lin. ft. on each track.

WEST WALL							
TIME, Elapsed in Minutes	LOADING, Uniform Load in lbs./lin.ft.	MEASURED DEFLECTION IN 10^{-4} INCH Of Anchor Pile at Section & Dial Gage No.					
		C - C				S - S	N - N
		1	2	3	4	5	6
0	0	0	0	0	0	0	0
30	56.4	+ 10	+ 13	+ 15	+ 10	+ 15	+ 10
60	112.8	+ 30	+ 28	+ 35	0	+ 30	+ 30
90	169.2	+ 50	+ 38	+ 45	+ 5	+ 35	+ 40
Calculated deflection at maximum loads		+ 20	0	+ 54	0	0	0

EAST WALL							
TIME, Elapsed in Minutes	LOADING, Uniform Load in lbs./lin.ft.	MEASURED DEFLECTION IN 10^{-4} INCH Of Anchor Pile at Section & Dial Gage No.					
		C - C				S - S	N - N
		1	2	3	4	5	6
0	0	0	0	0	0	0	0
30	56.4	- 45	- 12	+ 5	- 4	- 15	- 6
60	112.8	- 65	- 17	+ 5	- 6	- 15	- 13
90	169.2	- 70	- 21	+ 5	- 9	- 20	- 19
No calculations made for inward deflection		x	x	x	x	x	x

+ = outward deflection
- = inward deflection

TEST 9 - TEST SERIES II (Tests 8 to 12 inclusive)

LOADING SEQUENCE: - Tracks A & B each loaded with existing load of 169.2 lbs./lin. ft. resulting at end of Test 8.
- Loading on Track D to maximum load of 169.2 lbs./lin. ft.

WEST WALL

TIME, Elapsed in Minutes	LOADING, Uniform Load in lbs./lin.ft.	MEASURED DEFLECTION IN 10^{-4} INCH Of Anchor Pile at Section & Dial Gage No.					
		C - C				S - S	N - N
		1	2	3	4	5	6
0	0	0	0	0	0	0	0
60	169.2	0	+ 4	+ 5	0	+ 5	+ 5
Deflection at end of Test 8		+ 50	+ 38	+ 45	+ 5	+ 35	+ 40
Resulting deflection at end of Test 9		+ 50	+ 42	+ 50	+ 5	+ 40	+ 45

EAST WALL

TIME, Elapsed in Minutes	LOADING, Uniform Load in lbs./lin.ft.	MEASURED DEFLECTION IN 10^{-4} INCH Of Anchor Pile at Section & Dial Gage No.					
		C - C				S - S	N - N
		1	2	3	4	5	6
0	0	0	0	0	0	0	0
60	169.2	+ 45	+ 11	+ 20	- 3	+ 20	+ 10
Deflection at end of Test 8		- 70	- 21	+ 5	- 9	- 20	- 19
Resulting deflection at end of Test 9		- 25	- 10	+ 25	- 12	0	- 9

\+ = outward deflection
\- = inward deflection

TEST 10 - TEST SERIES II (Tests 8 to 12 inclusive)

LOADING SEQUENCE: - Tracks A, B & D each loaded with existing load of 169.2 lbs./lin. ft. resulting at end of Test 9.
- Loading on Track C to maximum load of 169.2 lbs./lin. ft. with load transferred directly from Track B.

WEST WALL

TIME, Elapsed in Minutes	LOADING, Uniform Load in lbs./lin.ft.	MEASURED DEFLECTION IN 10^{-4} INCH Of Anchor Pile at Section & Dial Gage No.					
		C - C				S - S	N - N
		1	2	3	4	5	6
0	0	0	0	0	0	0	0
60	169.2	+ 10	- 1	0	0	0	0
Resulting deflection at end of Test 9		+ 50	+ 42	+ 50	+ 5	+ 40	+ 45
Resulting deflection at end of Test 10		+ 60	+ 41	+ 50	+ 5	+ 40	+ 45

EAST WALL

TIME, Elapsed in Minutes	LOADING, Uniform Load in lbs./lin.ft.	MEASURED DEFLECTION IN 10^{-4} INCH Of Anchor Pile at Section & Dial Gage No.					
		C - C				S - S	N - N
		1	2	3	4	5	6
0	0	0	0	0	0	0	0
60	169.2	+ 40	+ 22	+ 20	+ 8	+ 20	+ 22
Resulting deflection at end of Test 9.		- 25	- 10	+ 25	- 12	0	- 9
Resulting deflection at end of Test 10.		+ 15	+ 12	+ 45	- 4	+ 20	+ 13

+ = outward deflection
- = inward deflection

TEST 11 - TEST SERIES II (Tests 8 to 12 inclusive)

LOADING SEQUENCE: - Tracks A, C & D each loaded with existing load of 169.2 lbs./lin. ft. resulting at end of Test 10.
- Unloading Track A only.

WEST WALL							
TIME, Elapsed in Minutes	LOADING, Uniform Load in lbs./lin.ft.	MEASURED DEFLECTION IN 10^{-4} INCH Of Anchor Pile at Section & Dial Gage No.					
		C - C				S - S	N - N
		1	2	3	4	5	6
0	169.2	0	0	0	0	0	0
60	0	- 25	- 22	- 20	+ 5	- 20	- 20
Resulting deflection at end of Test 10.		+ 60	+ 41	+ 50	+ 5	+ 40	+ 45
Resulting deflection at end of Test 11.		+ 35	+ 19	+ 30	+ 10	+ 20	+ 25

EAST WALL							
TIME, Elapsed in Minutes	LOADING, Uniform Load in lbs./lin.ft.	MEASURED DEFLECTION IN 10^{-4} INCH Of Anchor Pile at Section & Dial Gage No.					
		C - C				S - S	N - N
		1	2	3	4	5	6
0	169.2	0	0	0	0	0	0
60	0	+ 15	- 10	+ 5	+ 2	+ 10	+ 11
Resulting deflection at end of Test 10.		+ 15	+ 12	+ 45	- 4	+ 20	+ 13
Resulting deflection at end of Test 11.		+ 30	+ 2	+ 50	- 2	+ 30	+ 24
Calculated deflection with Tracks C & D at maximum load		+ 20	0	+ 54	0	0	0

+ = outward deflection
- = inward deflection

TEST 12 - TEST SERIES II (Tests 8 to 12 inclusive)

LOADING SEQUENCE: - Tracks C & D each loaded with existing load of 169.2 lbs./lin. ft. resulting at end of Test 11.
- Unloading Tracks C & D simultaneously.

WEST WALL							
TIME, Elapsed in Minutes	LOADING, Uniform Load in lbs./lin.ft.	MEASURED DEFLECTION IN 10^{-4} INCH Of Anchor Pile at Section & Dial Gage No.					
		C - C				S - S	N - N
		1	2	3	4	5	6
0	169.2	0	0	0	0	0	0
120	0	+ 15	+ 10	+ 10	+ 5	+ 10	+ 5
Resulting deflection at end of Test 11.		+ 35	+ 19	+ 30	+ 10	+ 20	+ 25
Resulting deflection at end of Test 12		+ 50	+ 29	+ 40	+ 15	+ 30	+ 30

EAST WALL							
TIME, Elapsed in Minutes	LOADING, Uniform Load in lbs./lin.ft.	MEASURED DEFLECTION IN 10^{-4} INCH Of Anchor Pile at Section & Dial Gage No.					
		C - C				S - S	N - N
		1	2	3	4	5	6
0	169.2	0	0	0	0	0	0
120	0	0	- 14	- 20	0	+ 5	- 6
Resulting deflection at end of Test 11.		+ 30	+ 2	+ 50	- 2	+ 30	+ 24
Resulting deflection at end of Test 12.		+ 30	- 12	+ 30	- 2	+ 35	+ 18

+ = outward deflection
- = inward deflection

TEST 13 - TEST SERIES III (Tests 13 to 16 inclusive)

LOADING SEQUENCE: - Loading Track A to maximum load of 169.2 lbs./lin. ft. and then unloading to no load.

WEST WALL							
TIME, Elapsed in Minutes	LOADING, Uniform Load in lbs./lin.ft.	MEASURED DEFLECTION IN 10^{-4} INCH Of Anchor Pile at Section & Dial Gage No.					
		C - C			S - S		N - N
		1	2	3	4	5	6
0	0	0	0	0	0	0	0
20	84.6	+15	+15	+15	+25	+ 5	+10
40	169.2	+20	+30	+30	+45	+30	+20
60	84.6	+15	+20	+25	+35	+30	+15
90	0	+ 5	+10	+10	+25	+30	+10
Calculated deflection at maximum load		+15	0	+40	+15	+40	+40

EAST WALL							
TIME, Elapsed in Minutes	LOADING, Uniform Load in lbs./lin.ft.	MEASURED DEFLECTION IN 10^{-4} INCH Of Anchor Pile at Section & Dial Gage No.					
		C - C			S - S		N - N
		1	2	3	4	5	6
0	0	0	0	0	0	0	0
20	84.6	-20	- 5	- 5	-20	-15	0
40	169.2	-25	-10	0	-25	-20	0
60	84.6	-30	-15	0	-30	-15	0
90	0	-30	-15	0	-30	-10	0
No calculations made for inward deflection		x	x	x	x	x	x

+ = outward deflection
- = inward deflection

TEST 14 - TEST SERIES III (Tests 13 to 16 inclusive)

LOADING SEQUENCE: - Loading Tracks A & B each to maximum load of 169.2 lbs./lin. ft. and then unloading to no load.

WEST WALL							
TIME, Elapsed in Minutes	LOADING, Uniform Load in lbs./lin.ft.	MEASURED DEFLECTION IN 10^{-4} INCH Of Anchor Pile at Section & Dial Gage No.					
		C - C			S - S		N - N
		1	2	3	4	5	6
0	0	0	0	0	0	0	0
20	84.6	+ 35	+ 20	+ 20	+ 50	0	+ 10
40	169.2	+ 75	+ 45	+ 65	+ 95	+ 30	+ 35
60	84.6	+ 75	+ 40	+ 55	+ 90	+ 30	+ 30
120	0	+ 55	+ 30	+ 40	+ 70	+ 25	+ 20
Calculated deflection with Tracks A & B at maximum load		+ 20	0	+ 54	+ 20	+ 54	+ 54

EAST WALL							
TIME, Elapsed in Minutes	LOADING, Uniform Load in lbs./lin.ft.	MEASURED DEFLECTION IN 10^{-4} INCH Of Anchor Pile at Section & Dial Gage No.					
		C - C			S - S		N - N
		1	2	3	4	5	6
0	0	0	0	0	0	0	0
20	84.6	- 20	- 10	0	- 15	+ 5	0
40	169.2	- 40	- 40	- 10	- 20	0	0
60	84.6	- 50	- 40	- 10	- 20	0	0
120	0	- 75	- 50	- 10	- 30	0	- 10
No calculations made for inward deflection		x	x	x	x	x	x

+ = outward deflection
- = inward deflection

TEST 15 - TEST SERIES III (Tests 13 to 16 inclusive)

LOADING SEQUENCE: - Loading Tracks C & D to maximum load of 169.2 lbs./lin. ft.

WEST WALL							
TIME, Elapsed in Minutes	LOADING, Uniform Load in lbs./lin.ft.	MEASURED DEFLECTION IN 10^{-4} INCH Of Anchor Pile at Section & Dial Gage No.					
		C - C			S - S		N - N
		1	2	3	4	5	6
0	0	0	0	0	0	0	0
30	84.6	0	- 5	- 5	0	- 5	- 5
60	169.2	- 5	- 10	- 10	- 5	- 10	- 10
No calculations made for inward deflection		x	x	x	x	x	x

EAST WALL							
TIME, Elapsed in Minutes	LOADING, Uniform Load in lbs./lin.ft.	MEASURED DEFLECTION IN 10^{-4} INCH Of Anchor Pile at Section & Dial Gage No.					
		C - C			S - S		N - N
		1	2	3	4	5	6
0	0	0	0	0	0	0	0
30	84.6	+ 15	0	+ 15	+ 5	+ 25	+ 20
60	169.2	+ 65	+ 20	+ 40	+ 65	+ 50	+ 45
Calculated deflection with Tracks C & D at maximum load		+ 20	0	+ 54	+ 20	+ 54	+ 54

+ = outward deflection
- = inward deflection

TEST 16 - TEST SERIES III (Tests 13 to 16 inclusive)

LOADING SEQUENCE: - Tracks C & D each loaded with existing load of 169.2 lbs./lin. ft. resulting at end of Test 15.
- Loading on Track A to maximum load of 169.2 lbs./lin. ft.

WEST WALL							
TIME, Elapsed in Minutes	LOADING, Uniform Load in lbs./lin.ft.	MEASURED DEFLECTION IN 10^{-4} INCH Of Anchor Pile at Section & Dial Gage No.					
		C - C			S - S		N - N
		1	2	3	4	5	6
0	0	0	0	0	0	0	0
60	169.2	+ 50	+ 10	+ 25	+ 45	+ 5	+ 20
Deflection at end of Test 15		- 5	- 10	- 10	- 5	- 10	- 10
Resulting deflection with Tracks A, C & D at maximum load		+ 45	0	+ 15	+ 40	- 5	+ 10
Resulting deflection with all loads removed		+ 25	- 10	+ 5	+ 25	- 5	+ 10

EAST WALL							
TIME, Elapsed in Minutes	LOADING, Uniform Load in lbs./lin.ft.	MEASURED DEFLECTION IN 10^{-4} INCH Of Anchor Pile at Section & Dial Gage No.					
		C - C			S - S		N - N
		1	2	3	4	5	6
0	0	0	0	0	0	0	0
60	169.2	+ 15	+ 10	0	+ 5	- 5	0
Deflection at end of Test 15		+ 65	+ 20	+ 40	+ 65	+ 50	+ 45
Resulting deflection with Tracks A, C & D at maximum load		+ 80	+ 30	+ 40	+ 70	+ 45	+ 45
Resulting deflection with all loads removed		+ 20	+ 10	+ 10	+ 45	+ 10	+ 10

+ = outward deflection
- = inward deflection

Fig.9-1 - Deflection curves for anchor pile on model.
(Test Series I)

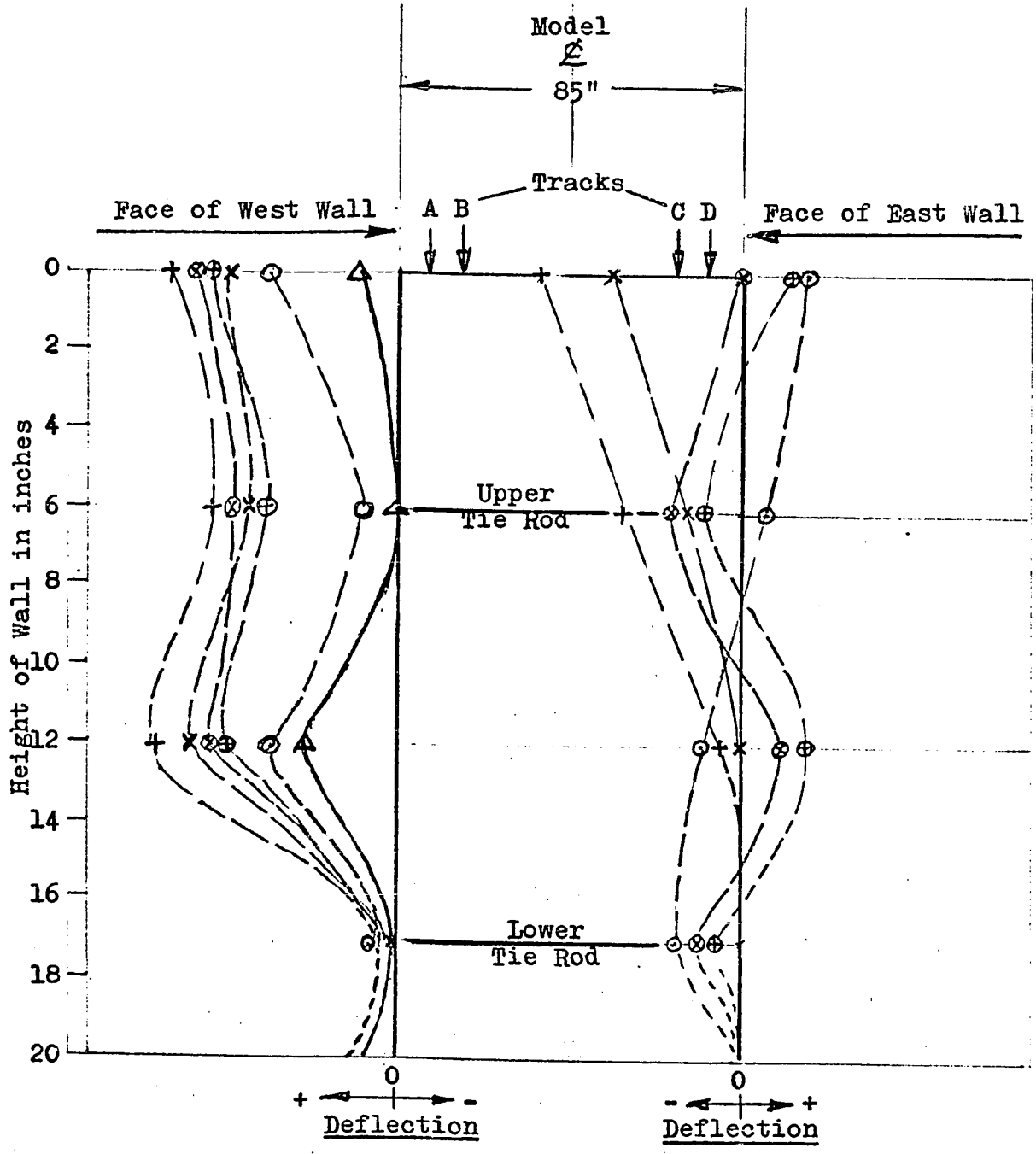

Scale: 1" = 40 x 10^{-4} inch

× = Loads on Track A
+ = Loads on Tracks A and B
⊗ = Loads on Tracks A, B and D
⊕ = Loads on Tracks A, C and D
⊙ = All loads removed.
△ = Loads on Tracks A and B (calculated deflection)

Fig.9-2 - Deflection curves for anchor pile on model.
(Test Series II)

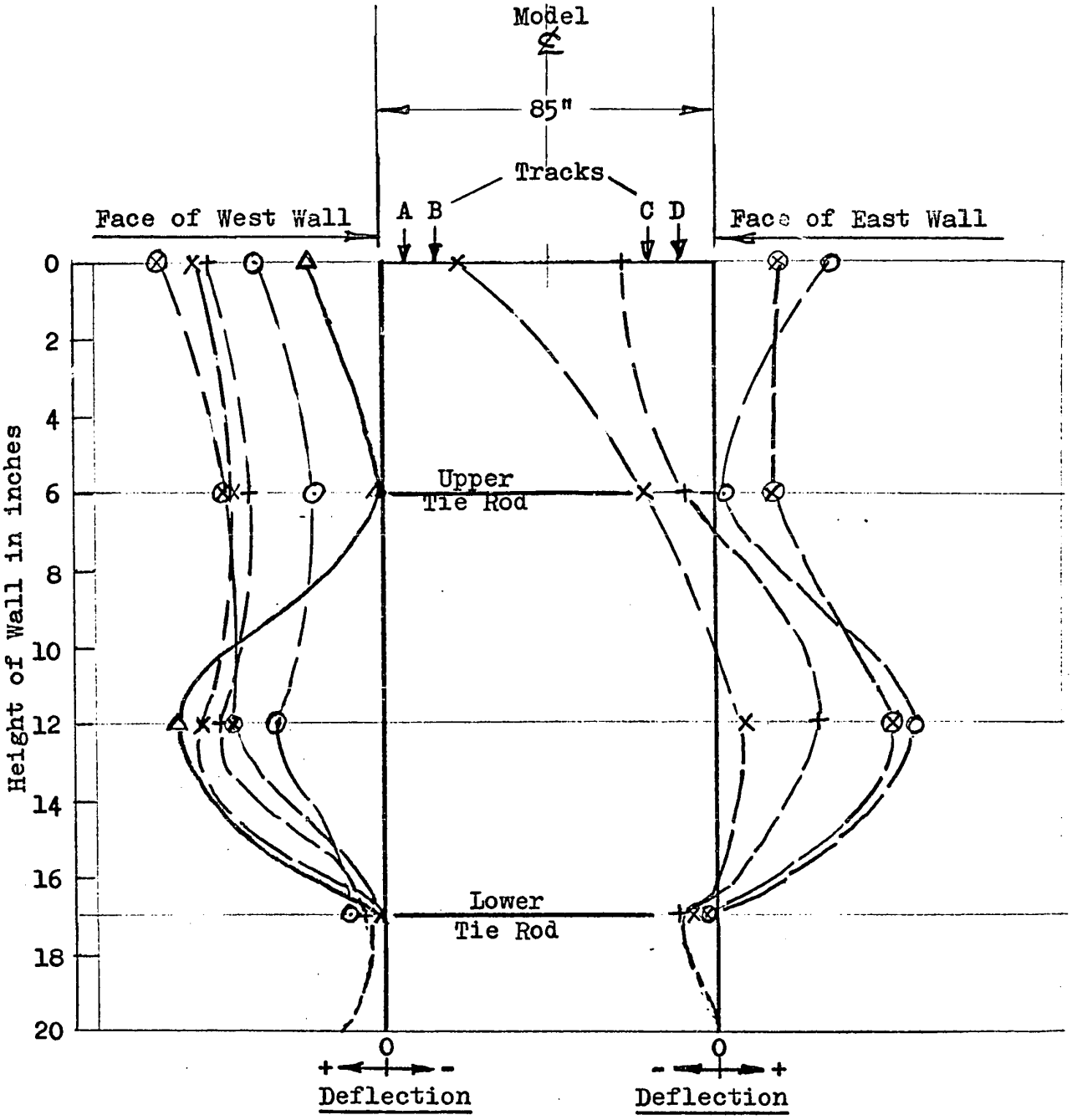

Scale: 1" = 40×10^{-4} inch

× = Loads on Tracks A and B
+ = Loads on Tracks A, B and D
⊗ = Loads on Tracks A, C and D
⊙ = All loads removed.
△ = Loads on Tracks A and B (calculated deflection)

Fig.9-3 - Deflection curves for anchor pile on model.
(Test Series III - Tests 15 and 16)

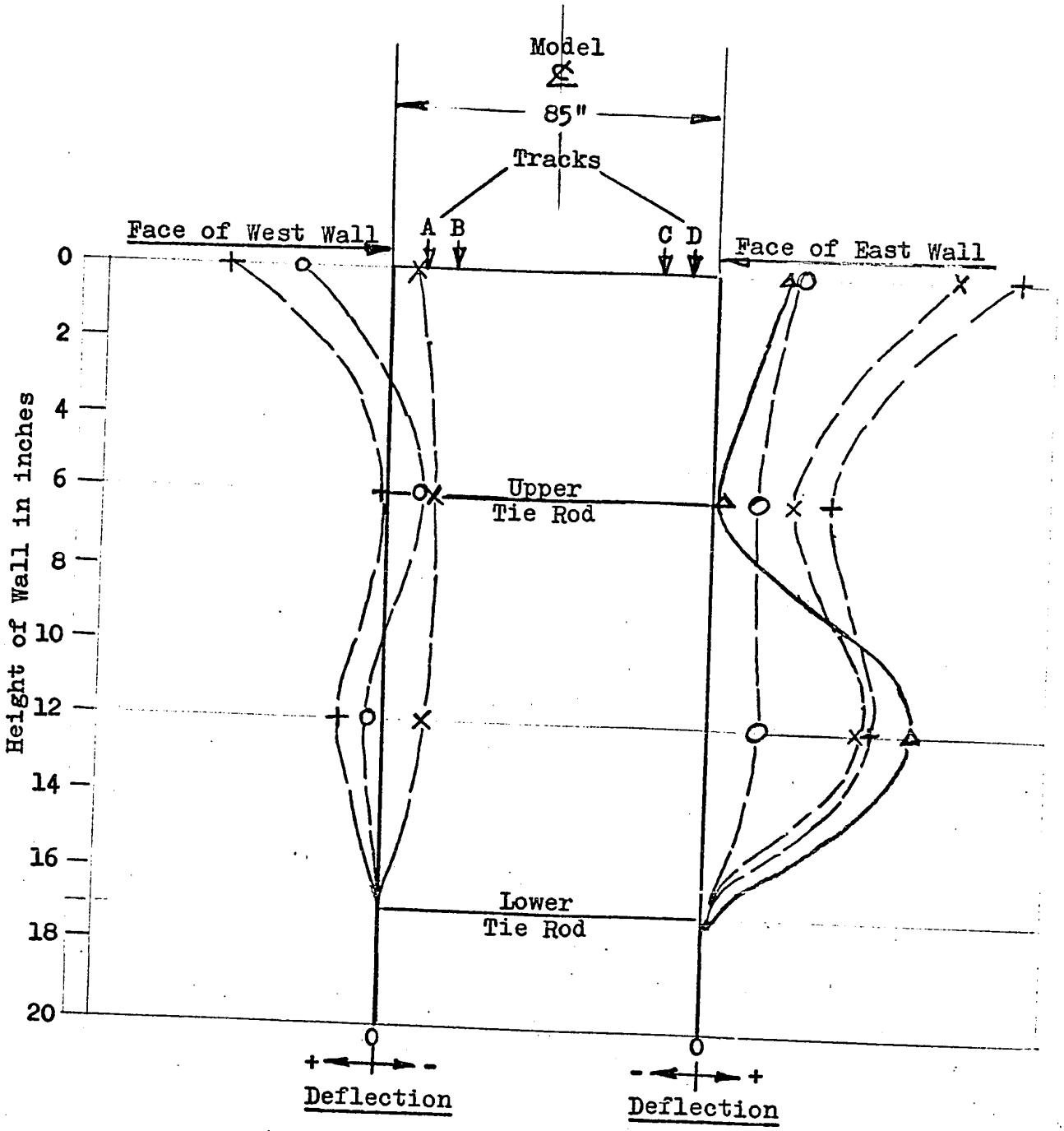

Scale : 1" = 40×10^{-4} inch

× = Loads on Tracks C and D
+ = Loads on Tracks A, C and D
⊙ = All loads removed.
△ = Loads on Tracks C and D (calculated deflection)

10. CONCLUSIONS

(1). The experimental results indicate that the deflections measured on the anchor piles under the application of surface loads generally fall along the pattern and the range predicted by theory. The actual values measured are small as expected, but they show that certain trend of movement took place simultaneously on both walls. Movement occurred mainly in the upper part of the wall. The test results show that when load was applied at one wall, that wall would move outward and pull the other wall inward with it. When the loads were reversed, there was generally some recovery from the movement. However, recovery was generally found to be non-linear, and full recovery was not evident even when all applied loads were removed.

(2). The response of one wall under load action to react against the other wall is obvious. The degree of response should relate to the flexibility or resistance of the walls to movement. It would be complex to evaluate the response by theory as the "equivalent beam" deforming elastically will be subjected to a continuously varying distribution of reactive loading. Measurements, however, show that it appeared to be dependent to a large extent on both the active and passive states of the fill placed against the walls, and the direct or reversible effects of the applied loads. It is evident from these observations that good compaction of the fill is an important factor in limiting and reducing possible large or undesirable deformation that may be produced by repetitive

loadings. Poor compaction and variation in fill density, local yield and separation between fill and inner face of the wall can significantly affect the movement and therefore the overall stability of the wall system.

(3). Both the Rankine's theory and the strip load method used for evaluating lateral pressures against the walls appeared to be adequate. Earth pressure is considered to have an advantageous balancing effect on the wall system. Hence, simultaneous filling on both walls and achieving uniformity in fill density would be important considerations in construction.

(4). As largest movement occurs in the upper section of the wall, the effect of surface loads on the upper tie rods can be considerable. These rods should be embedded in sufficient depth and protected to avoid abrasion and the possibility of distortion or displacement from alignment by impact and direct stress action from repetitive loadings. The lower tie rods were found to be comparatively more stable, and the measurements indicated that there was relatively little or no movement there.

(5). Since movements do occur along the tie rods, the analytical assumption that the anchor pile will not yield at the supporting points is not entirely valid. Since lower tie rods were found to have almost no movement, relative displacement between the two supporting points in the anchor pile should be considered. Considering unbalanced effects from applied loads, modification to the proposed design procedure

should make allowance for some relative displacement of the upper supporting point in the actual design of the anchor pile member. This allowance will depend on the degree of fixity and rigidity at both the supporting points.

(6). A balanced design for equal pull in tie rods, or for equal tensile and compressive stresses in the anchor pile is desirable and may be achieved by appropriate choice of depths for tie rods. The tie rod depth parameters "a" and "d" in the equations for axial forces and bending moments in Sections 3 and 6 can be used to advantage.

(7). Considering that both walls are tied against each other and that lateral pressures against walls are in an outward direction, the resultant axial force developed in each tie rod would be the sum of forces resulting from each of the various lateral pressures considered on each wall.

(8). Finally, performance of the wall system under the various loading conditions was observed to be satisfactory as there was no sign of yield or abnormal structural deformation in any part of the walls. The fact that the wall system was loaded to twice its maximum design load as carried out in Test Series II and III shows that such a wall is stable and can be designed for practical purpose.

APPENDIX A

NUMERICAL EXAMPLE CONSIDERING EARTH PRESSURE ONLY

Example considers only lateral earth pressure for design of 20 ft. high retaining wall to be constructed on each side of an existing railway embankment as shown in Fig.A-1. The equations derived in Section 3 will be used for design.

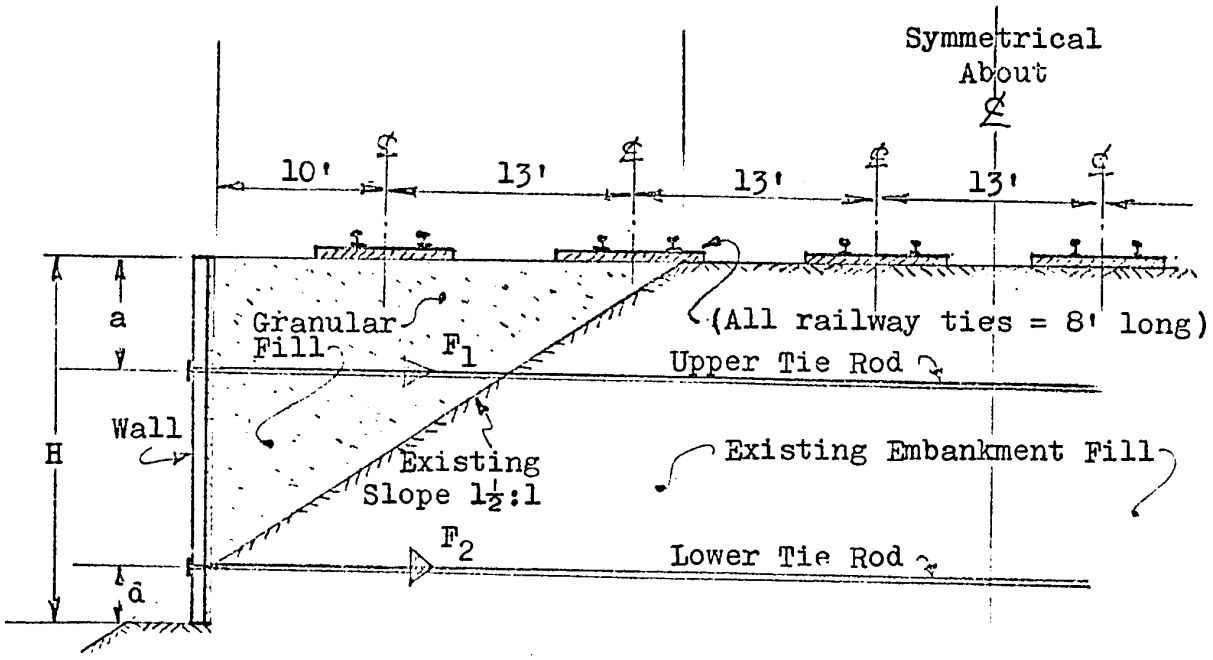

Fig.A-1 - Cross Section & Dimensions of Railway Embankment with retaining wall system.

Given data: H = 20 ft. γ = 125 lbs./cu. ft.

a = 6 ft. ϕ = 35°

d = 3 ft. K_a = 0.27

s = 14 ft.

Lateral pressure on anchor pile:

Substituting into Eq.(3-1),

P_b = 9,450 lbs./ft. of pile.

Forces in tie rods:

Substituting into Eqs.(3-2) and (3-3),

F_1 = 31,500 lbs.

F_2 = 63,000 lbs.

Shear in anchor pile:

Substituting into Eqs.(3-4),

Case (a), $S = 236.3x^2$

Case (b), $S = 236.3x^2 - 31{,}500$

Case (c), $S = 236.3x^2 - 94{,}500$

Above equations given in lbs. and results are represented by curve in Fig.A-2.

Bending moment in anchor pile:

Substituting into Eqs.(3-5),

Case (a), $M = 78.75x^3$

Case (b), $M = 78.75x^3 - 31{,}500(x - 6)$

Case (c), $M = 78.75x^3 - 31{,}500(x - 6) - 63{,}000(x - 17)$.

Above equations given in ft.-lbs. and results are represented by curve in Fig.A-2.

Maximum bending moment in anchor pile:

Substituting into Eqs.(3-6) and (3-7),

h = 11.55 ft.

M_{max} = 53,000 ft.-lbs.

Deflection in anchor pile:

Substituting into Eqs.(3-8),

Case (a), $y = -\frac{1}{EI}\left(3.94x^5 - 25{,}500x + 122{,}300 \right)$

Case (b), $y = -\frac{1}{EI}\left(3.94x^5 - 5{,}250x^3 + 94{,}500x^2 - 433{,}100x + 302{,}950 \right)$

Case (c), Deflection for this is comparatively small and will be omitted in this example.

Above equations given in ft. and results are represented by curve in Fig.A-2.

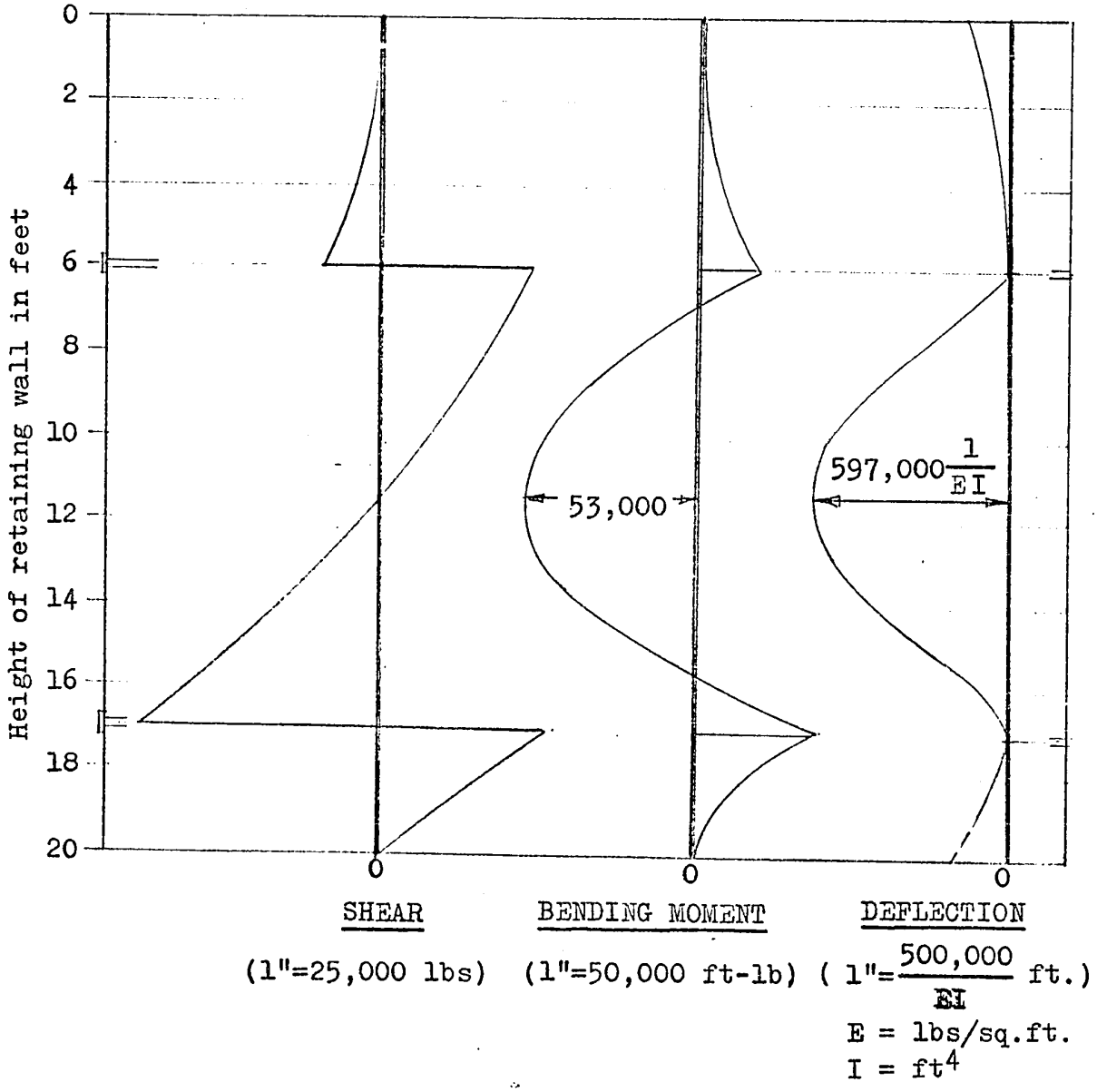

Fig.A-2 - Shear, bending moment and deflection on anchor pile due to lateral earth pressure.

APPENDIX B

NUMERICAL EXAMPLE CONSIDERING RAILWAY LOADING ONLY

Example considers only lateral pressure from railway loading for design of 20 ft. high retaining to be constructed on each side of an existing embankment as shown in Fig.A-1 of the numerical example in Appendix A. The lateral pressure exerted on each wall comes from loadings on the two new tracks adjacent to the wall, and design values are taken from the modified pressure diagram of Fig.5-4. The equations derived in Section 6 will be used for design.

Given data: $H = 20$ ft. $\quad \sigma_i = 750$ lbs./sq.ft.

$a = 6$ ft. $\quad \sigma_o = 300$ lbs./sq.ft.

$d = 3$ ft.

$s = 14$ ft.

Lateral pressure on anchor pile:

Substituting into Eqs.(6-1),

$P_1 = 10{,}500$ lbs./ft. of pile,

$P_o = 4{,}200$ lbs./ft. of pile.

Force in tie rods:

Substituting into Eqs.(6-4) and (6-5),

$F_1 = 84{,}000$ lbs.

$F_2 = 50{,}400$ lbs.

Shear in anchor pile:

Substituting into Eqs.(6-6),

Case (a), $S = 875x^2$,

Case (b), $S = -225x^2 + 13,200x - 123,600$

Case (c), $S = -225x^2 + 13,200x - 174,000$

Above equations given in lbs. and results are represented by curve in Fig.B-1.

Bending moment in anchor pile:

Substituting into Eqs.(6-7),

Case (a), $M = 291.7x^3$

Case (b), $M = -75x^3 + 6,600x^2 - 123,600x + 583,200$

Case (c), $M = -75x^3 + 6,600x^2 - 174,000x + 1,440,000$

Above equations given in ft.-lbs. and results are represented by curve in Fig.B-1.

Maximum bending moment in anchor pile:

Substituting into Eqs.(6-8) and (6-9),

$h = 12.11$ ft.

$M_{max} = 81,000$ ft.-lbs.

Deflection in anchor pile:

Substituting into Eqs.(6-10),

Case (a), $y = -\frac{1}{EI}(14.58x^5 - 94,400x + 453,500)$

Case (b), $y = -\frac{1}{EI}(-3.75x^5 + 550x^4 - 20,600x^3 + 291,600x^2 - 1,478,400x + 2,139,000)$

Case (c), Deflection for this case is comparatively small and will be omitted in this example.

Above results given in ft. and results are represented by curve in Fig.B-1.

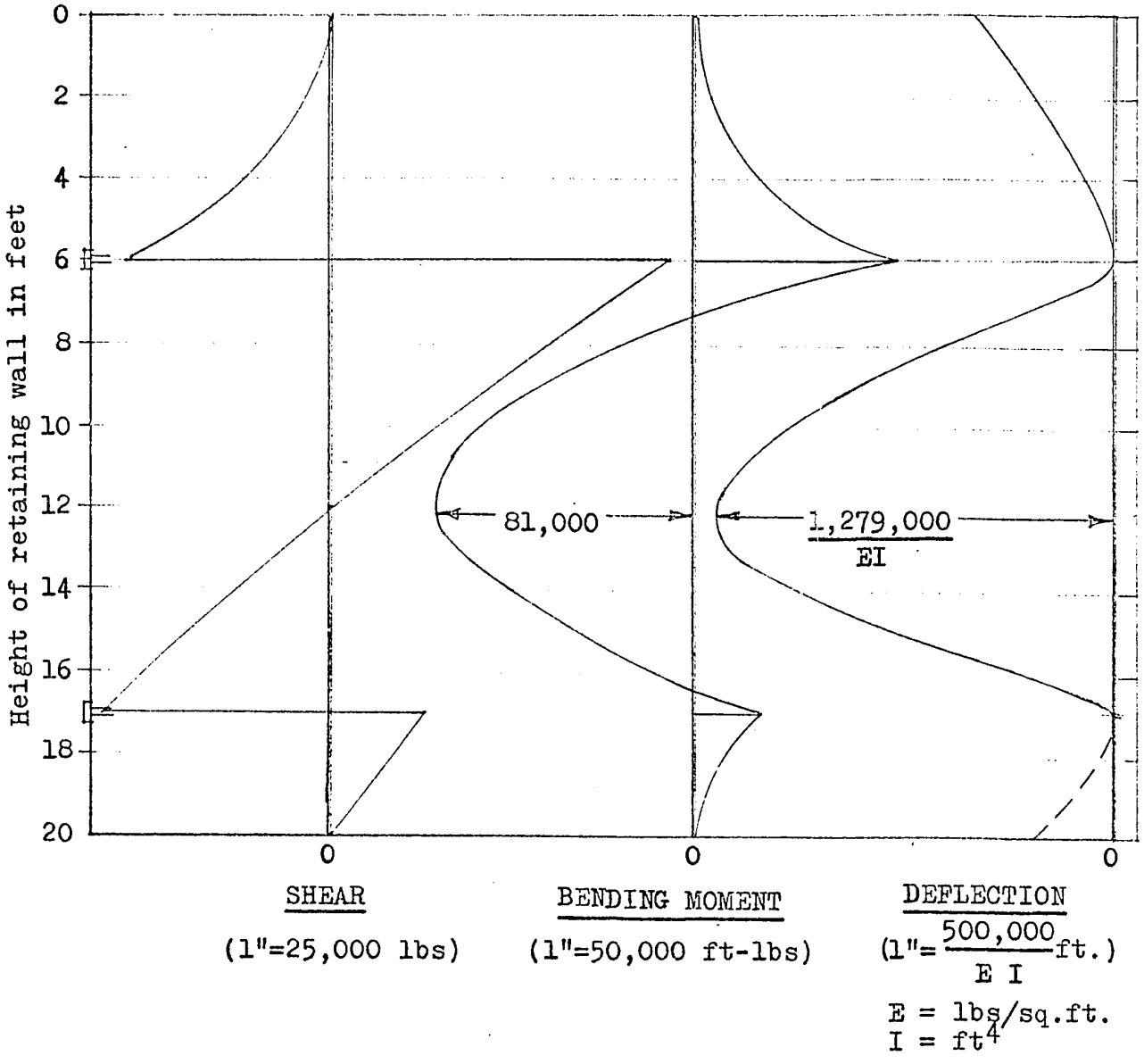

Fig.B-1 - Shear, bending moment and deflection on anchor pile due to lateral pressure from two tracks loading.

LIST OF TABLES AND PLATES

REFERENCES

1. Gerber, E., "Unterschungen uber die Druckverteilung im ortlich belasteten Sand," Technische Hochschule, Zurich, Switzerland, 1929.
2. Terzaghi, K., "Theoretical Soil Mechanics," John Wiley & Sons, New York, 1943, pp.376 - 377.
3. Murphy, G., "Similitude in Engineering," The Ronald Press Co., New York, 1950, pp. 57 - 93.
4. Lee, G. H., "An Introduction to Experimental Stress Analysis," John Wiley & Sons, New York, 1950, pp. 65 - 85.
5. Terzaghi, K., "Anchored Bulkheads," Trans. ASCE Vol. 119, 1954, pp. 1243 - 1324.
6. Spangler, M. G., and Mickle, J., "Lateral Pressure on Retaining Walls due to Backfill Surface Loads," Highway Research Board Bulletin 141, 1956, pp. 1 - 18.
7. Huntington W. C., "Earth Pressure and Retaining Walls," John Wiley & Sons, 1957, pp. 47 - 52.
8. "Timber Construction Manual," Canadian Institute of Timber Construction, 1963.
9. Bowles, J. E., "Foundation Analysis and Design," McGraw Hill, 1968, pp. 265 - 300.
10. Breen, J. E., "Fabrication and Tests of Structural Models," Journal of the Structural Division, ASCE, Proceeding Paper 5989, June 1968.

11. Haliburton, T. A., "Numerical Analysis of Flexible Retaining Structures," Journal of Soil Mechanics & Foundation Division, SM6, November 1968.

12. "Moment and Shear Tables for Heavy Duty Cars on Bridges," Association of American Railroads Research Centre, Chicago, July 1970.